EPA 550-B99-017

TECHNICAL BACKGROUND DOCUMENT FOR OFFSITE CONSEQUENCE ANALYSIS FOR ANHYDROUS AMMONIA, AQUEOUS AMMONIA, CHLORINE, AND SULFUR DIOXIDE

Chemical Emergency Preparedness and Prevention Office
U.S. Environmental Protection Agency

Prepared by:

Geoffrey D. Kaiser, Joseph D. Price, and José Urdaneta
Science Applications International Corporation
11251 Roger Bacon Drive
Reston, Virginia 20190

TABLE OF CONTENTS

Page

CHAPTER 1: INTRODUCTION **1-1**

1.1 BACKGROUND 1-1
1.2 PURPOSE 1-1
1.3 GENERAL APPROACH 1-1
1.4 ASSUMPTIONS 1-2

CHAPTER 2: UNCERTAINTIES AND MODELS USED **2-1**

2.1 ANHYDROUS AMMONIA 2-1
2.1.1 SAIC Proprietary Model *2-1*
2.1.2 USEPA RMP Offsite Consequence Analysis Guidance (OCAG) *2-3*
2.1.3 TFI *2-3*
2.1.4 DNV-UDM-Technica *2-5*
2.1.5 AWWARF Approach *2-6*
2.1.6 Additional ALOHA Run *2-6*
2.1.7 Comparison with Available Data *2-6*
2.1.7.1 Data from Accidents 2-6
2.1.7.2 Experimental Data--Desert Tortoise 2-9
2.1.7.3 Data from Modeling 2-10
2.1.7.4 Interpretation of Figures 2-2 and 2-3 2-10
2.1.7.5 Choice of a Single Curve for AR and WWTP Guidance 2-11
2.1.7.6 10-Minute vs. 60-Minute Releases 2-11
2.1.8 Anhydrous Ammonia--Urban Site, Worst-Case *2-13*
2.1.9 Anhydrous Ammonia--Alternative Scenarios *2-13*
2.2 AQUEOUS AMMONIA 2-17
2.3 CHLORINE 2-17
2.3.1 Worst-Case Scenarios *2-17*
2.3.2 Alternative Scenario *2-23*
2.4 SULFUR DIOXIDE 2-23
2.5 BACKGROUND DESCRIPTION OF SENSITIVITY STUDIES 2-24
2.5.1 Dry Deposition *2-24*
2.5.2 Puff Releases *2-25*
2.5.3 Qualitative Uncertainties and Conservatisms *2-25*
2.5.3.1 Duration of Worst-Case Weather Conditions 2-25
2.5.3.2 Pooling 2-25
2.5.3.3 Time Varying Toxic Endpoints 2-25
2.5.4 Conclusion–Sensitivity Studies *2-26*

CHAPTER 3: GASES LIQUEFIED UNDER PRESSURE **3-1**

CHAPTER 4: ADJUSTMENT OF MEAN CONCENTRATION FOR AVERAGING TIME **4-1**

CHAPTER 5: AMMONIA/MOIST-AIR THERMODYNAMICS **5-1**

5.1 CALCULATION OF THERMODYNAMIC PROPERTIES OF MIXTURES OF AMMONIA AND AIR 5-1
5.1.1 Methods *5-1*
5.1.1.1 Physical Property Data 5-2
5.1.1.2 Algorithm for Determination of Final Cloud Conditions 5-5
5.1.2 RESULTS *5-10*
5.2 EFFECT ON PREDICTION OF DISTANCES TO TOXIC ENDPOINT 5-12
5.3 POTENTIAL FOR LIFT-OFF 5-13

CHAPTER 6: EFFECT OF AMMONIA RELEASES ON STRUCTURES **6-1**

6.1 PROLONGED RELEASES 6-1

6.1.1 Building Structural Response *6-2*

6.1.2 Building Attenuation of Release *6-2*

6.2 SUMMARY OF CONCLUSIONS 6-3

REFERENCES .....

LIST OF FIGURES

Page

Figure 2-1. Sensitivity Studies for Worst-Case Anhydrous Ammonia Scenarios - Predicted Distances to Toxic Endpoint, Rural Site, Atmospheric Stability F, Windspeed 1.5 m/s 2-4

Figure 2-2. Ammonia Dispersion Data Accidents and Desert Tortoise Experiments 2-8

Figure 2-3. Ammonia Dispersion Data (Enlarged) 2-12

Figure 2-4. Sensitivity Studies For Worst-Case Anhydrous Ammonia Scenarios Predicted Distances To Toxic Endpoint, Urban Site, Atmospheric Stability F, Windspeed 1.5 m/s 2-14

Figure 2-5. Sensitivity Studies for Alternative Anhydrous Ammonia Scenarios Predicted Distances to Toxic Endpoint, Rural Site, Atmospheric Stability Category D, Windspeed 3 m/s 2-15

Figure 2-6. Sensitivity Studies for Alternative Anhydrous Ammonia Scenarios Predicted Distances To Toxic Endpoint, Urban Site, Atmospheric Stability Category D, Windspeed 3 m/s 2-16

Figure 2-7. Sensitivity Studies for Worst-Case Aqueous Ammonia Scenarios Predicted Distances to Toxic Endpoint, Rural Site, Atmospheric Stability F, Windspeed 1.5 m/s 2-18

Figure 2-8. Sensitivity Studies For Worst-Case Aqueous Ammonia Scenarios Predicted Distances to Toxic Endpoint, Urban Site, Atmospheric Stability F, Windspeed 1.5 m/s 2-19

Figure 2-9. Sensitivity Studies for Alternative Aqueous Ammonia Scenarios Predicted Distances to Toxic Endpoint, Rural Site, Atmospheric Stability D, Windspeed 3 m/s 2-20

Figure 2-10. Sensitivity Studies for Alternative Aqueous Ammonia Scenarios - Predicted Distances to Toxic Endpoint, Urban Site, Atmospheric Stability Category D, Windspeed 3 m/s 2-21

Figure 2-11. Sensitivity Study Predicted Distances To Toxic Endpoint For Chlorine 2-22

Figure 3-1. Fraction of Liquid Chlorine Falling to the Ground as a Function of Superheat 3-2

Figure 4-1. Illustration of Meandering 4-3

Figure 5-1. Algorithm for Determination of Final Cloud Conditions for Mixing of Ammonia and Moist Air Clouds 5-6

Figure 5-2. Algorithm for Calculation of Dew Point Pressure 5-10

LIST OF TABLES

Page

Table 2-1. Maximum Center Line Concentrations Measured in the Desert Tortoise Experiments (ppm) 2-9

Table 2-2. Comparison of Worst-Case Hazard Assessments for Anhydrous Ammonia 2-10

Table 2-3. Examples of AWWARF and SACRUNCH/AR Predictions Worst Case, Urban Site 2-13

Table 2-4. Ratios of AWWARF Alternative Case Predictions 2-13

Table 2-5. Distances to Toxic Endpoint (ft)--Sensitivity Studies for Chlorine 2-23

Table 4-1. Example of Effect of Meandering of Anhydrous Ammonia Releases, Worst-Case, Rural Conditions 4-4

Table 4-2. Example of Effect of Meandering of Anhydrous Ammonia Releases, Worst-Case Urban Conditions 4-5

Table 5-1. Comparison of Measured and Predicted Vapor Pressure of Water 5-4

Table 5-2. Comparison of Measured and Predicted Vapor Pressure of Ammonia 5-4

Table 5-3. Comparison of Measured and Predicted Vapor Pressures Above Ammonia/Water Solutions 5-4

Table 5-4. Heat Capacity and Heat of Vaporization Data 5-5

Table 5-5. Final Cloud Conditions for a Worst-Case Scenario, Two-Phase Release with Moist Air* 5-11

Table 5-6. Final Cloud Conditions for a Worst-Case Scenario, Two-Phase Release with Dry Air* 5-11

Table 5-7. Final Cloud Conditions for All Vapor Release with Dry Air* 5-12

Table 5-8. Example of the Effect of New Thermodynamic Model and Meandering of Anhydrous Releases, Worst-Case, Rural Conditions, 75% RH 5-12

Table 5-9. Illustration of the Potential for Lift-Off 5-13

Table 6-1. Ten-Minute Building Release Attenuation Factors for Continuous Releases of Ammonia 6-4

Table 6-2. Ten-Minute Building Release Attenuation Factors for Prolonged Releases of Chlorine and Sulfur Dioxide 6-5

CHAPTER 1: INTRODUCTION

1.1 BACKGROUND

Following the publication of the US Environmental Protection Agency's (EPA's) Risk Management Program (RMP) regulations, 40 CFR Part 68, EPA developed generic guidance for the offsite consequence analyses required by the regulation. This document, *RMP Offsite Consequence Analysis Guidance (OCAG)*, is intended to provide simple methods and reference tables for determining distances to toxic and flammable endpoints for worst-case and alternative release scenarios. The generic approach is based on parameters required by the rule and on conservative assumptions about other conditions and may not reflect site-specific conditions. Use of the guidance is not required; facilities may conduct their own air dispersion modeling, provided that they use the parameters specified in the rule and a model appropriate for the substance.

EPA also developed industry-specific guidance for ammonia refrigeration (AR) and wastewater treatment plants (WWTPs). In developing these documents, EPA conducted chemical-specific modeling for anhydrous ammonia, aqueous ammonia, chlorine, and sulfur dioxide, including consideration of liquid droplet formation (except in the case of aqueous ammonia). This chemical-specific modeling was incorporated into the OCAG. The modeling for these four toxic substances is different from, and less conservative than, the generic modeling that applies to other regulated substances covered in the OCAG.

1.2 PURPOSE

The purpose of this document is to provide the technical background of the methodology and assumptions used to develop the chemical-specific tables.

1.3 GENERAL APPROACH

Modeling the consequences of large-scale accidental releases of toxic vapors involves many uncertainties. These uncertainties may arise from the capability of different models to describe the physical phenomena, the selection of input parameters, and the lack of data to validate the models. When the same inputs are used, different models may produce widely varying results; the same model may also produce widely varying results if the input parameters are varied across their range of uncertainty. The range of predicted distances can be as much as a factor of 10.

The modeling conducted to develop the chemical-specific tables differs from the modeling for the generic tables found in the OCAG in the following ways:

(1) Models developed by SAIC (referred to as SACRUNCH and SADENZ) were used rather than SLAB. Sensitivity analyses were conducted using various models, experimental data, and accident data to evaluate the reasonableness of the results. Chapter 2 provides the results of these analyses, which illustrate the range of outcomes possible when performing analyses of the type required by EPA. Because SACRUNCH, SADENZ, and SAPLUME (1994) are proprietary

dispersion models, and thus not readily available for review, some information about these models is provided in Appendix A.

(2) Liquid anhydrous ammonia, chlorine, and sulfur dioxide are frequently stored as gases liquefied under pressure. In the OCAG, for the worst-case release, gases liquefied under pressure are assumed to behave similarly to gases. Based on relevant studies, absent obstacles, liquid anhydrous ammonia, chlorine, and sulfur dioxide released at typical ambient temperatures are assumed to become and remain airborne as a mixture of vapor and fine liquid droplets and, for the purposes of RMP, can be modeled as a gas. Chapter 3 discusses this issue.

(3) The effect of averaging time on plume spread was considered and a method for adjusting the predicted mean concentration for averaging time developed. Chapter 4 discusses this issue.

(4) The thermodynamics of mixtures of moist air and anhydrous ammonia were analyzed using the techniques reported by Wheatley (1987). (See Chapter 5, which also discusses whether the ammonia/moist air mixing will generate enough heat to cause the plume to become buoyant.)

(5) For scenarios in which the release from a vessel is indoors, the effect of hold-up of vapors within a building has been incorporated into the industry-specific models, but not the OCAG, which uses a simpler approach. Chapter 6 discusses this issue.

1.4 ASSUMPTIONS

As previously mentioned, the RMP rule requires that certain parameters be used in the offsite consequence analysis modeling (40 CFR 68.22). The analyses presented in this document use these required assumptions.

- For anhydrous ammonia, chlorine, and sulfur dioxide (i.e., gases liquefied under pressure), the worst-case scenario consists of the sudden release of the whole contents of the largest vessel or pipeline. For the purposes of the modeling, it is assumed that the release is spread over 10 minutes, whether the release is outside or inside a building.

- The worst-case weather conditions consist of Atmospheric Stability Category F, with a windspeed of 1.5 m/s, unless it can be shown that such conditions have not occurred at the site during the past three years.

- The toxic endpoints are 200 ppm for ammonia, 3 ppm for chlorine, and 3 ppm for sulfur dioxide, irrespective of the duration of exposure. EPA is currently developing Acute Exposure Guideline Levels (AEGLs), which will consist of different values of toxic endpoint for a number of exposure times. However, until the AEGLs have been published and the rule has been changed, toxic endpoints are fixed.

CHAPTER 2: UNCERTAINTIES AND MODELS USED

Developing offsite consequence analysis guidance that is simple and easy to use, yet scientifically defensible, is difficult because a large range of uncertainty exists for predictions of distances to the toxic endpoint. For example, 40 CFR Part 68 requires that worst-case modeling be carried out assuming atmospheric stability category F and a windspeed of 1.5 m/s. However, very few experimental data exist for these weather conditions with which to validate models. To develop an understanding of the plausible uncertainty range, a comparative study was conducted in which the same input parameters were used in the different available models, release rate varied, and the outputs compared. The following is a description of analyses performed to support the reference tables and provides an explanation of how reference tables, plots, and formulas were selected from within the range of possibilities. Anhydrous ammonia is discussed first because, for this particular chemical, there are many examples and calculations available from which to develop an understanding of the range of uncertainties.

2.1 ANHYDROUS AMMONIA

In many parts of a typical refrigeration system, ammonia is liquefied under pressure. If the pressure and temperature are sufficiently high, and if there is a sudden release of ammonia, it will become and remain airborne as a mixture of vapor and very fine liquid droplets that do not fall to the ground. The droplets evaporate quickly cooling the air so that a cold mixture of air and ammonia vapor is formed. The mixture is initially denser than air.

The comparative study was conducted for a worst-case scenario release of anhydrous ammonia at a rural site. The toxic endpoint for ammonia as specified in the RMP Rule is 0.14 mg/L (200 ppm). For the purposes of the RMP, this is a fixed value no matter the duration of release. The worst-case weather conditions consist of Atmospheric Stability Category F, with a windspeed of 1.5 m/s. The worst-case scenario consists of an outdoor, sudden release of the whole contents of the largest vessel or pipeline. For the purposes of this comparative study, the worst-case release was varied from 1,000 to 400,000 lbs. It is assumed that the release is spread over 10 minutes, therefore, the rate of release varied from 100 to 40,000 lbs./min.

Figure 2-1 displays several different answers to the question: "For worst-case scenarios at a rural site, what is the predicted distance to the toxic endpoint as a function of the rate of release of anhydrous ammonia?" The various models used to prepare Figure 2-1 are described below. [On the tables and plots in this chapter, it was sometimes necessary to extrapolate data presented by other authors. This was done by assuming a linear relationship between distance and release rate on a log-log plot.]

2.1.1 SAIC Proprietary Model

The May 1996 draft guidance for ammonia refrigeration (USEPA, 1996b) made use of two SAIC proprietary computer models—SACRUNCH, which is suitable for the modeling of ground-level, horizontal releases of denser-than-air vapors, and a companion model, SADENZ, for denser-than-air puffs. These models are described in SAIC (1994), and a summary is

provided in Appendix A. These models were used because they allow the easy use of sensitivity studies, including the phenomenon of dry deposition, a highly effective mechanism for depleting clouds of reactive gases such as ammonia, and because they allowed the easy insertion of an ammonia/moist air thermodynamics module.

1. The models are 2-D "box" models with gravitational slumping, edge entrainment, and top entrainment of air given by simple but reasonably well-established formulas in the initial, heavier-than-air phase. The model was essentially "tuned" by comparison with the Thorney Island experiments (McQuaid, 1986).

2. The model finally evolves from being denser-than-air to being neutrally buoyant when $\Delta\rho/\rho_a = 0.001$, where ρ_a is the density of air and $\Delta\rho$ is the difference between the density of the vapor cloud (averaged across a continuous-plume cross section or throughout a puff) and the density of the surrounding air[1].

3. In the neutrally buoyant phase, the models evolve to the "Green Book" horizontal and vertical standard deviations of σ_y and σ_z (i.e., the rural or urban parameterizations proposed by Briggs (1973a) and reproduced in the "Green Book." The "Green Book" is EPA's *Technical Guidance for Hazards Analysis* (USEPA, 1987), which contains a Gaussian model with vertical and horizontal standard deviations from Briggs (1973a).

4. For ammonia, chlorine, and sulfur dioxide released from the liquid space of vessels in which they are liquefied under pressure at 25 °C or at the highest daily temperature, it is assumed that a portion of the released liquid immediately flashes to vapor (e.g., 20 percent). The user calculates the percentage outside the model from thermodynamic principles. The remaining liquid atomizes and remains airborne. See Chapter 3 for justification of this assumption. See Chapter 6 for a discussion of how buildings could mitigate this effect.

5. SACRUNCH makes a simplifying assumption: the turbulence generated by the flash atomization process is such that, almost immediately, the mass mixing ratio is 10 (i.e., the ratio of entrained air to airborne ammonia, chlorine, or sulfur dioxide mass is 10). For anhydrous ammonia, the density and temperature of this mixture are calculated using the ammonia/moist air thermodynamic model described in Chapter 5. For chlorine and sulfur dioxide, the mixture is assumed to be air and Cl_2 vapor or air and SO_2 vapor, respectively, at their atmospheric boiling points. The initial horizontal momentum of the escaping liquid jet and the entrained air is conserved to define the initial conditions for SACRUNCH. A similar assumption is made for an instantaneous puff release in SADENZ. The predictions of the model at distances at which the toxic endpoints of Cl_2 or SO_2 are encountered (3ppm) are not sensitive to this assumption, although it does mean that predictions near the source may not be accurate.

[1] Some reviewers criticized this assumption because it is a simpler transition criterion than is found in other models. However, as is shown in Appendix A, the models do a reasonable job of fitting the large-scale experimental databases. They evolve in the far field into a well-established Gaussian model with well-known standard deviations provided by Briggs (1973a). In addition, sensitivity studies (not shown here) indicate that the results do not change significantly when the $\Delta\rho/\rho_a$ criterion is varied between 0.01 and 0.001.

6. In SACRUNCH, the toxic endpoint is compared to the peak centerline concentration, which, for worst-case scenarios, is assumed to jump up to that value when the puff arrives and to remain constant for exactly 10 minutes, independent of location. In SADENZ, the model calculates the average centerline concentration over the duration of cloud passage. This duration is a function of distance downwind.

7. SACRUNCH and SADENZ have simple dry deposition modeling algorithms (see Section 2.5.1). None of the other computer programs discussed herein have these capabilities, which is one of the reasons the authors consider it useful to use SACRUNCH and SADENZ.

8. There is an issue concerning the use of models such as SACRUNCH with high surface roughness length (this issue is discussed below in some detail in the context of the use of DEGADIS). The concern is that, at a truly urban site, a heavy vapor will flow in among the obstructions on the surface (e.g., large buildings) and will not be exposed to the turbulence in the atmosphere above those obstructions. For the present work, it has been assumed that, while in the denser-than-air phase, the surface roughness length is 10 cm at both urban and rural sites. When $\Delta\rho/\rho a < 0.001$, the model is a Gaussian one in which σy and σz are different for urban and rural sites. This approach should be somewhat conservative for the urban site.

Three sensitivity studies are shown on Figure 2-1:

A. A conservative case, in which SACRUNCH defaults into the "Green Book" rural dispersion model in the far field, when the initial denser-than-air behavior has been "forgotten".

B. A case in which a dry deposition velocity of 1 cm/sec has been used. See Section 2.5.1 for further discussion of dry deposition. The authors also looked at a case in which the dry deposition velocity was 0.3 cm/sec, but that case is not reproduced on Figure 2-1.

C. A case in which the puff model SADENZ has been used.

2.1.2 USEPA RMP Offsite Consequence Analysis Guidance (OCAG)

The OCAG (USEPA, 1996a) was developed using the SLAB model (Ermak, 1989). It is intentionally conservative. The distances are obtained simply by reading from tables provided in the OCAG. The nearest entry in the OCAG table that is conservative is the one that is chosen. In addition, a second OCAG curve has been provided – one that has been interpolated between the discrete values of release rate and toxic endpoint that are given in the OCAG lookup tables. This gives somewhat less conservative predictions.

2.1.3 TFI

The Fertilizer Institute (TFI) has produced its own guidance on large-scale releases of anhydrous ammonia. TFI used the DEGADIS model (USEPA, 1989), with its transient option. In this option, the initial ten-minute "slug" of ammonia gradually evolves into a puff as it travels

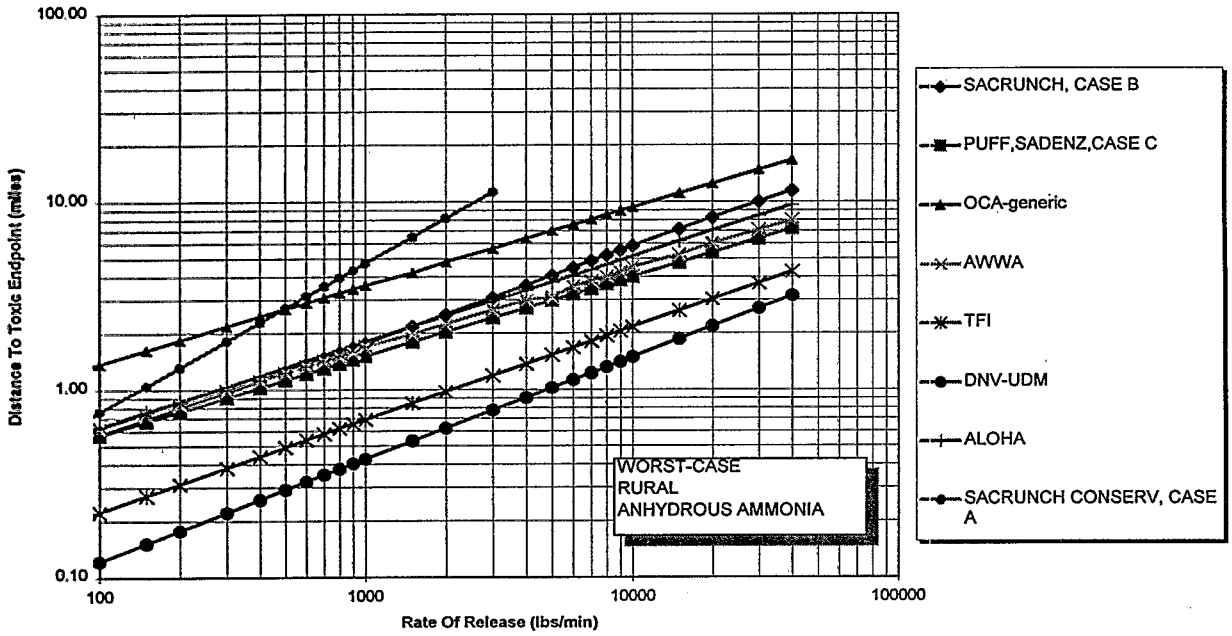

Figure 2-1. Sensitivity Studies for Worst-Case Anhydrous Ammonia Scenarios - Predicted Distances to Toxic Endpoint, Rural Site, Atmospheric Stability F, Windspeed 1.5 m/s

downwind because there is along-wind lengthening of the slug due to the action of atmospheric turbulence. This lengthening effect is most dramatic in Atmospheric Stability Category F conditions with a low windspeed. The transient release model that TFI has used is conceptually realistic.

Note that TFI uses roughness lengths of 3 cm and 1 m to characterize rural and urban areas, respectively. There are two potential concerns about this:

1. The authors of DEGADIS have previously expressed the opinion that DEGADIS should not be used with surface roughness lengths in excess of 10 cm. This issue was extensively discussed in 1990/91 during the South Coast Air Quality Management Districts rulemaking on hydrogen fluoride storage and use (SCAQMD, 1991a,b). SCAQMD states:

   "The slumping and stably stratified flow characteristic of dense gas releases produces dense gas plumes that have height scales significantly less than the height of the atmospheric boundary layer. The surface roughness parameter is used by the models to characterize the dense gas vertical dispersion. The mathematical concept of the surface roughness parameter dictates the use of a value that is much less than the height scale of the dispersing cloud. This is not a problem when simulating dense gas dispersion in a desert environment, but it becomes more complicated when applying the models in urban areas.

"Since dense gas models have been developed to simulate test releases conducted in non-urban (desert) settings, most models, including DEGADIS, are designed to simulate rural dispersion when the cloud enters the passive phase. A surface roughness value characteristic of urban scale roughness elements is inappropriate unless the dense gas cloud height is approximately 30 times the height of the surface roughness elements. Until the issue of extrapolating the use of the models from non-urban settings to urban settings is better understood, a surface roughness value of 0.1 meter shall be used as the input to DEGADIS for the entire transport and dispersion calculation."

This limitation on the use of DEGADIS was supported by one of the original authors of DEGADIS, Jerry Havens, in testimony to SCAQMD.

2. When moving from a rural to an urban area, increased intensity of atmospheric turbulence arises from two sources, mechanical (due to the presence of buildings) and convective (due to the presence of large heat sources). It is questionable whether a model in which changed surface roughness alone is responsible for the enhanced intensity of turbulence at urban sites correctly characterizes the physics of the situation (this comment also applies to SLAB).

2.1.4 DNV-UDM-Technica

The work presented by Woodward (1998) is of considerable interest because the model used is based on experimental data obtained at very low windspeeds in stable weather conditions. There are few such data available for any hazardous vapor; DNV made use of a database of large-scale propane releases (Heinrich et al., 1988/1989). The releases ranged in size from a few hundred kilograms to several thousand kilograms, and the duration of release varied from 40 seconds to 600 seconds. It is pertinent to try to understand why the DNV predictions on Figure 2-1 are relatively low.

1. The model that DNV "tuned" based on the TUV experiments is known as UDM (Unified Dispersion Model). It has considerable merit because, as noted above, it was actually based on experiments at low windspeeds in stable weather conditions. However, the appreciably lower predictions of the UDM model in Figure 2-1 are, in part, due to an assumption about averaging. Basically, the author appears to have divided the model's predicted concentrations by a factor of six to take account of the 10-minute duration of release, whereas the ammonia toxic endpoint of 200 ppm is valid for an exposure time of 60 minutes. This amounts to assuming that Haber's law is valid for ammonia. As noted above, such exposure time-dependent relationships for toxic endpoints are not permitted under the current rule.

2. The principal aim of the original TUV papers from the *Journal of Hazardous Materials* (Heinrich et al., 1988; 1989) was to examine the lower flammable distance (LFD) (i.e., the distance to the lower flammable limit, which is 2.1 v% [~ 20,000 ppm] for propane). Experimental measurements were taken down to concentration levels of a few thousand ppm. To make predictions for ammonia at 200 ppm, extrapolations of more than an order of magnitude are required. Therefore, it should be noted that the

experimental results upon which the "tuning" of the UDM models is based are strictly near-field results and do not provide information about concentrations at or near the toxic endpoint of ammonia. (UDM is no different from any of the other models in this respect; however, it is also true to say that it is no better than the others, either.)

3. Two types of instruments were used to record propane concentration – "catalytic-type" instruments (details not given) that were regularly distributed across the field, and infrared (IR) spectrometers that used the 3.7 m propane absorption band for detection. It turned out that, in the original publication (Heinrich et al., 1988), the IR measurements were incorrectly interpreted because the results were distorted by the presence of ice crystals, which led to considerable overestimates of the LFDs. These overestimates were corrected in 1989 (Heinrich et al., 1989).

   Woodward points out inconsistencies between the readings of the catalytic sensors and the IR sensors in experiments in which the rate of release and other conditions were nearly identical and, on this basis, states that the IR results are preferable. The IR results appear to be generally lower than the catalytic sensor results, presumably biasing the tuning of the UDM model towards lower predicted distances. It would seem that caution is advisable in ignoring one set of results just because the experimental fluctuations appear to be large, while accepting another set of results that required major post facto corrections.

2.1.5 AWWARF Approach

The American Water Works Association Research Foundation (AWWARF, 1998) approach is based on the ALOHA model (NOAA and USEPA, 1995) and is provided here as a representative application of that computer model. It is likely that many facilities that do their own modeling will use ALOHA.

2.1.6 Additional ALOHA Run

When preparing the RMP Guidance for Ammonia Refrigeration (USEPA, 1998), EPA engaged in continuous dialog with the International Institute of Ammonia Refrigeration (IIAR). Early in 1996, one of IIAR's consultants provided an ALOHA output[2], which is also shown on Figure 2-1.

2.1.7 Comparison with Available Data

2.1.7.1 Data from Accidents

No data set (or sets) was identified that unequivocally distinguishes among all of the models on Figure 2-1. However, there are sufficient data available to make some judgments about where to place reasonably conservative guidance.

Markham (1986) provides an instructive review of the consequences of quite a large number of accidents that have resulted in the release of anhydrous ammonia. The results of Markham's

[2] IIAR, Private Communication, March 1996

work are summarized on Figure 2-2, which is a little complicated, but which is worth further study. The letters A, B, - - - MM identify the estimated concentrations from a list of 12 accidents that Markham analyzed. The lengths of the bars represent the uncertainty in recovering data from accident descriptions. *Note that these bars do not represent actual measured concentrations. They represent post-facto reconstructions from observations of effects on plants and birds.*

Markham defines the releases as follows:

- A, B, C and D-45-ton release of cold product (presumably refrigerated) in approximately 30 minutes, Bainesville, MN (6/10/81)
- E-puncture in 82-ton railcar, ambient temperature, Belle, WV (1/21/70)
- F and G-160 tons of cold product over 2□ hours, Blair, NE (11/16/70)
- H, J and K-truck train collision, 18 tons of anhydrous ammonia at ambient temperature released in a few minutes, Boitte, LA (12/15/70)
- L, M and N-pipeline rupture, 230 tons at ambient temperature released in under eight hours, Conway, KS (12/6/73)
- O-160 tons released instantaneously, presumably ambient temperature, Crestview, FL (4/8/79)
- P-70 tons from train wreck, ambient temperature, Crete, NE (2/18/69)
- Q and R-pipeline rupture, 400 tons over four hours, ambient temperature, Enid, OK (5/7/76)
- U, V and W-train wreck, 50 tons rapidly released, ambient temperature, Pensacola, FL (11/9/77)
- X, Y, Z, AA, BB and CC-bullet tank failure, instantaneous release of 30 tons, ambient temperature, Potchefstroom, South Africa (7/13/73)
- DD and EE-railcar failure, 75-ton release, ambient temperature, Verdigis, OK (6/10/79)
- FF, GG, HH, II, JJ, KK, LL and MM-19 tons instantaneous release from a tank truck, ambient temperature, Houston, TX (5/11/76)

Thus, most of the data from accidents on Figure 2-2 are from spills of anhydrous ammonia at ambient temperature, with two releases of refrigerated ammonia. Markham does not specify the weather conditions associated with each specific release.

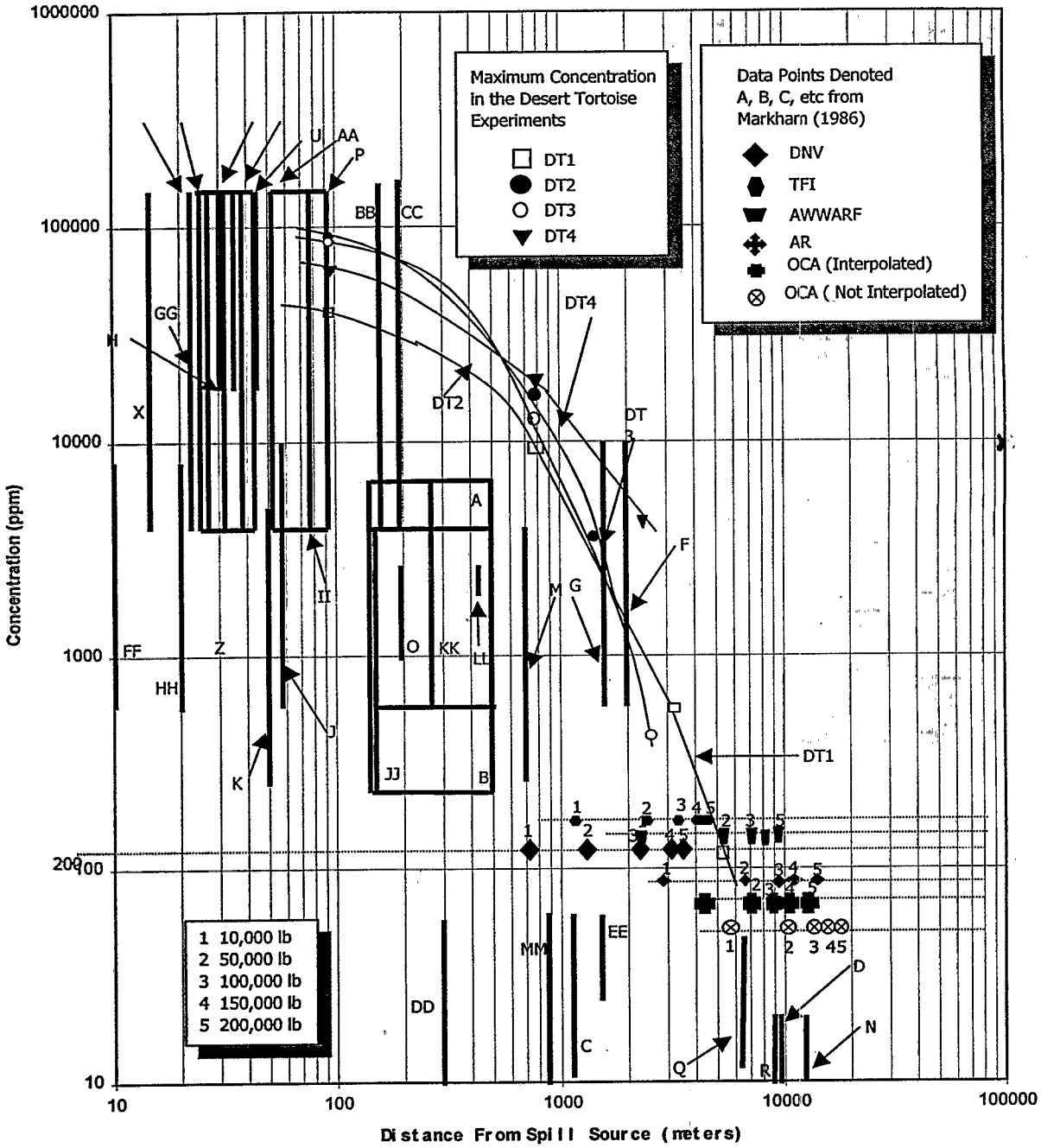

Figure 2-2. Ammonia Dispersion Data Accidents and Desert Tortoise Experiments

2.1.7.2 *Experimental Data--Desert Tortoise*

The solid curves on Figure 2-2 are data from the so-called "Desert Tortoise" (DT) large-scale experimental releases of flashing liquid ammonia, which were carried out at the Nevada Test Site (Goldwire et al., 1985). The release rates in the experiments were about 100 kg/sec (220 lb/sec, 13,200 lb/min), and the durations of release were a few minutes. The masses released in the four DT experiments were ~ 24,500 lb, 66,000 lb, 50,000 lb, and 90,000 lb in atmospheric stability classes D, D, D, and E, respectively, with windspeeds 7.42 m/s, 5.76 m/s, 7.38 m/s, and 4.5 m/s, respectively. The surface roughness length was 0.003 m. The actual data points are reproduced on Table 2-1. No estimates of experimental error were provided by Goldwire et al.

Some pertinent observations are as follows:

1. The solid curves connecting the Desert Tortoise data points on Figure 2-1 are drawn by eye to connect the points. They are not intended to be model fits to the data.

2. The Desert Tortoise data points themselves are peak concentrations taken from plots in the Desert Tortoise Series Data Report (Goldwire et al., 1985). Comparisons with some other publications show the following: (1) in a comparison with the numerical computer model, FEM3, Chan et al. (1987), use almost the same concentrations as in Table 2-1 for DT4; (2) Spicer et al. (1987) use 75,000, 21,000, and 5,000 ppm for the three DT4 measurements at 100, 800, and 2,800 m, respectively, in DT4, also close to the values given in Table 2-1. Therefore, there is precedent for the interpretation of the Desert Tortoise data in the way they are presented in Table 2-1.

Table 2-1. Maximum Center Line Concentrations Measured in the Desert Tortoise Experiments (ppm)

Distance Downwind (m)	DT1[a]	DT2[b]	DT3[c]	DT4[d]
100	50,000	80,000	80,000	65,000
800	10,000	15,000	12,500	17,500
1,400	---	5,000	---	---
2,800	---	---	600	5,000
3,500	650	---	---	---
5,600	150	---	---	---

[a]24,500 lb over 2 minutes (12,250 lb/min), stability category D, windspeed 7.42 m/s
[b]66,000 lb over 4 minutes (16,500 lb/min), stability category D, windspeed 5.76 m/s
[c]50,000 lb over 3 minutes (16,700 lb/min), stability category D, windspeed 7.38 m/s
[d]90,000 lb over 6 minutes (15,000 lb/min), stability category E, windspeed 4.51 m/s

3. Beyond 800 m, the ammonia concentration was measured by portable sensor stations. These data should be regarded as less reliable than those taken at 800 m and 100 m (with a full range of stationary instruments), but, nonetheless, do provide information that is helpful when making judgments.

2.1.7.3 Data from Modeling

Refer to Table 2-2 for a brief summary of some of the modeling data plotted on Figure 2-1. The predicted distance to the toxic endpoint is given for five discreet total masses, 10,000, 50,000, 100,000, 150,000 and 200,000 lb, respectively. Note that, for OCAG, two columns are presented. One, "without interpolation," consists of reading the predicted distances from the OCAG tables using the nearest conservative value that is directly tabulated therein. The other, "with interpolation," involves interpolating between values in the OCAG tables, assuming linear relationships on log-log plots. The AR data is the SACRUNCH, Case B from Figure 2-1 and is close to the OCAG guidance published in 1996.

The data from Table 2-2 are plotted on Figure 2-2. They should all lie along the 200-ppm line, but have been broken apart for greater clarity. For each model, the points labeled 1, 2, 3, 4, and 5 correspond to total mass released of 10,000, 50,000, 100,000, 150,000, and 200,000 lb, respectively. A portion of Figure 2-2 has been enlarged on Figure 2-3.

Table 2-2. Comparison of Worst-Case Hazard Assessments for Anhydrous Ammonia

Total Mass Released (lb)	PREDICTED DISTANCE TO TOXIC ENDPOINT (m)					
	OCAG[a]		AR[b]	AWWARF[c]	TFI[d]	DNV[e]
10,000	4,800[f]	5,800[g]	2,900	2,700	1,200	720
50,000	9,200	11,000	6,500	5,300	2,400	1,500
100,000	12,000	15,000	9,400	7,200	3,400	2,300
150,000	14,300	17,700	11,600	8,500	4,200	3,100
200,000	16,000	19,300	13,500	9,700	4,700	3,600

[a]OCAG – Offsite Consequence Analysis Guidance
[b]AR – Risk Management Program Guidance for Ammonia Refrigeration
[c]AWWARF – American Water Works Association Research Foundation
[d]TFI – Fertilizer Institute
[e]DNV – Det Norske Veritas-Technica
[f]OCAG with interpolation
[g]OCAG without interpolation

2.1.7.4 Interpretation of Figures 2-2 and 2-3

Recognizing that there is great uncertainty in the data on Figures 2-2 and 2-3, it is nevertheless pertinent to try to come to some tentative conclusions.

- Bars F and G represent the farthest observed distance to which accidental releases of ammonia have been seen to generate vapor clouds in the 1,000 to 10,000 ppm range, namely about 2,000 m. The data from Markham represent a prolonged release of refrigerated ammonia□160 tons over 22 hours, or about 2,000 lb/min. This is the release rate that would be expected from an RMP worst-case release of 20,000 lb, although the comparison is not quite apt because bars F and G come from a steady-state release, whereas the worst-case release is transient. Nonetheless, one would expect worst-case releases with larger release rates than 2,000 lb/min (e.g., points 2, 3, 4, and 5 with release rates of 5,000, 10,000, 15,000, and 20,000 lb/min, respectively) to be farther to the right

beyond bars F and G along the 200 ppm level. Therefore, at the 200-ppm level, the largest releases (e.g., 100,000 lb, representative of a railcar-sized release) ought to give predicted distances considerably in excess of this. For DNV and TFI, the predicted distances for a 100,000-lb release are 2,300 and 3,400 m, respectively. From this perspective, they seem a little low.

- The Desert Tortoise experiments have provided some data, albeit uncertain, in the 100 to 1,000 ppm range. These data were taken in Stability Categories D and E, with windspeeds considerably in excess of 1.5 m/s. If experiments had been performed in Atmospheric Stability Category F, with a windspeed of 1.5 m/s, the distances would be expected to increase. The surface roughness length at the Desert Tortoise was 0.003 cm, characteristic of a very smooth rural site (e.g., TFI gives rural terrain a surface roughness length of ~ 0.03 m, while DNV gives a surface roughness length of 0.003 m). Therefore, it seems reasonable that model predictions for releases of about the size of Desert Tortoise releases should propagate somewhat farther than do the Desert Tortoise curves on Figures 1 and 2. Both the DNV and TFI models give predictions that seem a little low from this perspective (e.g., DT1 shows a 150-ppm result at 5,600 m).

- In the 10 to 100 ppm range, the worst-case data from accident scenarios propagates out to about 12,500 m. Assuming that the worst-case accident data come close to the worst theoretically possible case, the predictions at the 200-ppm level should not propagate as far as (or, at least not much beyond) this distance. From the perspective, the OCAG predictions are perhaps too high.

2.1.7.5 Choice of a Single Curve for AR and WWTP Guidance

In conclusion, based on an analysis of what are admittedly highly uncertain data, it appears that the AWWARF and AR models fit well with what is observed. The OCAG model is more conservative (as intended), and the TFI and DNV models seem perhaps a little optimistic. Therefore, given the paucity of currently available data in the few hundred ppm range, it would seem reasonable to choose something in the region of the AWWARF/AR predictions. In the AR and WWTP guidance, the SACRUNCH, Case B, curve has been chosen.

2.1.7.6 10-Minute vs. 60-Minute Releases

In the OCAG, a distinction is drawn between releases that last for 10 minutes and releases that last for 60 minutes, and separate lookup tables are provided for each. However, in the guidance for WWTPs and ARs, no distinction is made. The main reason for this is that differences between the two are expected to be small relative to the uncertainties that have been identified in this section.

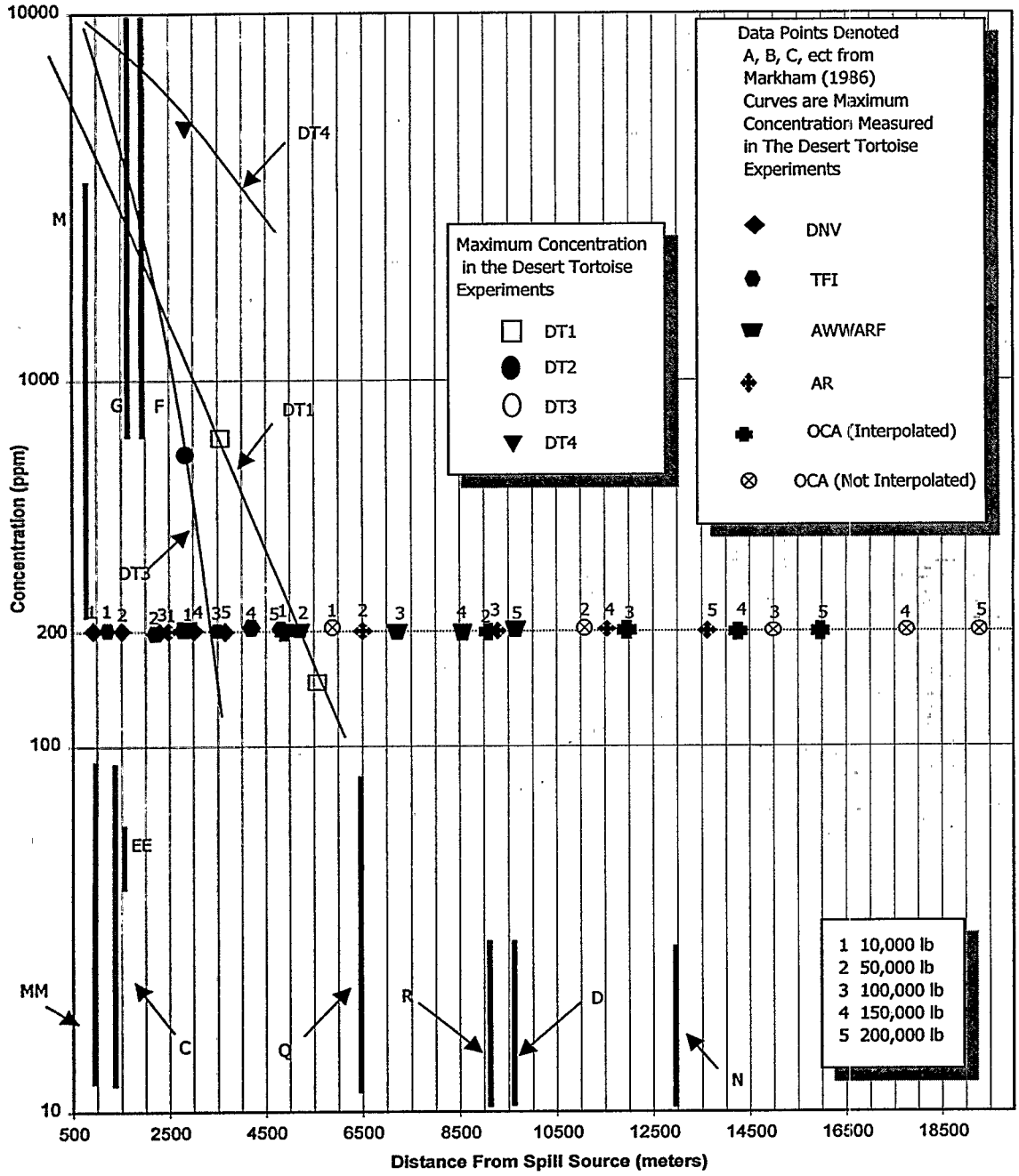

Figure 2-3. Ammonia Dispersion Data (Enlarged)

2.1.8 Anhydrous Ammonia--Urban Site, Worst-Case

The discussion so far has been for a rural site. Figure 2-4 is similar to Figure 2-1, except that it is for worst-case anhydrous ammonia on an urban site. (There is no modeling available for DNV at an urban site.) The pattern is similar to that for the rural site, except that the range of uncertainties is not so great. Again, the SACRUNCH, Case B, has been chosen for the generic worst-case, urban-site guidance for AR and WWTPs.

2.1.9 Anhydrous Ammonia--Alternative Scenarios

There is alternative scenario guidance for flashing liquid releases of anhydrous ammonia in AR and WWTPs. This guidance is displayed on Figures 2-5 and 2-6 in comparison with data from TFI, AWWARF, and the OCAG. These curves do not lie as far apart as do the curves for the worst case and much less attention has been devoted to justifying the choice of the SACRUNCH curve than was done for the worst-case scenarios. However, it is pertinent to make the following observations.

Examples of AWWARF and SACRUNCH/AR predictions from Figure 2-6 are given in Table 2-3. The distances generated by ALOHA as used by AWWARF are about a factor of 4 higher. It is instructive to look at the additional examples of data taken from Figures 2-5 and 2-6 and shown on Table 2-4. These show that, within the context of the large uncertainties that exist in the modeling, there is essentially no difference between the AWWARF predictions at rural and urban sites. For SACRUNCH, the corresponding ratios lie between 2 and 3 (i.e., SACRUNCH does show that there is a difference between an urban and a rural site in alternative-case weather conditions).

Table 2-3. Examples of AWWARF and SACRUNCH/AR Predictions Worst Case, Urban Site

Release Rate	AWWARF	SACRUNCH	AWWARF/SACRUNCH Ratio
100 lb/min	0.32 mi	0.08 mi	4.0
1,000 lb/min	1.0 mi	0.24 mi	4.2
3,000 lb/min	1.8	0.4	4.5

Table 2-4. Ratios of AWWARF Alternative Case Predictions

Release Rate	AWWARF (Rural)	AWWARF (Urban)	Ratio Rural/Urban
100 lb/min	0.4 mi	0.32 mi	1.25
1,000 lb/min	1.2 mi	1.0 mi	1.2
3,000 lb/min	2.0 mi	1.8 mi	1.1

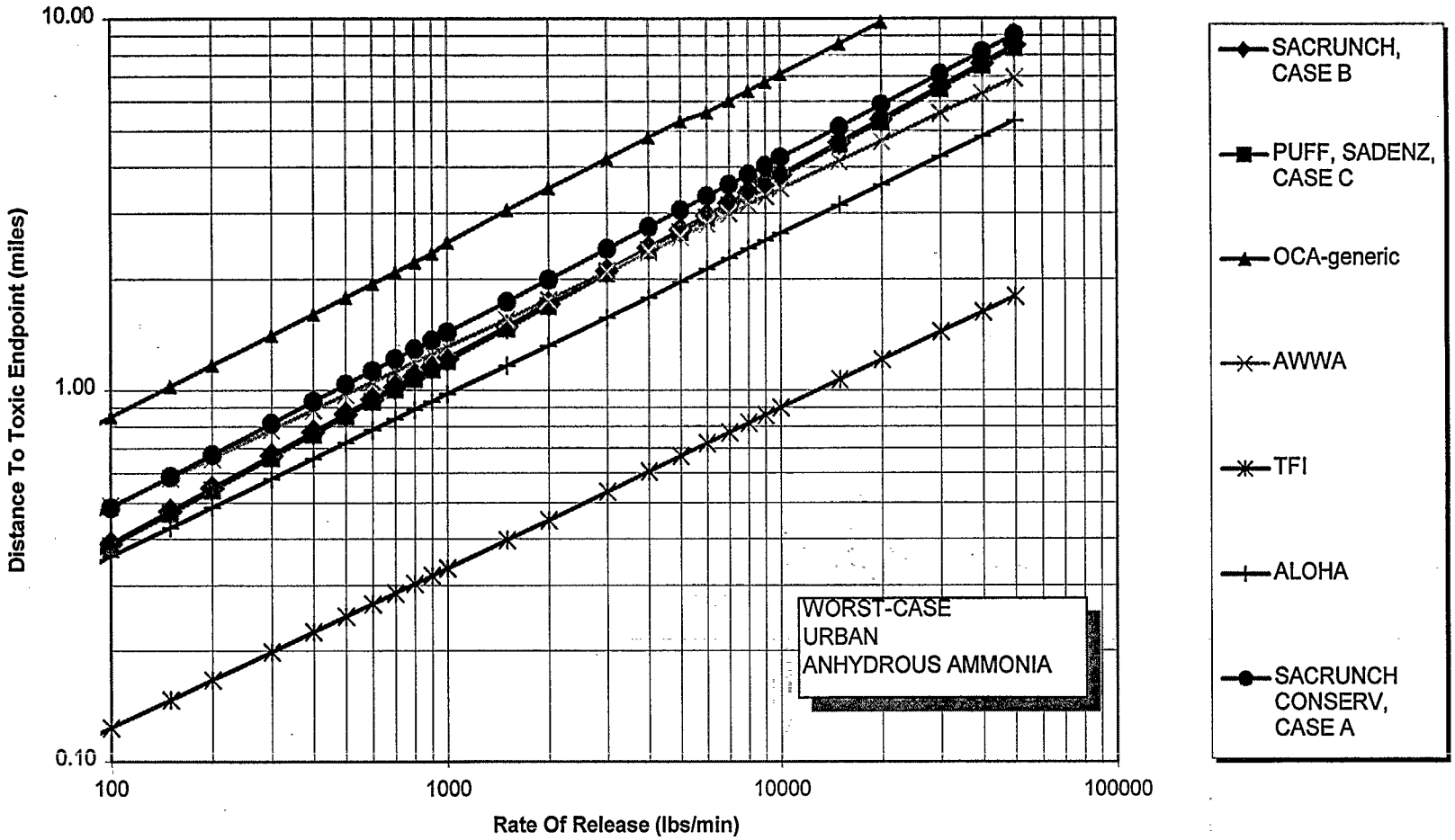

Figure 2-4. Sensitivity Studies For Worst-Case Anhydrous Ammonia Scenarios Predicted Distances To Toxic Endpoint, Urban Site, Atmospheric Stability F, Windspeed 1.5 m/s

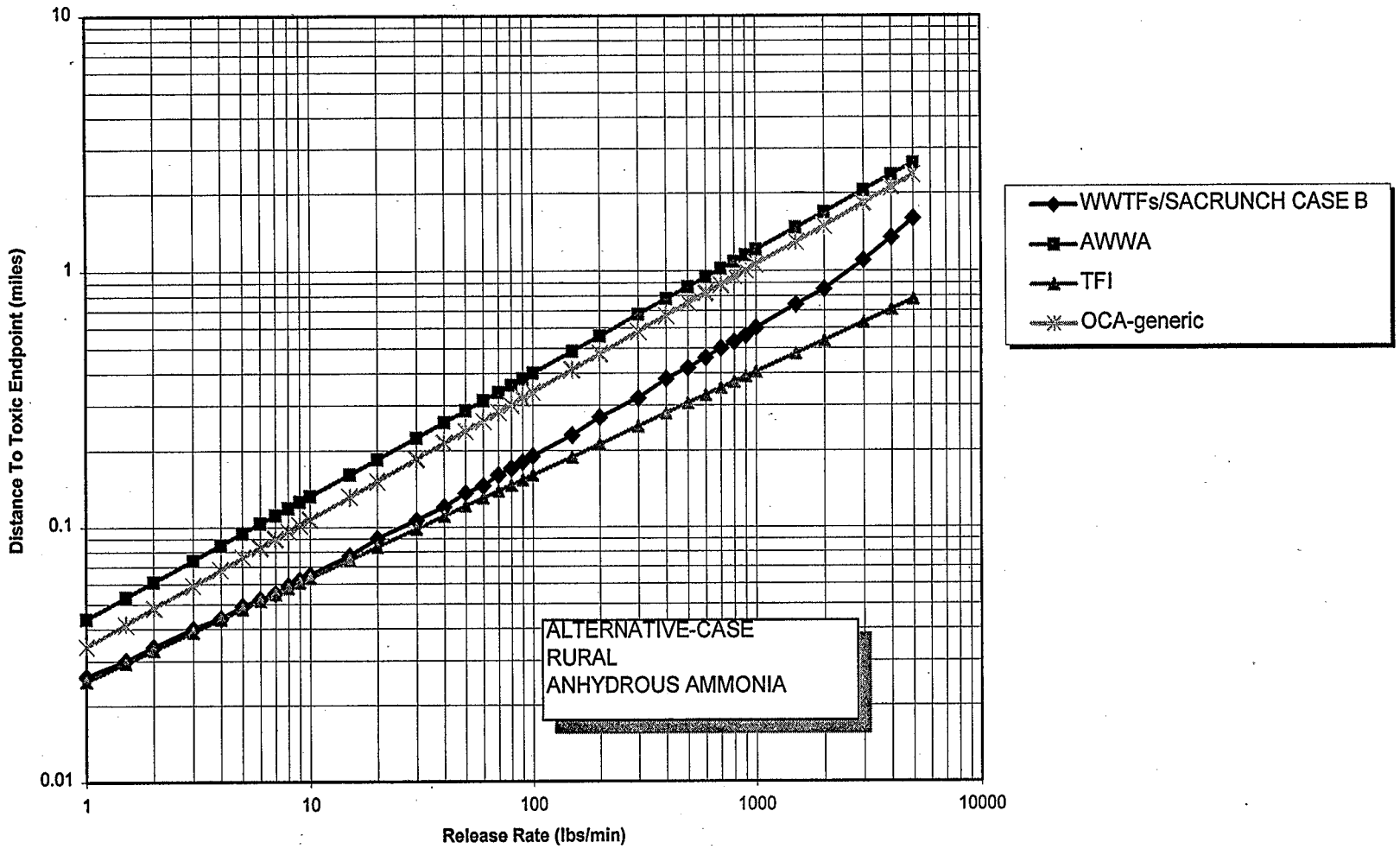

Figure 2-5. Sensitivity Studies for Alternative Anhydrous Ammonia Scenarios Predicted Distances to Toxic Endpoint, Rural Site, Atmospheric Stability Category D, Windspeed 3 m/s

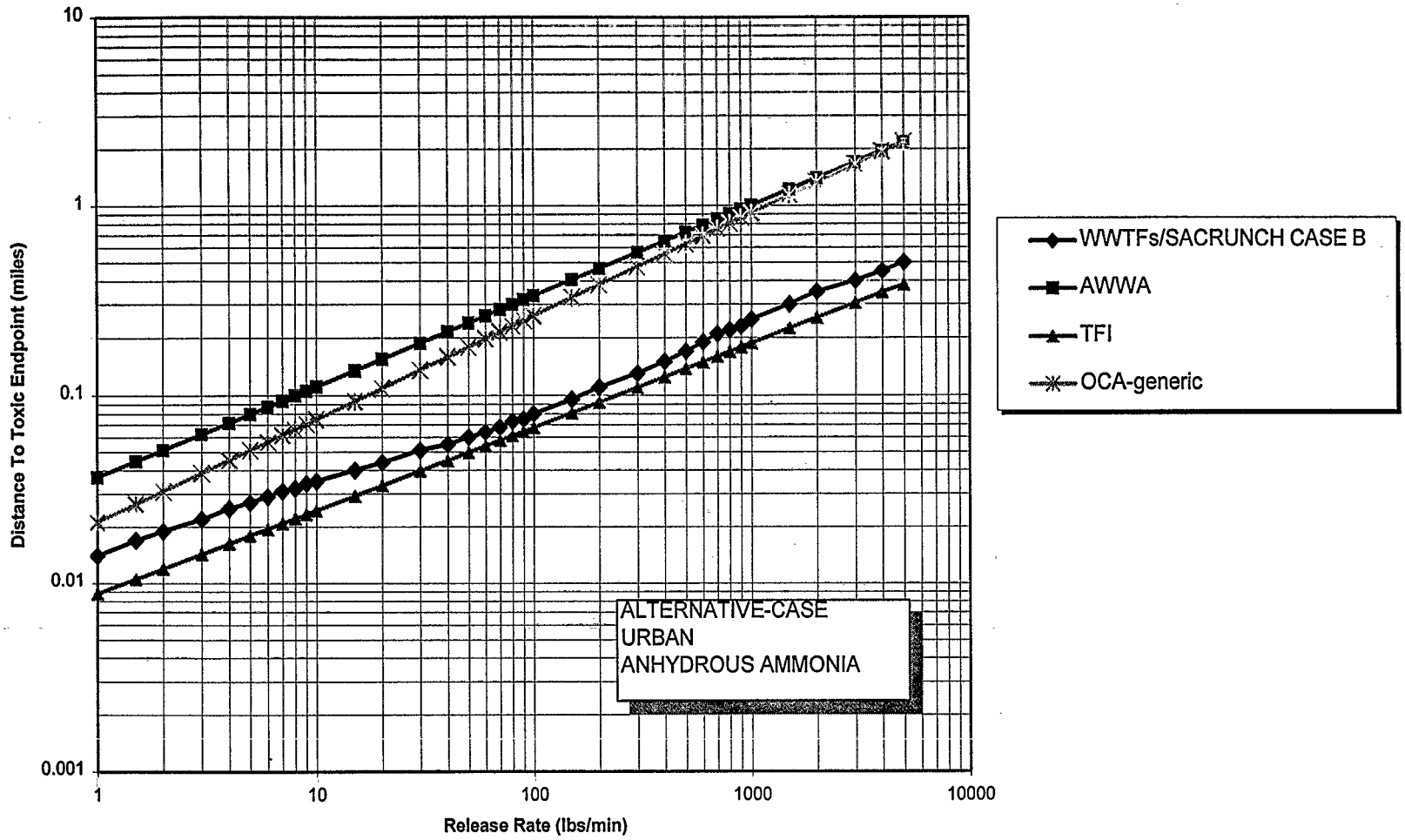

Figure 2-6. Sensitivity Studies for Alternative Anhydrous Ammonia Scenarios Predicted Distances To Toxic Endpoint, Urban Site, Atmospheric Stability Category D, Windspeed 3 m/s

2.2 AQUEOUS AMMONIA

Aqueous ammonia is sometimes found at WWTPs, but not at ammonia refrigeration facilities. In the WWTP guidance, it is assumed that a solution of 30 percent ammonia spills onto the ground: this is conservative for the range of concentrations found at such sites. Both diked and undiked areas are considered. The WWTP guidance contains methods for predicting the rate of evaporation. These methods are taken from the OCAG and are not discussed further here. The discussion that follows concerns how to predict the distance to the toxic endpoint, assuming that the rate of evaporation is known.

The principal difference between aqueous and anhydrous ammonia, in the context of atmospheric dispersion modeling, is that the former evaporates relatively slowly from a pool, entirely as vapor, whereas the latter consists of a mixture of vapor and liquid droplets that is initially denser than air. By contrast, the vapor from a pool of aqueous ammonia is neutrally buoyant, or even marginally lighter than air. Therefore, it is appropriate to use the passive Gaussian dispersion model for a neutrally buoyant plume (which will be somewhat conservative if the plume is buoyant).

Figure 2-7 shows the worst-case SACRUNCH Case B for aqueous ammonia at a rural site, and Figure 2-8 for that at an urban site. Here, the SACRUNCH Case B is the "Green Book" Gaussian model, modified by assuming a dry deposition velocity of 1 cm/s. The other models shown are those proposed by TFI, AWWARF, and OCAG.

In Figure 2-9, the alternative scenario SACRUNCH case for aqueous ammonia is displayed, together with the AWWARF, TFI, and draft OCAG suggestions. Figure 2-10 is a similar plot for an urban site.

2.3 CHLORINE

2.3.1 Worst-Case Scenarios

The results of various sensitivity studies are shown on Figure 2-11 and Table 2-5, taking chlorine with a 150-lb cylinder, a one-ton cylinder, a 17-ton cylinder, and a 90-ton railcar as examples. These are container sizes that are most common at WWTPs.

None of the sensitivity studies on Table 2-5 is the "right" sensitivity study to choose for a "point estimate." The approach adopted here has been to exclude the SACRUNCH conservative case and the OCAG as being too conservative, and then to choose values that are approximately in the middle of the range defined in the various sensitivity studies. This leads to the choice of the SACRUNCH case with 1 cm/s dry deposition velocity as the representative choice for the guidance tables, the same as was the case for anhydrous ammonia (SACRUNCH Case B).

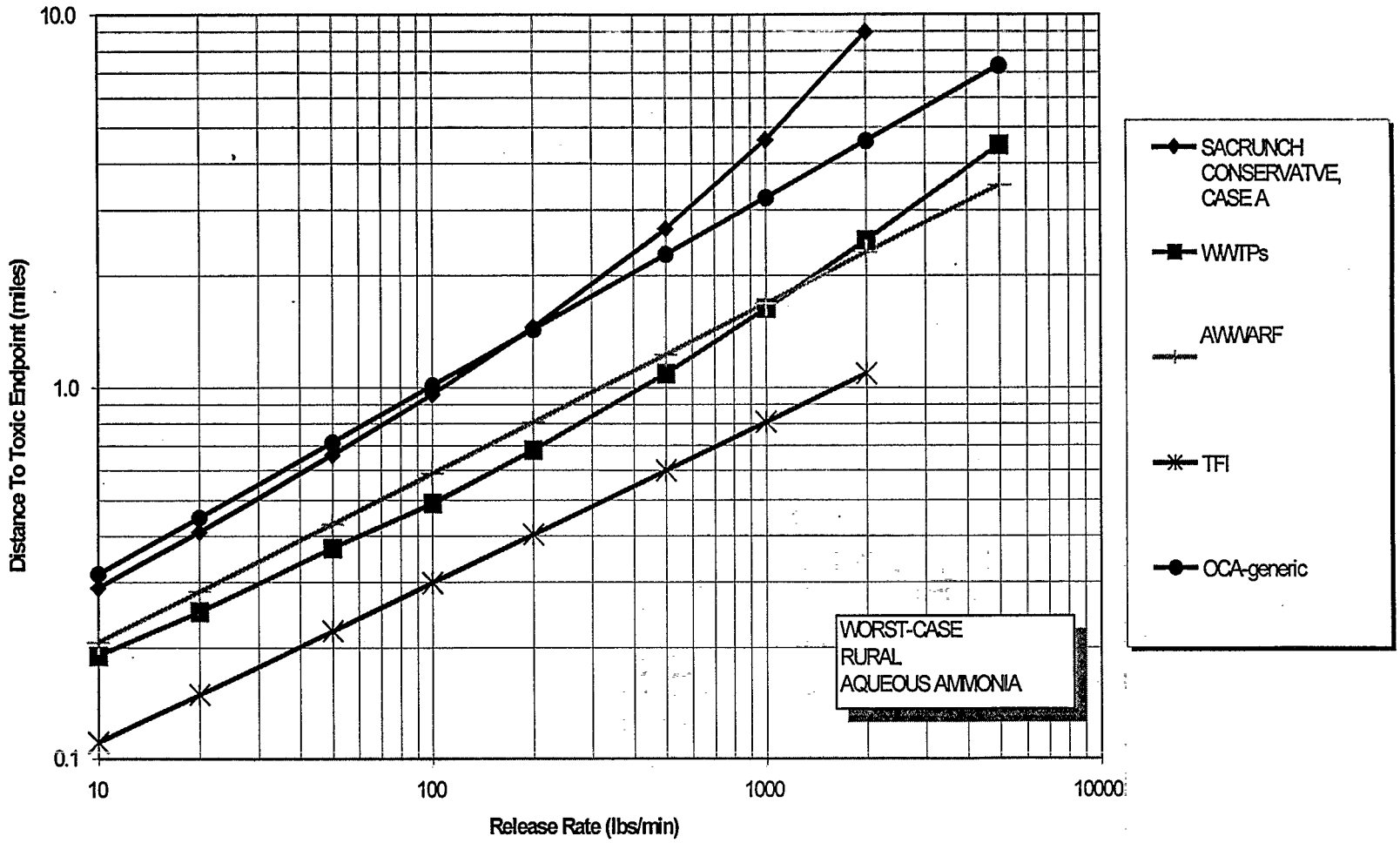

Figure 2-7. Sensitivity Studies for Worst-Case Aqueous Ammonia Scenarios Predicted Distances to Toxic Endpoint, Rural Site, Atmospheric Stability F, Windspeed 1.5 m/s

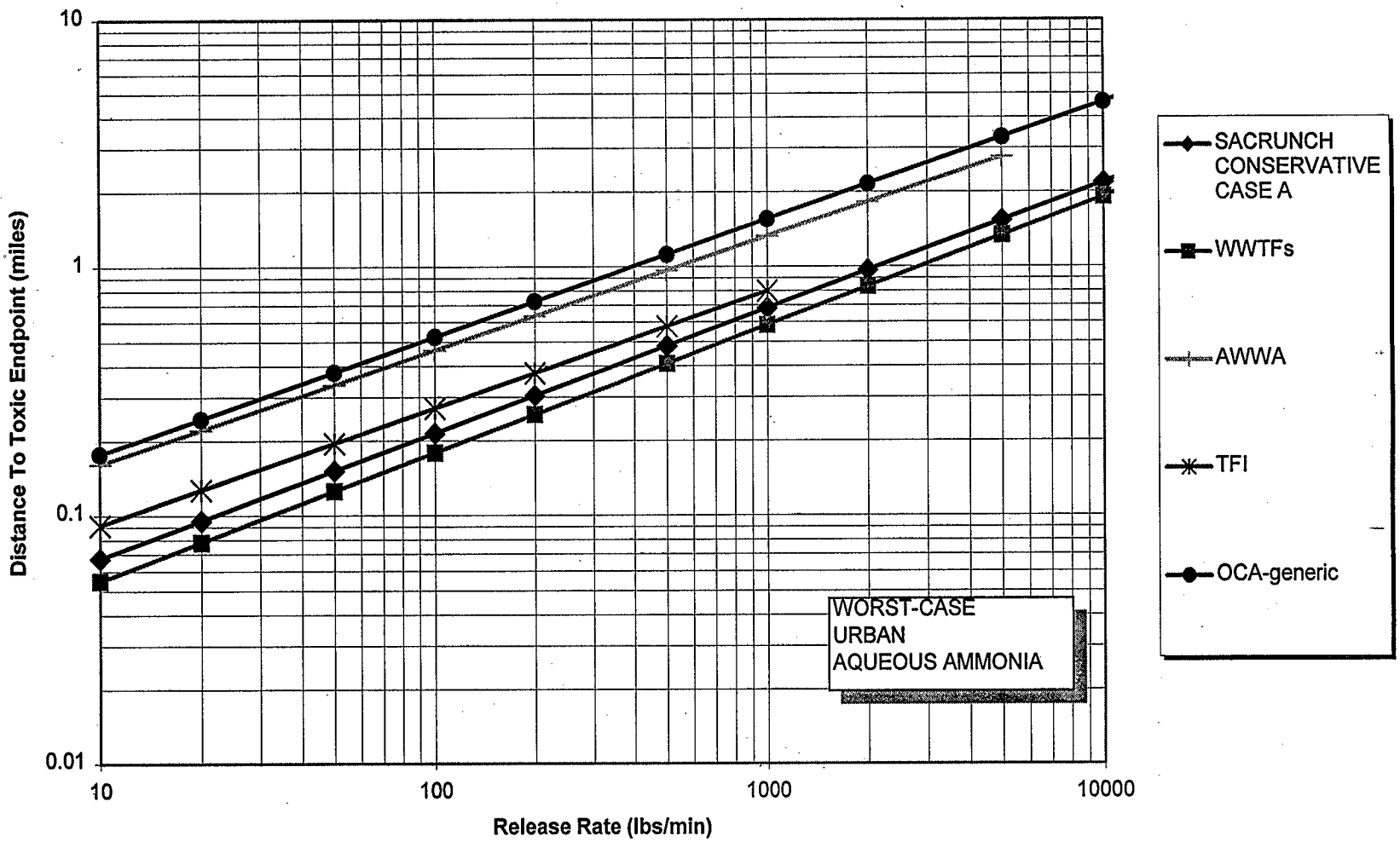

Figure 2-8. Sensitivity Studies For Worst-Case Aqueous Ammonia Scenarios Predicted Distances to Toxic Endpoint, Urban Site, Atmospheric Stability F, Windspeed 1.5 m/s

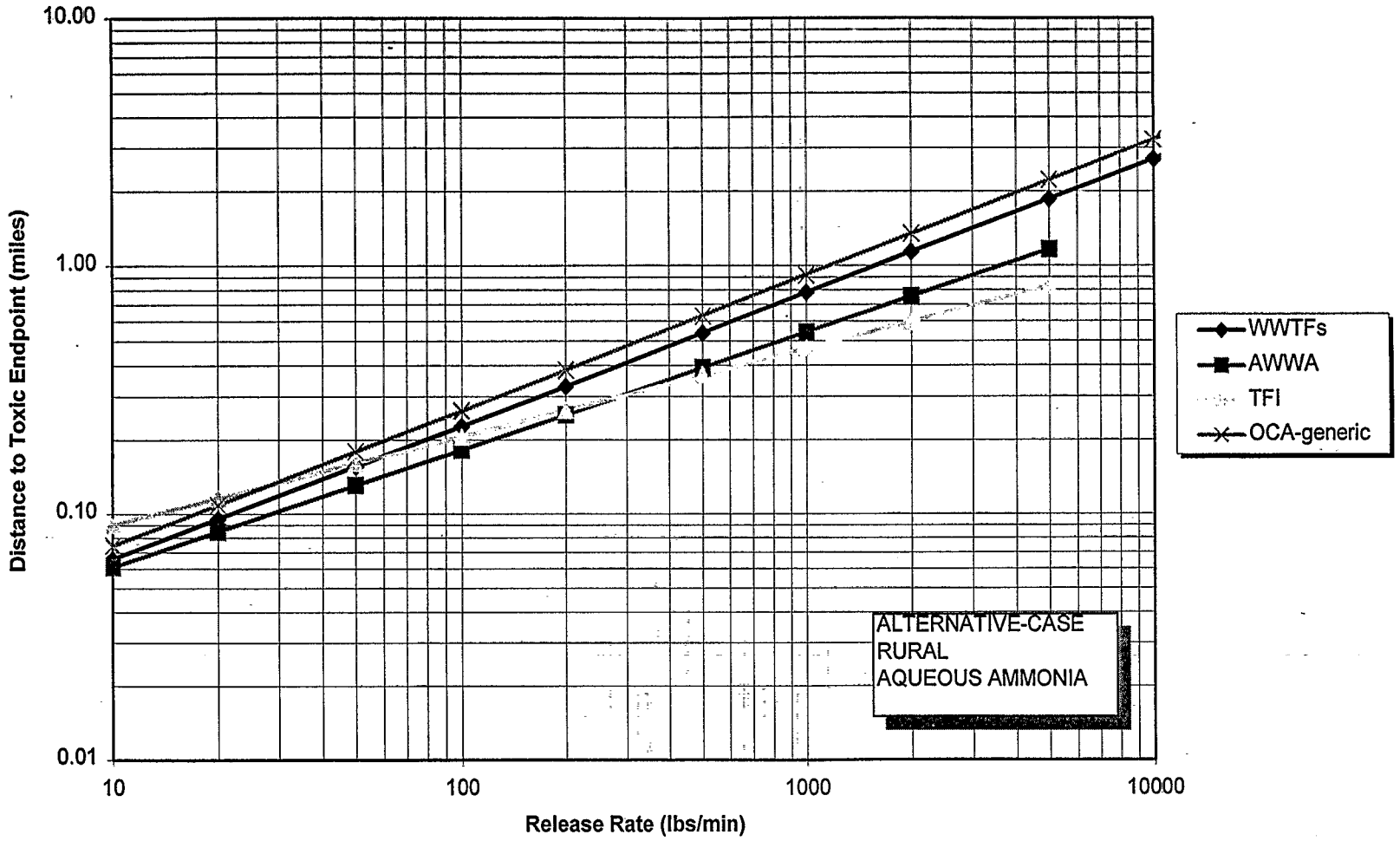

Figure 2-9. Sensitivity Studies for Alternative Aqueous Ammonia Scenarios Predicted Distances to Toxic Endpoint, Rural Site, Atmospheric Stability D, Windspeed 3 m/s

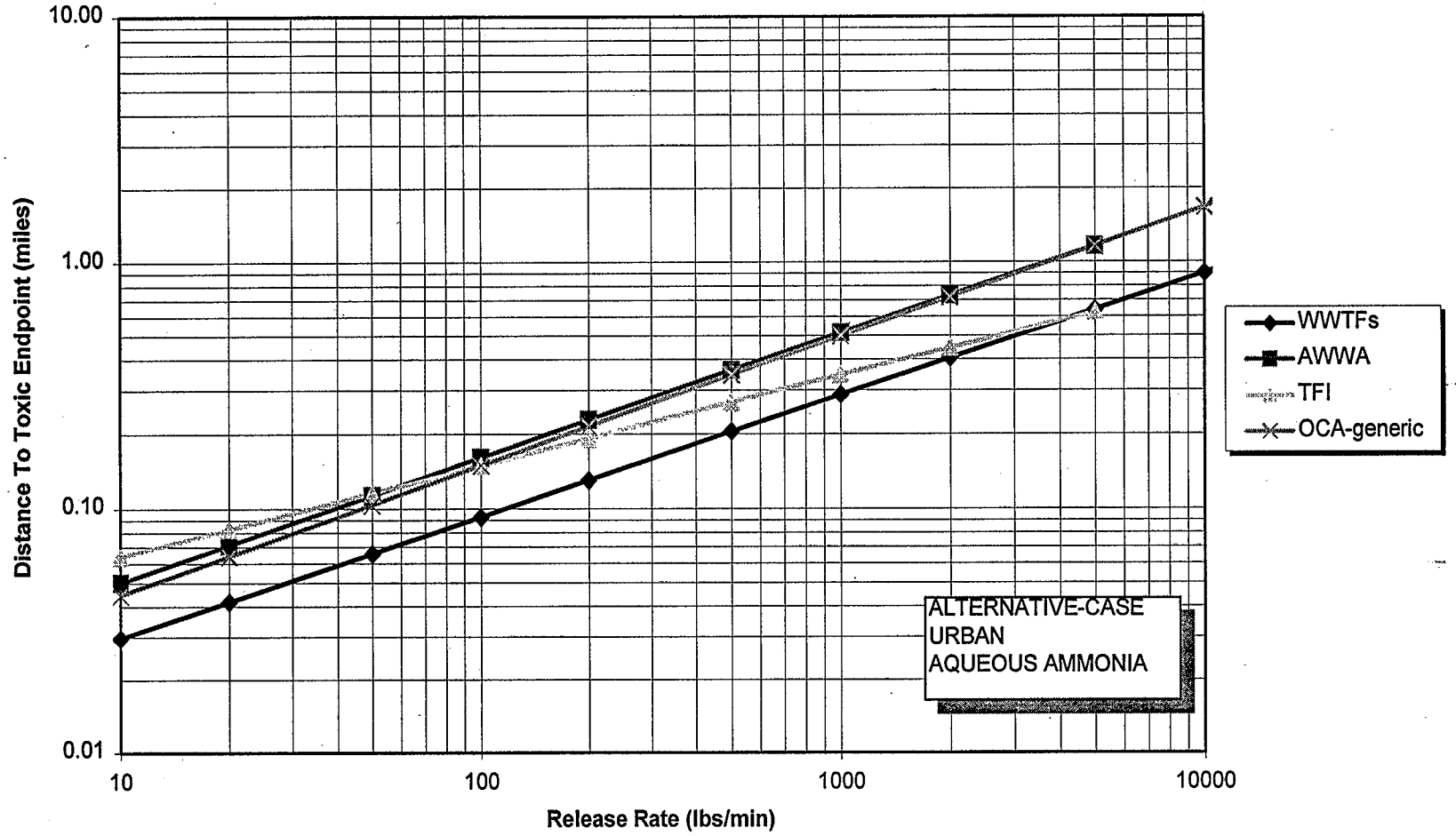

Figure 2-10. Sensitivity Studies for Alternative Aqueous Ammonia Scenarios - Predicted Distances to Toxic Endpoint, Urban Site, Atmospheric Stability Category D, Windspeed 3 m/s

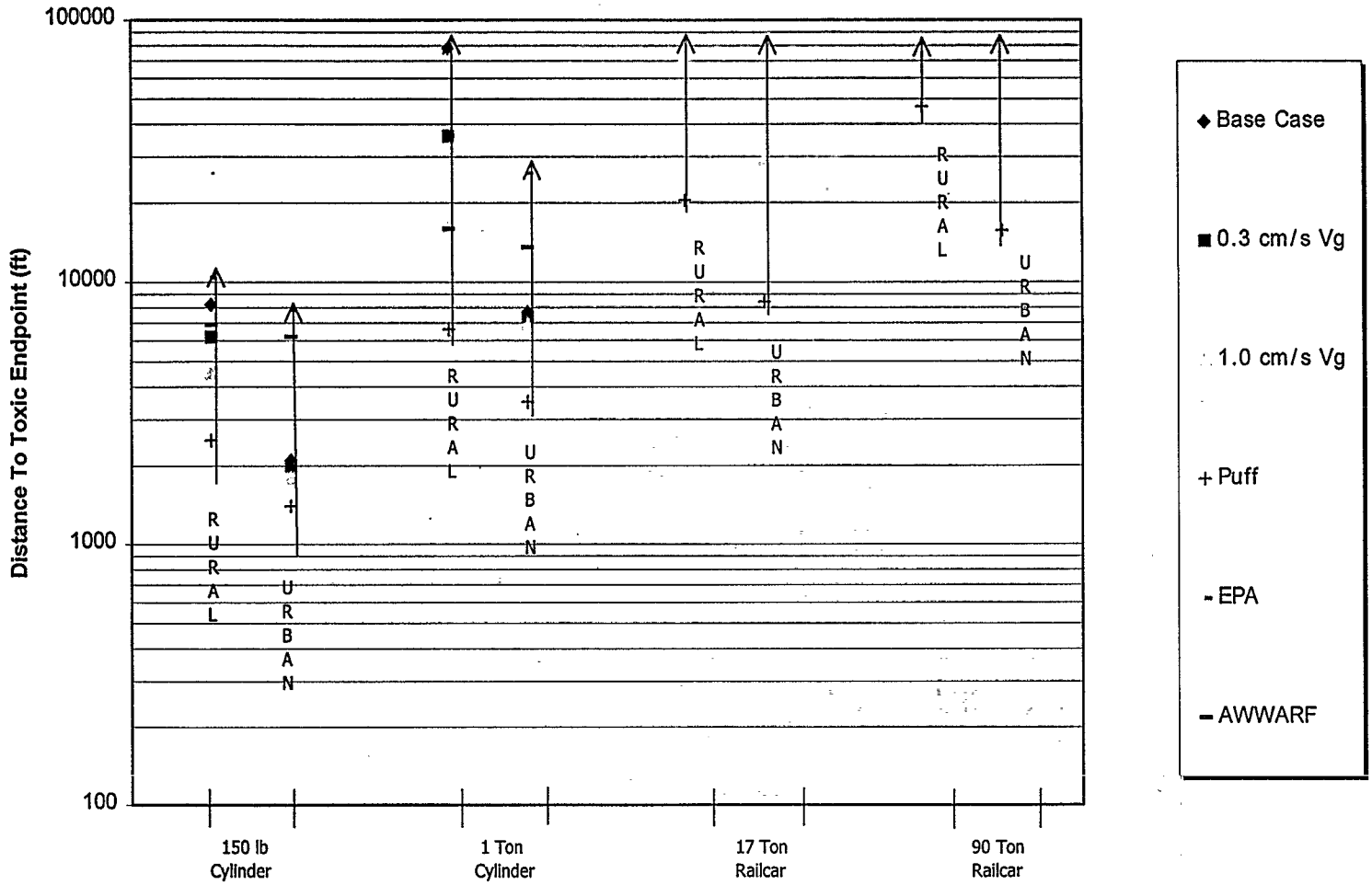

Figure 2-11. Sensitivity Study Predicted Distances To Toxic Endpoint For Chlorine

Table 2-5. Distances to Toxic Endpoint (ft)--Sensitivity Studies for Chlorine

	150-lb Cylinder		1-ton Cylinder		17-ton Tank Car		90-ton Cylinder	
	Rural	Urban	Rural	Urban	Rural	Urban	Rural	Urban
- EPA OCAG[1]	10400	7800	36000	26000	**	**	**	**
▬ AWWARF[2]	6900	6200	16000	13600	> 6 mi	> 6 mi	> 6 mi	> 6 mi
◆ SACRUNCH Conservative Case[3]	8200	2100	78000	7700	**	**	**	**
o 0.3 cm/s v_g[4]	6200	2000	36000	7400	**	**	**	**
Δ 1.0 cm/s v_g[5]	4500	1790	16000	6800	**	29000	**	**
+ Puff[6]	2500	1400	6600	3500	20400	8400	46700	15700

** Not evaluated or beyond limits of model
1. From EPA's 1996 OCAG Guidance
2. From AWWARF Guidance for the Water Industry
3. Conservative Case Run with SACRUNCH Model
4. SACRUNCH with a dry deposition velocity of 0.3 cm/s
5. SACRUNCH with a dry deposition velocity of 1 cm/s
6. Puff Case

Pertinent conclusions and observations are as follows:

- The results of worst-case scenario modeling should not be quoted without a caveat that states the range of uncertainty. As can be seen from Figure 2-11 and Table 2-5, the range of uncertainty is not necessarily the same for each prediction, but a reasonable statement for the predictions made using the methods presented in the WWTP guidance is that the result is uncertain by up to a factor of 2-3 below and a factor of 2-3 above. However, based upon the analysis of uncertainties provided above, it is reasonable to choose a single, point estimate that is towards the middle or lower end rather than the higher end of the range.
- The 17-ton tank truck and 90-ton railcar case illustrates a difficulty with essentially all models that are available for modeling worst-case scenarios at low toxic endpoints like the 3 ppm for chlorine, namely that the predicted distances become increasingly uncertain.

2.3.2 Alternative Scenario

As for ammonia and aqueous ammonia, the WWTP guidance for alternative scenarios for chlorine is simply based upon the SACRUNCH with $v_g = 1$ cm/s case for alternative weather conditions, atmospheric stability category D and windspeed 3 m/s. See Section 2.5.1. for a definition of dry deposition velocity.

2.4 SULFUR DIOXIDE

Once the characteristics of the source term have been determined, vapor clouds formed from flashing liquid chlorine or sulfur dioxide releases should disperse in much the same way (the molecular weights are similar, and the toxic endpoints are the same (3 ppm)). Therefore, the

sulfur dioxide guidance for WWTPs (for both the worst-case and alternative scenarios) has been calculated using the SACRUNCH case with a dry deposition velocity $v_g = 1$ cm/s.

2.5 BACKGROUND DESCRIPTION OF SENSITIVITY STUDIES

As discussed above, the biggest single difficulty encountered when attempting to provide guidance on how to calculate the distance to the toxic endpoint is that there are large uncertainties in the predictions of atmospheric dispersion models. This section contains further background on uncertainties.

2.5.1 Dry Deposition

The toxic gases that are under discussion here — ammonia, chlorine, and sulfur dioxide — are highly reactive. They will interact with vegetation, moisture, and surfaces as they travel downwind. This mechanism depletes the vapor cloud and can effectively reduce predicted downwind distances. This phenomenon is known as dry deposition.

Deposition is often expressed in terms of an empirical deposition velocity (Hanna and Hosker, 1980). The dry deposition velocity is used as follows:

$$CD = v_g CA \tag{2-1}$$

where CD is the rate of deposition of the material onto unit area of the ground, and CA is the airborne concentration immediately above the ground.

Erisman and Draaijers (1995) have published a book titled *Atmospheric Deposition in Relation to Acidification and Eutrophication.* They reviewed more than 30 experiments on the dry deposition of sulfur dioxide and concluded that "In the literature, average values for the deposition velocity range from 0.1 to over 2 cm/s with daytime values usually between 0.8 and 1.2 cm/s. Large values (> 2 cm/s) are observed above water surfaces and forests and relatively small values (< 0.13 cm/s) are measured above snow and bare soil." Therefore, a choice of 0.3 cm/s or 1 cm/s is within the observed range.

Sehmel (1984) has written a chapter on deposition and resuspension in *Atmospheric Sciences and Power Production.* He reports that measured dry deposition velocities for all gases range from 0.002 up to 26 cm/s. He quotes one result for chlorine in the range 1.2 – 2.1 cm/s. Erisman and Draaijers, in the reference cited above, quote a dry deposition velocity of 0.8 cm/s for ammonia, but with a large range of uncertainty that includes 1 cm/s.

In SACRUNCH, the dry deposition model does not start until the plume has evolved out of the heavy vapor phase because very little work has been done on models for dry deposition in the denser-than-air phase. This approach should be conservative when predicting the distance to the toxic endpoint.

2.5.2 Puff Releases

The worst-case release is assumed to occur over a period of 10 minutes. Close to the source, a continuous release model is a good approximation. However, as the vapor cloud travels further downwind, it begins to look more and more as it would if it had been released as a puff. As a puff travels downwind, the action of atmospheric turbulence lengthens it along the wind, as well as causing the width and height to grow. This causes the average concentrations seen by an individual far downwind to be lower than they would be if modeled as a quasi-continuous "slug" that goes by in 10 minutes. Some atmospheric dispersion computer programs, such as DEGADIS, model this transition explicitly. In the present work, a further sensitivity study has been undertaken in which the worst-case contents of a vessel are released as a puff. It shows that the case chosen for use as guidance has an element of conservatism to it.

2.5.3 Qualitative Uncertainties and Conservatisms

There are a number of other uncertainties that have not been explicitly modeled in this chapter, but which add strength to the proposition that many atmospheric dispersion models have considerable conservatisms built into them.

2.5.3.1 Duration of Worst-Case Weather Conditions

For the very largest releases (e.g., chlorine from a 90-ton railcar), almost all available models predict very large worst-case distances, usually 25 miles or more. However, traveling at 1.5 m/s, a plume would take ~ 7 hours to travel 25 miles. It is unlikely that atmospheric stability category F weather conditions with a windspeed of 1.5 m/s will persist for this long. Before the vapor cloud has traveled anything like 25 miles, the weather is likely to change to a condition that will cause more rapid dilution.

2.5.3.2 Pooling

In very low windspeeds, heavy vapor clouds often "pool" on the ground (this is not the same as a liquid pool). This was explicitly demonstrated in the early heavy vapor experiments at Porton Down (Picknett, 1978), consisting of puff releases of freon-12, which, at low windspeeds, slumped until they were only a few inches deep and then remained on site, barely moving. This might well happen to some or all of the vapor clouds in worst-case conditions.

2.5.3.3 Time Varying Toxic Endpoints

The toxic endpoint established by the rule is valid for an exposure time of one hour, but used even if the duration of exposure is much less than one hour, as it would be for a worst-case gas release that takes place in 10 minutes. As a general rule, for a given health effect, an individual can withstand higher concentrations at smaller exposure times. Consequently, using a 60-minute endpoint adds to the conservatism of the predictions.

EPA has begun the process of developing concentrations that will have different toxic endpoints for various exposure times. These alternatives are known as Acute Exposure Guideline Levels (AEGLs) for Hazardous Substances. Proposed AEGLs for 12 chemicals have been published in the *Federal Register* (62 FR 58839-58851, October 30, 1997) (notice

published by the National Advisory Committee for Acute Exposure Guideline Levels for Hazardous Substances). The 12 chemicals are 1,1-dimethylhydrazine; methylhydrazine; aniline; ethylene oxide; hydrazine; 1,2-dichloroethene; 1,2-dimethylhydrazine; nitric acid; fluorine, chlorine, arsine; and phosphine. The only one of these relevant to the present work is chlorine.

For chlorine, the proposed AEGL-1 is 1 ppm for a one-hour exposure (the same as ERPG-1); the proposed AEGL-2 is 2 ppm (just below the toxic endpoint [ERPG-2] of 3 ppm); and the proposed AEGL-3 is 20 ppm (the same as the ERPG-3). Thus, AEGLs and ERPGs are roughly equivalent. To incorporate exposure-time dependence, the National Advisory Committee for AEGLs states that

$$C^2t = k \tag{2-2}$$

where k is a constant that has different values for AEGL-1, AEGL-2, and AEGL-3, C is the average airborne concentration and t is the exposure time. For AEGL-1, $C^2t = 60$ ppm^2-min; for AEGL-2, $C^2t = 240$ ppm^2-min; and for AEGL-3, $C^2t = 24{,}000$ ppm^2-min. Focusing on the AEGL-2 as being closest to the EPA's toxic endpoint, C for chlorine is 2 ppm for t = 1 hour (as noted above), 2.8 ppm for t = 30 minutes and 4.9 ppm for t = 10 minutes.

It is also pertinent to address the question of whether Haber's law applies to substances such as chlorine, sulfur dioxide, and ammonia. Gephardt and Moses (1989) looked at published literature and focused on the effects of airborne concentrations of 3-20 ppm of chlorine over a duration of exposure of 1 hour (i.e., concentrations in the ERPG-2 to ERPG-3 range). They concluded that Haber's law is valid as an extrapolation of the 3 ppm/1 hour exposure (i.e., the ERPG-2) with Ct = 180 ppm-min.

Gephardt and Moses expressed the caveat that Ct = k is not expected to apply for C > 100 ppm, where different types of more severe health effects begin to occur. For ERPG-2, C = 100 ppm corresponds to an exposure time of less than 2 minutes. For t = 10 min, C = 18 ppm and for t = 30 min, C = 6 ppm.

Gephardt and Moses also consider ammonia, for which the Haber's law constant k for the ERPG-2 is Ct = (200)(60) = 12,000 ppm-min, provided that C < 5,000 ppm (equivalent to t < 2.4 min.)

2.5.4 Conclusion–Sensitivity Studies

The qualitative sensitivities discussed above would reduce the predicted distances to the toxic endpoint, if they were analyzed quantitatively. This gives added confidence that the choice of guidance for AR and WWTPs still contains some elements of conservatism.

CHAPTER 3: GASES LIQUEFIED UNDER PRESSURE

The purpose of this chapter is to discuss how the phenomenon of aerosolization from liquid chlorine, sulfur dioxide, or anhydrous ammonia releases is handled in the AR and WWTP guidance documents.

Chlorine, sulfur dioxide, and anhydrous ammonia in WWTPs and anhydrous ammonia in such vessels as the high-pressure receiver in ammonia refrigeration facilities are kept liquefied under pressure. If the pressure and temperature are sufficiently high, if there is a sudden liquid release of one of these materials, and if there are no obstructions, it will all become and remain airborne as a mixture of vapor and very fine liquid droplets that do not fall to the ground. Experimental results clearly show that this is a real physical phenomenon (Goldwire et al., 1985; Kaiser, 1989). The airborne droplets evaporate quickly as air is entrained. The evaporation process cools the air so that a cold mixture of air and vapor is formed. The mixture is denser than air, even in the case of ammonia, and a heavy vapor dispersion model is required to adequately predict airborne concentrations downwind of the point of release.

Figure 3-1 shows the results of some experiments that were carried out on liquid chlorine and reported by Johnson (1991). Similar experiments were not performed for ammonia, but ammonia results should look similar because chlorine and ammonia have similar density ratios of liquid to vapor and have similar atmospheric boiling points. It is also a reasonable assumption that sulfur dioxide will exhibit the same type of behavior.

Figure 3-1 shows the percentage of liquid chlorine that falls to the ground as a function of superheat, which is the difference between the temperature of the chlorine initially in the vessel and its atmospheric pressure. Figure 3-1 also shows for comparison the results of the Dow Model (Dow, 1993), which predicts that the fraction of airborne liquid droplets is five times the vapor flash fraction (the fraction of chlorine that immediately vaporizes as it is released to the atmosphere). As can be seen, the Dow Model appears to be non-conservative (i.e., it predicts that too much chlorine falls back to the ground).

Figure 3-1 also shows the results of a model (Ianello 1989), known as the "RELEASE" model, that was used by Johnson (1991) to try to reproduce the experimental results. As can be seen, agreement is poor[3]. Other models that take into account this evaporation lead to better agreement with experiments (e.g., Woodward and Papadourakis, 1991; Woodward et al., 1995).

The principal conclusion is that, even at superheats of only 10 °C (which would be a temperature of only about -23 °C for ammonia and chlorine and about 0 ° C for sulfur dioxide), only a small fraction of released liquid would fall to the ground. Therefore, at most, a small degree of conservatism is introduced if it is assumed that, for superheats exceeding 10 °C, all of the released chlorine, sulfur dioxide, or ammonia remains airborne as a mixture of vapor and fine liquid droplets.

[3] CCPS has been funding further development of the RELEASE model. A private communication from Johnson, D.J., Quest Consultants, Norman Oklahoma (October 1997) indicates that RELEASE has been modified so that agreement with experiment is much improved. However, at the time of writing, RELEASE was not available to the authors.

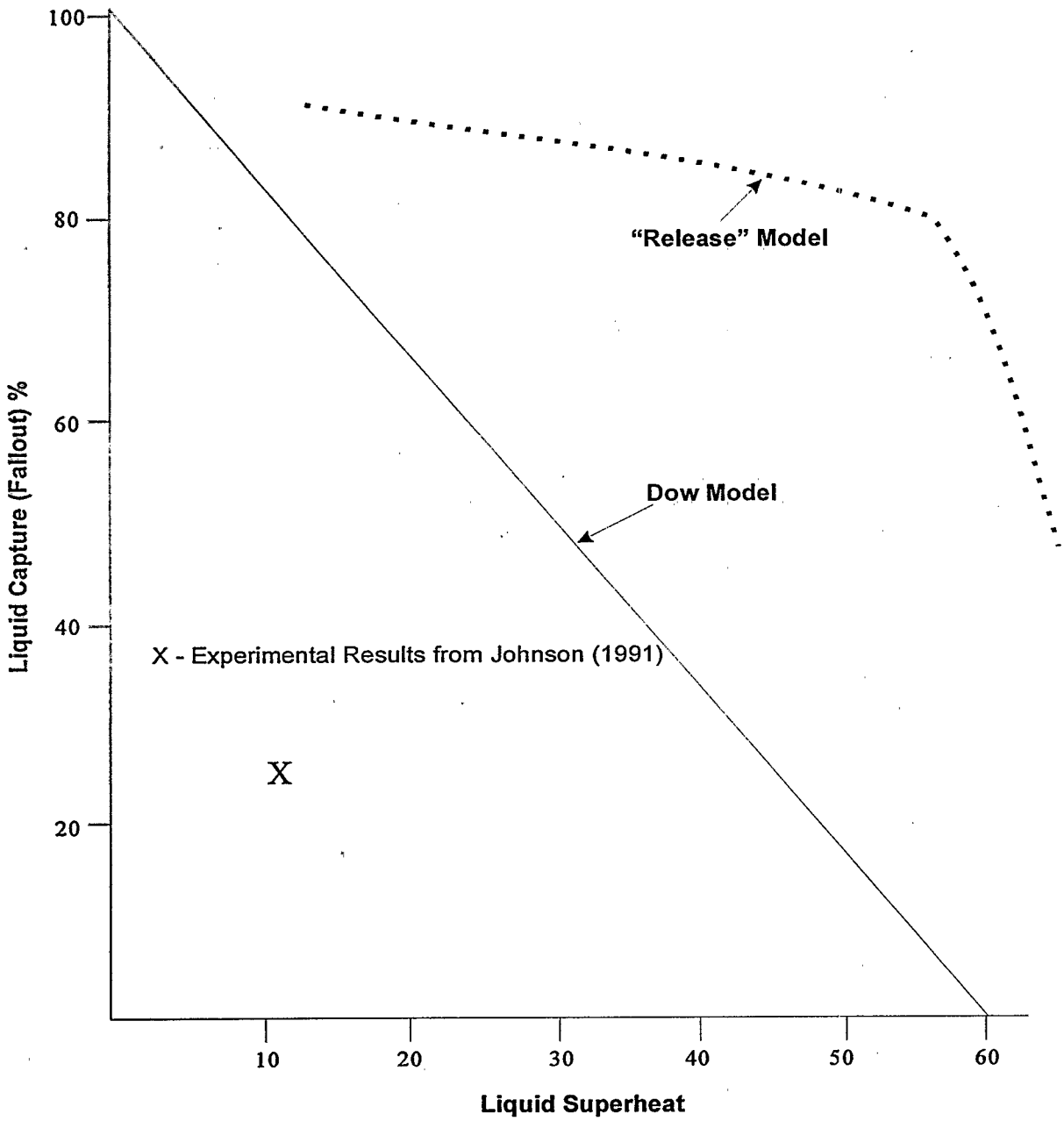

Figure 3-1. Fraction of Liquid Chlorine Falling to the Ground as a Function of Superheat

If a jet of liquid droplets and vapor impinges upon a surface close to the point of release, there can be efficient recovery of droplets, which will form a relatively slowly evaporating pool on the ground. Experiments with ammonia have shown that up to 75 percent of the airborne droplets can be removed in this way (Resplandy, 1969: Kaiser, 1989). For worst-case scenario modeling, the use of this or similar reduction factors is probably not justified if it is possible that the release would not encounter obstructions. However, when considering mitigation, this phenomenon can be taken into account. For example, if vessels are indoors, there will almost certainly be a surface upon which the jet will impinge and the jet will likely change direction (e.g., impingement of the floor and subsequent upward movement of the vapor cloud). This arrangement is similar to the design of separators in chemical processes and would be expected to be very efficient at removing liquid droplets from the vapor stream. This issue is further discussed in Chapter 6. For the purposes of discussing the effects of obstacles, it is assumed that obstacles cause the recovery of 75 percent of any airborne liquid droplets. Thus, if the initial airborne release consists of 20 percent vapor and 80 percent liquid droplets, an obstacle-impeded release would consist of the original 20 percent vapor plus 20 percent liquid droplets (i.e., a mixture split equally between vapor and liquid and containing only 40 percent of the mass in an unobstructed release).

The above amounts only to a rule of thumb. In fact, the percent capture of the liquid depends on several factors, among which is the path length of the jet before it encounters an obstruction. A model that shows this effect explicitly has been developed by Muralidhar et al. (1995). This model was specifically developed for escaping jets of a mixture of hydrogen fluoride and a proprietary additive. The mixture is being used as a catalyst in the alkylation unit at Mobil's Torrance, CA, refinery. However, the general picture is applicable to all jet releases that consist of a mixture of fine droplets and vapor. The droplets present a very large surface area for evaporation; as long as they remain airborne, they evaporate rapidly. On encountering an obstacle, they run down to form a pool on the ground, which has a much smaller surface area to volume ratio, so the rate of evaporation is much decreased. Some typical results show that the airborne reduction factor (essentially the percentage of hydrogen fluoride that ends up on the ground) is 50-70 percent for a 40' travel distance, 75-85 percent for a 5' travel distance, and ~ 90 percent for a 3" travel distance.

These figures cannot be directly applied to ammonia, chlorine, or sulfur dioxide, but illustrate the general idea. They show that the percentage collecting on the floor (or the percentage of the original release remaining airborne) is going to be highly configuration dependent. However, compressor rooms in ammonia refrigeration facilities and chlorine or sulfur dioxide rooms in WWTPs are often highly crowded.

The rule-of-thumb presented above, that 60 percent of the initial flashing liquid release of ammonia, chlorine, or sulfur dioxide ends up on the floor as a slowly evaporating pool, is, therefore, offered as a simple means of taking some advantage of the presence of obstructions in buildings. This number is highly uncertain, but it is not possible to produce configuration-specific guidance that is also simple to use.

CHAPTER 4: ADJUSTMENT OF MEAN CONCENTRATION FOR AVERAGING TIME

The work in this section is based on a monograph by D.J. Wilson (1995), *Concentration Fluctuations and Averaging Time in Vapor Clouds*, that contains the most comprehensive existing summary of the theories and experimental data relating to the subject of the effect of averaging time on mean concentrations.

This issue is easily illustrated in the context of the Gaussian model, in which the cloud centerline concentration C is inversely proportional to the crosswind standard deviation σ_y:

$$C \propto 1/\sigma_y \tag{4-1}$$

There is a widely used relationship for the dependence of σ_y on averaging time t_a:

$$\sigma_y \propto (t_a)^p \tag{4-2}$$

There are few direct measurements of the exponent p. Wilson documents experiments by Yersel, Gobel, and Morrill (1983) in which the value of p close to the source varied from 0.0 to 0.18. Studying releases from a high stack, Mueller and Reisinger (1986) found far downwind (25 km) an average p = 0.25, with at least a factor of two variability in p from one test to another.

Wilson has proposed a more realistic estimate of averaging time effects on plume spread using a power law model that accounts for initial source size and plume travel time on averaging time effects. Basically, a wide plume (with large σ_y) meanders less than does a narrow plume because meandering is caused by turbulent eddies that are larger than the plume, and there are a wider range of turbulent atmospheric eddies to push the smaller plume around. Wilson's recommended working equation is, for an atmospheric sampling time t_s equal to the mean concentration averaging time t_a,

$$\frac{\sigma_y}{\sigma_{y,ref}} = \left(\frac{1.5\left(\frac{\sigma_o}{\sigma_{y,t_s=\infty}}\right)^2 + \frac{t_t}{T_{Lv}} + r_1 \frac{t_s}{T_{Lv}}}{1.5\left(\frac{\sigma_0}{\sigma_{y,t_s=\infty}}\right)^2 + \frac{t_t}{T_{Lv}} + r_1 \frac{t_{s,ref}}{T_{Lv}}} \right)^{0.5} \tag{4-3}$$

where $\sigma_{y,ref}$ is the plume spread for a short sampling time, typically - $t_{s,ref}$ = 180s. As an approximation in the source size σ_o term, use $\sigma_{y,ts=\infty} \approx 2\ \sigma_{y,ref}$ to estimate the long-sampling-time plume spread. Equation 4-3 was derived for stationary processes and should be limited to sampling times less than about 3 hours in the atmosphere. The parameter r_l is given by

$$r_l = \frac{1}{2\left(1 + 0.6\frac{t_t}{T_{Lv}} + 0.3\frac{t_s}{T_{Lv}}\right)} \tag{4-4}$$

The power law in Equation 4-3, with atmospheric sampling time t_s equal to the averaging time t_a is more physically realistic than the purely empirical one-parameter Equation 4-2. The major difficulty applying this power law is estimating the Lagrangian turbulent time scale T_{Lv}. Here, a value of T_{Lv} = 10,000 seconds is recommended, based on plume dispersion data for long travel times (Barr and Gifford (1987)).

Surprisingly, considering the importance of averaging time effects, there is a lack of available data with statistically independent measurements of plume spread σ_y needed to validate (4-3). The only data used by Wilson for validation are from Briggs (1993) for plume spread measurements in unstable atmospheric conditions. Equation 4-3 gave a plausible fit to this data, but there was so much scatter that other functional forms would have done equally well.

It has been conventional wisdom in models for dense gas dispersion that the strong density gradients across the top of a dense plume reduce its entrainment and suppress both meandering and vertical mixing inhomogeneities that produce concentration fluctuations. To refute this claim, Hanna, Chang, and Strimaitis (1993), in a review of hazard assessment models, showed that large one-second averaged concentration fluctuations were present in the repeat realizations of various dense vapor field test experiments. In fact, it is apparent that fluctuations caused by inhomogeneous mixing, *excluding* meandering, are as strong in dense plumes as they are in neutrally buoyant releases.

In addition, dense plumes should also experience crosswind meandering, because they entrain atmospheric air with crosswind velocity fluctuations. These crosswind fluctuations should not be much affected by the density gradient that suppresses the vertical turbulence fluctuations and effectively reduces the rate of entrainment of air across the top surface of the vapor cloud (see Britter (1989)). Once the dense plume has been diluted by about a factor of five, it is mostly ambient air and should meander in much the same way as a passive plume.

One important obstacle to applying meandering plume models to dense releases is the substantial difference in shape of crosswind velocity profiles between a dense plume and a passive plume. Gravity-driven spreading produces a wider, more uniform concentration across the center of a dense plume, as shown in Figure 4-1.

Crosswind meandering simply flips this relatively uniform core back and forth across the centerline, causing considerably smaller fluctuations in the center and considerably more near the edges than would be caused by a Gaussian profile plume, shown superimposed on the dense plume developed. More work is needed in this area before an operational model can be recommended.

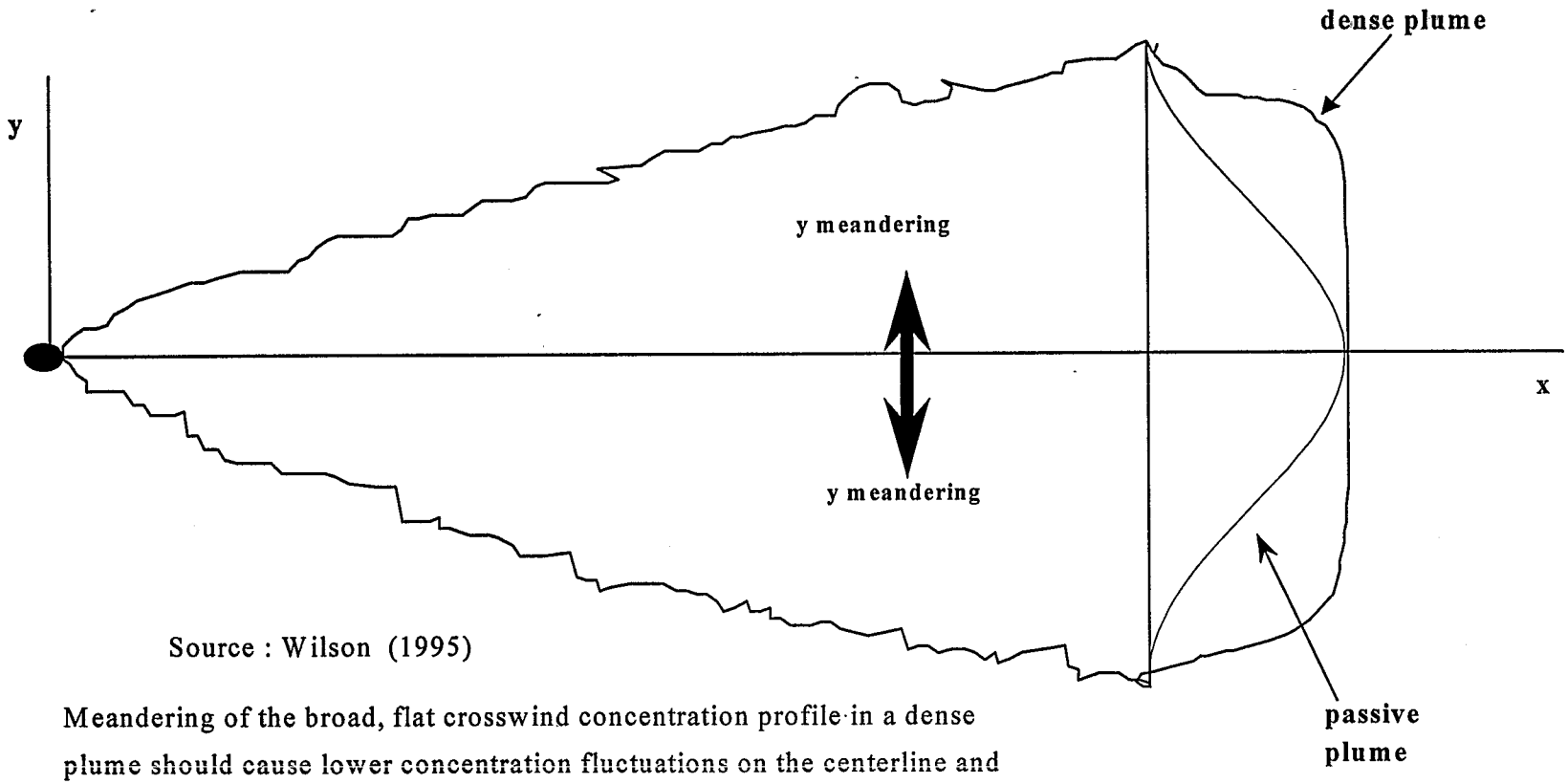

Source : Wilson (1995)

Meandering of the broad, flat crosswind concentration profile in a dense plume should cause lower concentration fluctuations on the centerline and higher fluctuations near the edges than observed in a passive plume.

Figure 4-1. Illustration of Meandering

Tables 4-1 and 4-2 show how the implementation of Wilson's meandering model affects predicted distances to the toxic endpoint for worst-case anhydrous ammonia releases. An exposure duration of 10 minutes has been assumed. In addition, to take account the lack of a good meandering model for dense plumes, the meandering effect is not allowed to start until the plume has essentially become neutrally buoyant, at which point σ_o is determined from the half-width L of the plume at the transition point:

$$\sigma_o = L/2.14 \tag{4-5}$$

That is, at the transition to neutral buoyancy, the plume becomes Gaussian with the 10 percent edge at a crosswind distance L from the centerline.

It can be seen that the distances are not much affected (the influence of meandering would be considerably larger for durations of exposure of an hour or more). The SACRUNCH Case B that was chosen as the guidance nevertheless contains the Wilson meandering correction.

The predicted effect of meandering is smaller for chlorine and sulfur dioxide than it is for ammonia, given the same rate of release. This is because the toxic endpoints of chlorine and sulfur dioxide are much smaller than for ammonia (3 ppm vs 200 ppm). Therefore, a chlorine or sulfur dioxide plume has to travel much further to the toxic endpoint than does an ammonia plume. Equation 4-3 shows that the ratio $\sigma_y/\sigma_{y,ref}$ tends to unity for very large travel times.

Table 4-1. Example of Effect of Meandering of Anhydrous Ammonia Releases, Worst-Case, Rural Conditions

Rate of Release (lbs/min)	Distance to Toxic Endpoint (miles)	
	"Old" Model	With Wilson Meandering
10	0.19	0.19
20	0.27	0.26
50	0.41	0.40
100	0.57	0.56
200	0.80	0.78
500	1.28	1.26
1,000	1.85	1.82
2,000	2.72	2.68
5,000	4.59	4.54
10,000	6.74	6.69
20,000	9.59	9.55
50,000	14.27	14.23

Table 4-2. Example of Effect of Meandering of Anhydrous Ammonia Releases, Worst-Case Urban Conditions

Rate of Release (lbs/min)	Distance to Toxic Endpoint (miles)	
	"Old" Model	With Wilson Meandering
10	0.10	0.10
20	0.14	0.13
50	0.21	0.20
100	0.28	0.28
200	0.39	0.39
500	0.61	0.60
1,000	0.84	0.83
2,000	1.18	1.17
5,000	1.86	1.84
10,000	2.64	2.62
20,000	3.89	3.83

CHAPTER 5: AMMONIA/MOIST-AIR THERMODYNAMICS

A rigorous consideration of ammonia/moist air thermodynamics will have some effect on predicted distances to the toxic endpoint. In this chapter, the basic thermodynamic model is described in Section 5.1, and the effect on predicted distances to the toxic endpoint is discussed in Section 5.2.

A related issue is that of potential lift-off of the plume. A flashing liquid release of ammonia is initially denser than air, but could potentially become buoyant as it travels downwind and entrains air. This issue is addressed in Section 5.3.

5.1 CALCULATION OF THERMODYNAMIC PROPERTIES OF MIXTURES OF AMMONIA AND AIR

A quantity of material released into the atmosphere entrains air both during the release process and the atmospheric transport process. In the case of ammonia, the release may involve pure vapor or a mixture of vapor and liquid, and considerable turbulence is generated in the release process as ammonia storage pressures are usually well above atmospheric pressure. Estimation of cloud concentration, position, velocity, and dimensions during atmospheric transport involves consideration of a variety of physical processes, including rate of entrainment of air, gravitational slumping, transfer of heat from the atmosphere and the ground, and fall-out of entrained aerosols. Performance of these calculations is facilitated by independent analysis of the changes in thermodynamic properties that occur when ammonia is mixed with air containing water vapor. This chapter discusses calculation of the temperature, density, quantities, and compositions of vapor and liquid phases comprising a cloud formed by mixing known quantities of ammonia and moist air. In all cases, the total pressure is one atmosphere, and both the initial clouds and the final cloud are at thermodynamic equilibrium.

5.1.1 Methods

The equilibrium state of a mixture of known quantities of ammonia, air, and water is completely determined by specification of two independent variables. If the number of independent intensive variables[4] determined by Gibb's phase rule[5] is greater than two, specification of temperature and pressure determines the state of the system, including composition and quantities of vapor and liquid phases. If the number of intensive variables determined by Gibb's phase rule is less than two, specification of pressure and relative quantities of vapor and liquid phases determines the state of the system for the cases considered in this analysis. Given specification of the properties of the initial ammonia cloud and the initial moist air cloud, the conditions of the final cloud may be calculated using vapor/liquid equilibrium relationships and mass and energy balances. The following sections describe physical property

[4]An intensive variable is a property of a system that does not depend on the quantity of material comprising the system. Temperature and pressure are examples of intensive variables.

[5]Gibbs's Phase Rule determines the minimum number of independent variables that must be specified to uniquely establish the intensive state of a system at equilibrium comprising given numbers of components and phases.

data and the algorithm combining mass and energy balances with vapor/liquid equilibrium relationships to determine the final cloud conditions.

5.1.1.1 Physical Property Data

Physical property data required to calculate the state of a system includes pressure/volume/temperature (PVT) relationships, vapor/liquid equilibrium data, and enthalpy data. Because the mixing process occurs at atmospheric pressure, the ideal gas law was used to represent PVT behavior for vapor phases. For liquid phases, densities were taken to be constant at a value of 690 kg/m^3 for ammonia and 1,000 kg/m^3 for water.

The vapor pressure exerted by ammonia/water systems depends on temperature and the composition of the liquid phase. Correlations proposed to represent this dependence (Wheatley, 1987) are:

$$P_1(X_2,T) = (1-X_2)\, P_{s,1}(T)\, \mathrm{EXP}\, [-A_1/T + B_1] \tag{5-1}$$

and

$$P_2(X_2,T) = X_2\, P_{s,2}(T)\, \mathrm{EXP}\, (-A_2/T + B_2) \tag{5-2}$$

where:

$P_1(X_2,T)$	=	partial pressure of water (component 1) as a function of temperature and liquid phase composition, Pa
X_2	=	mole fraction of ammonia (component 2) in the liquid phase
T	=	temperature, K
$P_{s,1}(T)$	=	partial pressure of pure water as a function of temperature, Pa
$P_2(X_2,T)$	=	partial pressure of ammonia as a function of temperature and liquid phase composition, Pa
$P_{s,2}(T)$	=	partial pressure of pure ammonia as a function of temperature, Pa

and A_1, B_1, A_2, and B_2 are estimated as:

$$A_1 = (1 + 3R_a/2 - R_aX_2)\, X_2^2\, W_a \tag{5-3}$$

$$A_2 = (1 + R_a - R_aX_2)\, (1-X_2)^2\, W_a \tag{5-4}$$

$$B_1 = (1 + 3R_b/2 - R_bX_2)\, X_2^2\, W_b \tag{5-5}$$

$$B_2 = (1 + R_b - R_bX_2)\, (1-X_2)^2\, W_b \tag{5-6}$$

R_a, R_b, W_a, and W_b are empirically determined constants with recommended values of -14, -14, -174 and -0.74 (Wheatley, 1987).

Pure component vapor pressures were estimated using Antoine's equation (Smith and Van Ness, 1975):

$$P_{s,i}(T) = \exp [A_{a,i} - B_{a,i}/(T + C_{a,i})] \tag{5-7}$$

where:

$P_{s,i}(T)$ = equilibrium vapor pressure of pure component i at temperature T, Pa
T = temperature, K

and $A_{a,i}$, $B_{a,i}$ and $C_{a,i}$ are empirically determined coefficients with recommended values of 16.4981, 2132.5 and -32.98 for ammonia and 18.3036, 3816.44 and -46.13 for water, respectively. The utility of these relations is supported by the comparison with pure component and mixture vapor/liquid equilibrium data presented in Tables 5-1, 5-2 and 5-3. The pure component predictions of Equation 5-7, which are summarized in Tables 5-1 and 5-2, are incorporated into the Wheatley model as indicated in Equations 5-1 and 5-2. The accuracy of the comparison of the mixture data (Table 5-3) is limited by interpolation of the reported measured data.

The dependence of enthalpy on temperature for vapor phase components is represented as:

$$h_{v,i} = C_{pv,i} (T-T_r) + \Delta H_{v,i} \tag{5-8}$$

where:

$h_{v,i}$ = enthalpy per unit quantity of component i in the vapor phase, J/g-mole

$C_{pv,i}$ = heat capacity at constant pressure of component i in the vapor phase J/g-mole/K

T = temperature of vapor phase, K

T_r = reference temperature, K

$\Delta H_{v,i}$ = latent heat of vaporization of component i, J/g-mole.

The enthalpy of pure liquid components was calculated as:

$$h_{l,i} = C_{pl,i} (T-T_r) \tag{5-9}$$

where:

$h_{l,i}$ = enthalpy per unit quantity of component i in the liquid phase, J/g-mole

$C_{pl,i}$ = heat capacity at constant pressure of component i in the liquid phase, J/g-mole/K

T = temperature of the liquid phase, K

T_r = reference temperature, K

Table 5-1. Comparison of Measured and Predicted Vapor Pressure of Water

Temperature (K)	Saturation Pressure (Pa)	
	Measured*	Predicted
273	611.3	593.1
283	1,164.5	1,204.5
293	2,290.4	2,313.3
303	4,165.5	4,219.9
313	7,253.4	7,358.8

* data from Table 1 of Keenan and Keyes, 1969

Table 5-2. Comparison of Measured and Predicted Vapor Pressure of Ammonia

Temperature (K)	Saturation Pressure (MPa)	
	Measured*	Predicted
210	0.01775	0.01793
230	0.06044	0.06091
250	0.16496	0.16515
270	0.38100	0.37841
290	0.77413	0.76211
310	1.4235	1.3873

*data from Table 15 of ASHRAE, 1981

Table 5-3. Comparison of Measured and Predicted Vapor Pressures Above Ammonia/Water Solutions

T	Liquid Phase NH_3 Mole Fraction	Measured*		Predicted	
(K)		Vapor Phase NH_3 Mole Fraction	Total Pressure (Pa)	Vapor Phase NH_3 Mole Fraction	Total Pressure (Pa)
273	0.06	0.74	2.0×10^3	0.73	2.0×10^3
	0.25	0.98	2.0×10^4	0.99	2.6×10^4
253	0.29	1.0	9.8×10^3	1.0	1.2×10^4
	0.37	1.0	2.0×10^4	1.0	2.4×10^4
	0.50	1.0	4.9×10^4	1.0	5.6×10^4
	0.63	1.0	9.8×10^4	1.0	9.8×10^4
233	0.28	1.0	2.0×10^3	1.0	2.6×10^3
	0.53	1.0	2.0×10^4	1.0	2.2×10^4
	0.74	1.0	4.9×10^4	1.0	4.9×10^4
213	0.42	1.0	2.0×10^3	1.0	2.5×10^3
	0.63	1.0	9.8×10^3	1.0	1.0×10^4
	0.87	1.0	2.0×10^4	1.0	1.9×10^4

*adapted by interpolation of Figure 3-17 of Perry and Chilton, 1973

Values of heat capacities and heats of vaporization are presented in Table 5-4.

Table 5-4. Heat Capacity and Heat of Vaporization Data

Component	Vapor Phase Heat Capacity (J/g-mole/K)	Liquid Phase Heat Capacity (J/g-mole/K)	Heat of Vaporization (J/g-mole)
Ammonia	23.0	77.1	21459.9
Water	32.5	75.4	45009.2
Air	29.0	--	--

The enthalpy of ammonia/water solutions was calculated as:

$$h_{soln} = (1-X_2)\, h_{l,H2O} + X_2\, h_{l,NH3} + \Delta H_{mix} \qquad (5\text{-}10)$$

where:

h_{soln} = enthalpy per unit quantity of ammonia/water solution, J/g-mole

X_2 = mole fraction of ammonia in the final solution, dimensionless

$h_{l,H2O}$ = enthalpy per unit quantity of pure liquid water, J/g-mole

$h_{l,NH3}$ = enthalpy per unit quantity of pure liquid ammonia, J/g-mole

ΔH_{mix} = enthalpy of mixing of ammonia and water per unit quantity of final solution, J/g-mole

and ΔH_{mix} is estimated as (Wheatley, 1987):

$$\Delta H_{mix} = -\,(1 + R_a - R_a X_2/2)\, X_2\, (1-X_2)\, R\, W_a \qquad (5\text{-}11)$$

where R is the universal gas constants and all other terms are as defined above.

5.1.1.2 Algorithm for Determination of Final Cloud Conditions

Mixing of initial clouds of ammonia and moist air produces a final cloud whose temperature, composition, and physical state are initially unknown. In addition, the nature of the equilibrium relationships and mass and energy balances describing the mixing process is such that direct calculation of the final conditions is not possible. Thus, the iterative procedure represented in Figure 5-1 was adopted to solve this problem. The procedure involves three primary elements: calculation of final cloud conditions assuming that the final cloud contains solely vapor; calculation of dew point pressure for the all-vapor final cloud; and calculation of conditions for a final cloud containing both vapor and liquid phases. Calculation of the dew point pressure of the assumed all-vapor final cloud is used to identify the physical state of the final cloud. If the sum of the vapor pressures of ammonia and water in the all-vapor final cloud is less than their pressures at the dew point, the final cloud is all vapor. If the sum of the pressures of ammonia

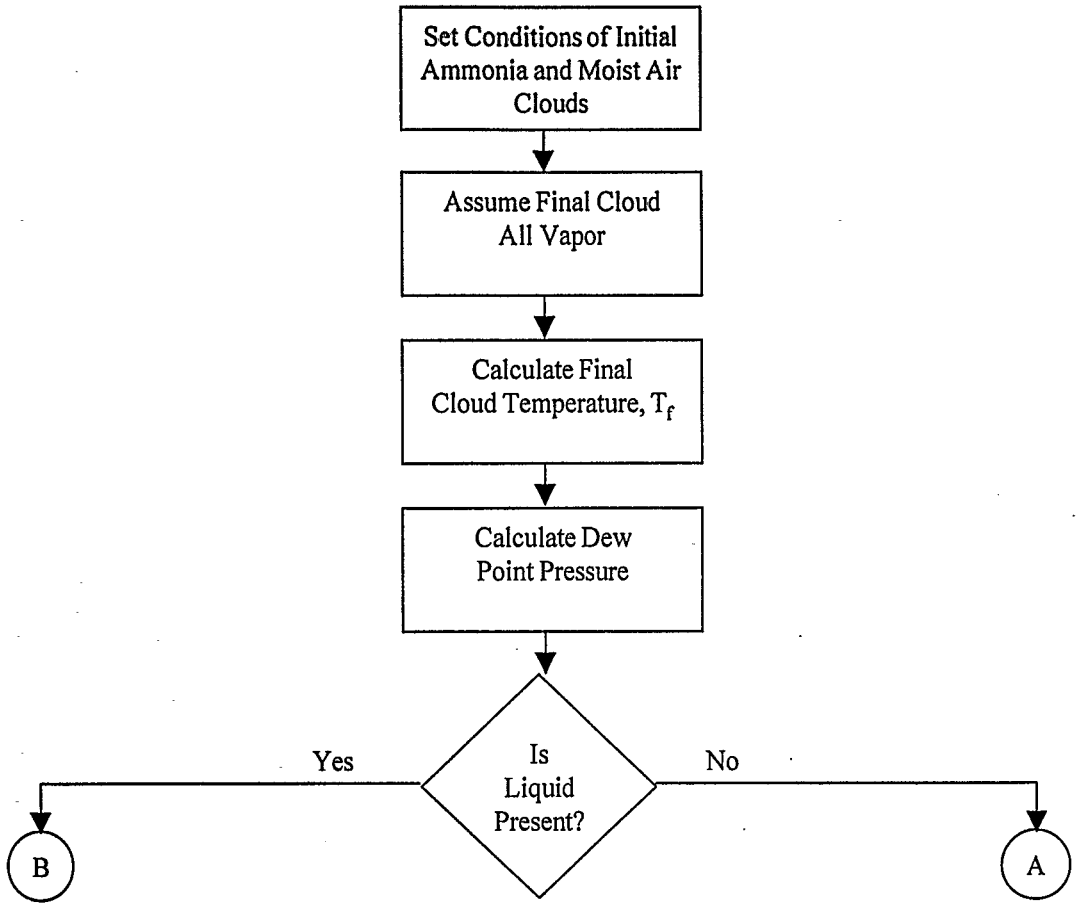

Figure 5-1. Algorithm for Determination of Final Cloud Conditions for Mixing of Ammonia and Moist Air Clouds

(continued)

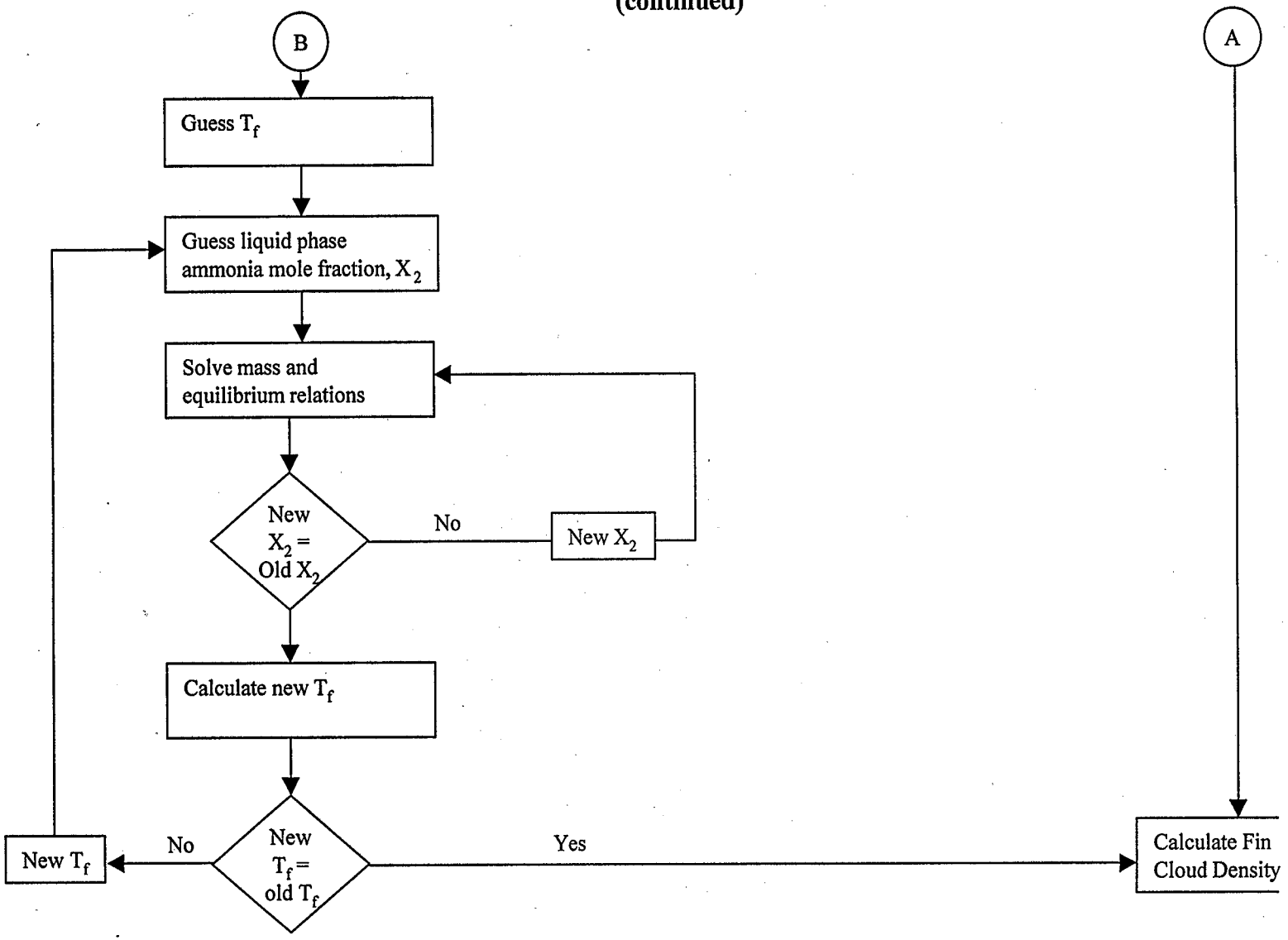

Figure 5-1. Algorithm for Determination of Final Cloud Conditions for Mixing of Ammonia and Moist Air Clouds (Continued)

and water in the all-vapor final cloud is greater than their dew point pressure, the final cloud contains both vapor and liquid phases. The following paragraphs describe execution of the three elements comprising the solution algorithm.

For given initial conditions, the temperature and composition of a final cloud containing solely vapor may be determined using mass and energy balances. The mass balance for each component was expressed as:

$$(N_{v,i} + N_{l,i})\Big|_{final} = (N_{v,i} + N_{l,i})\Big|_{initial} \qquad (5\text{-}12)$$

where:

$N_{v,i}$	=	number of moles of component i in the vapor phase, g-mole
$N_{l,i}$	=	number of moles of component i in the liquid phase, g-mole

and the vertical brackets indicate evaluation at initial and final conditions. For the case of no liquid present in the final cloud, Nl,i final is equal to zero in each of Equations 5-12, and Nv,i $-_{final}$ can be calculated directly for each component. The energy balance for the mixing process was expressed as:

$$\Sigma\,(N_{v,i}h_{v,i} + N_{l,i}h_{v,i})\,-_{final} + \Sigma\,(N_{l,i})\,\Delta H_{mix}\,-_{final} = \Sigma\,(N_{v,i}h_{v,i} + N_{l,i}h_{l,i})\,-_{initial} + \Sigma\,(N_{l,i})\,\Delta H_{mix}\,-_{initial} \qquad (5\text{-}13)$$

where all quantities are as defined above, the summations are taken over components, and the vapor and liquid phase enthalpies are evaluated according to Equations 5-8 and 5-9. For the assumed conditions of an all-vapor final cloud and the final cloud component masses determined by Equation 5-12, Equation 5-13 can be directly solved for the final cloud temperature.

Calculation of the dew point pressure is based upon specification of the temperature and vapor phase mole fractions of the cloud and identification of the liquid phase composition in equilibrium with the specified vapor phase composition. By definition, the liquid phase mole fractions sum to unity:

$$\Sigma\, X_i = 1 \qquad (5\text{-}14)$$

where X_i are liquid phase mole fractions. The vapor/liquid equilibrium constraints may be expressed as:

$$Y_i = K_i\, X_i \qquad (5\text{-}15)$$

where Y_i and X_i are vapor and liquid phase mole fractions, respectively, and the K_i are vapor/liquid equilibrium constants calculated as:

$$K_i = (1/X_i)\, P_i/P_t \qquad (5\text{-}16)$$

where the P_i are calculated using Equations 5-1 and 5-2, P_t is total pressure, and air is taken to be non-condensible. The dew point constraint, Equation 5-14, becomes:

$$\Sigma\,(Y_i/K_i) = 1 \tag{5-17}$$

where the Y_i are the specified vapor cloud mole fractions, and the K_i are functions of liquid phase mole fraction and the specified temperature. Because air is effectively non-condensible under conditions occurring in ammonia releases, the vapor phase mole fractions may be expressed on an air-free basis, and use of Equations 5-14, 5-15 and 5-16 was reduced to the condition of locating the liquid phase ammonia composition (X_2) in equilibrium with the specified vapor phase at the specified temperature. The algorithm for this procedure is presented in Figure 5-2. If the calculated dew point pressure is less than the sum of the specified partial pressures of water and ammonia, the final cloud is solely vapor, and the density was calculated using the ideal gas law. If the sum of the partial pressures of water and ammonia is greater than the dew point pressure, a liquid phase will form, and the procedure described in the following paragraphs was used to determine final cloud conditions.

For a final cloud containing both vapor and liquid phases, the algorithm presented in the portion of Figure 5-1 below connection point B was used to determine final cloud conditions. The mass balances of Equation 5-12 were combined with the vapor/liquid equilibrium relationships of Equations 5-15 to derive the constraint:

$$\Phi = \Sigma\,\{\,[Z_i\,(1-K_i)]/[1-(1-K_i)\beta]\,\} = 0 \tag{5-18}$$

where:

Φ = vapor/liquid equilibrium objective function, dim
Z_i = mole fraction of component i based on total quantity, dim
K_i = vapor/liquid equilibrium constant, dim
β = molar ratio of vapor to liquid in the final cloud, dim

K_i is calculated using Equations 5-1, 5-2 and 5-16, and the summation is over components.

As indicated in Figure 5-1, the solution procedure involves generation of initial estimates of final cloud temperature (T_f) and liquid phase ammonia mole fraction (X_2), which allows calculation of the K_i. After solving Equation 5-18 for β, the number of moles of each component in the vapor and liquid phases was calculated using the mass balances of Equations 5-12 and the equilibrium constraints of Equations 5-15. The composition of the liquid phase was then compared with the initial estimate and a new estimate of X_2 generated to allow re-calculation of cloud composition. When the final cloud composition is successfully determined for a given estimate of cloud temperature, the cloud temperature is re-calculated using the energy balance of Equation 5-13. The mass and energy balance procedure is iterated until final cloud temperature and composition are determined. The density of the final cloud is calculated using the ideal gas law and the assumption of complete entrainment of the liquid phase.

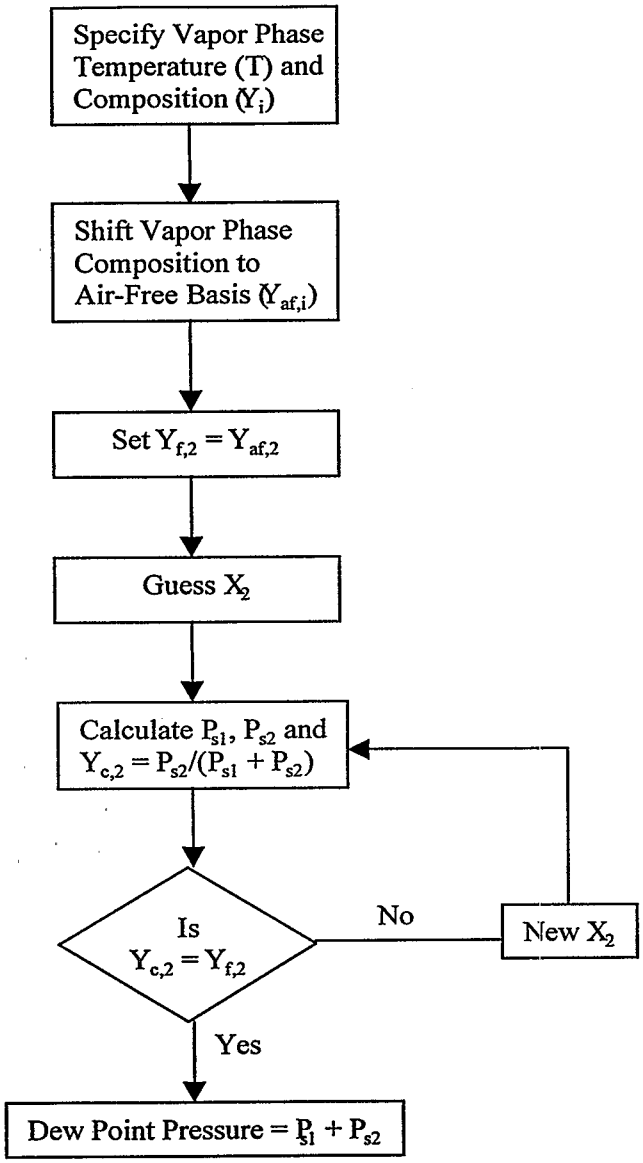

Figure 5-2. Algorithm for Calculation of Dew Point Pressure

5.1.2 RESULTS

Representative results were developed for three cases bounding potential conditions. The first case, representative of worst-case scenario conditions, involves release of vapor and liquid ammonia at the atmospheric pressure boiling point (240 K), with 80 percent of the ammonia in the liquid phase and mixing with warm, moist air (relative humidity = 50 percent). The results presented in Table 5-5 indicate that the final cloud initially experiences evaporative cooling and remains denser than ambient air even after entrainment of enough air to fully vaporize the ammonia. Liquid droplets, comprised primarily of condensed water, persist at high air-to-ammonia mixing ratios at moderate relative humidities. The second example, also a worst-case

scenario, involves release of a two-phase cloud of ammonia and mixing with warm, dry air. The results presented in Table 5-6 show the evaporative cooling step, but indicate that the ammonia liquid phase is completely evaporated after mixing with 11 kilograms of air per kilogram of ammonia. Comparison of the results of Tables 5-5 and 5-6 indicates that heat of mixing offsets the evaporative cooling effect and decreases the density of the final cloud. The third case involves release of vapor ammonia into dry air of variable temperature. The results presented in Table 5-7 indicate that the final cloud remains less dense than air even at relatively low ambient air temperatures.

Table 5-5. Final Cloud Conditions for a Worst-Case Scenario, Two-Phase Release with Moist Air*

Mass of Air / Mass of Ammonia	Final Cloud Conditions			
	T (K)	Density(kg/m^3)	Fraction of NH3in Liquid Phase (%)	Mole Fraction of NH3 in Liquid Phase
1	221.5	2.053	67.1	0.986
3	214.7	1.711	48.7	0.945
6	214.0	1.597	23.7	0.808
9	226.7	1.492	9.5	0.530
11	238.8	1.424	6.8	0.397
20	266.8	1.294	3.3	0.176
100	293.3	1.190	0.6	0.021

* Initial Conditions

- 80% of ammonia in Liquid Phase, T = 240
- air temperature = 298 K
- relative humidity = 50%
- air density = 1.186 kg/m^3

Table 5-6. Final Cloud Conditions for a Worst-Case Scenario, Two-Phase Release with Dry Air*

Mass of Air / Mass of Ammonia	Final Cloud Conditions		
	T (K)	Density (kg/m^3)	Fraction of NH3 in Liquid Phase
1	221	2.100	69.3
5	209.3	1.689	41.6
11	205.9	1.626	2.4
20	243.1	1.407	0.0
100	286.4	1.225	0.0

*Initial Conditions

- 80% of ammonia in Liquid Phase, T = 240
- air temperature = 298 K
- relative humidity = 0%
- air density = 1.186 kg/m^3

Table 5-7. Final Cloud Conditions for All Vapor Release with Dry Air*

Ambient Air Conditions		Final Cloud Conditions	
T (K)	Density (kg/m^3)	T (K)	Density (kg/m^3)
263	1.344	249	1.048
273	1.295	253	1.031
283	1.249	258	1.014
293	1.219	263	0.997

*Initial Conditions

- ammonia release all vapor, T = 240 K
- air-to-ammonia mass mixing ratio equal to unity
- 0% relative humidity

5.2 EFFECT ON PREDICTION OF DISTANCES TO TOXIC ENDPOINT

Table 5-8 shows an example of the effect on SACRUNCH runs of including the new thermodynamics, Wilson meandering, and both. As can be seen, the effect is small, but does lead to a small reduction in predicted distances, which has been taken into account in the AR and WWTPs guidance.

Table 5-8. Example of the Effect of New Thermodynamic Model and Meandering of Anhydrous Releases, Worst-Case, Rural Conditions, 75% RH

Rate of Release (lbs/min)	Distance to Toxic Endpoint (miles)			
	Old Model	With Wilson Meandering	With New Thermodynamics	With Wilson Meandering & New Thermodynamics*
10	0.19	0.19	0.20	0.20
20	0.27	0.26	0.28	0.27
50	0.41	0.40	0.42	0.42
100	0.57	0.56	0.58	0.58
200	0.80	0.78	0.81	0.80
500	1.28	1.26	1.27	1.25
1,000	1.85	1.82	1.79	1.77
2,000	2.72	2.68	2.54	2.52
5,000	4.59	4.54	4.11	4.07
10,000	6.74	6.69	5.94	5.90
20,000	9.59	9.55	8.60	8.54
50,000	14.27	14.23	13.8	13.74

* These results do not exactly match those in the AR. Minor details of input have been changed.

5.3 POTENTIAL FOR LIFT-OFF

There are certain types of initially heavy plumes that can potentially become buoyant and may lift off the ground. These include hydrogen fluoride (HF) releases in moist air, where the heat liberated by condensation of HF/water droplets can cause the plume's buoyancy to become positive as air is entrained. Another possibility is the uranium hexafluoride (UF_6)/moist air system because the UF_6-water reaction is highly exothermic. Finally, it is conceivable that initially denser-than-air ammonia plumes could become buoyant as they dilute.

Briggs (1973b) has developed a simple approach that requires the calculation of a lift-off parameter:

$$L_p = gh\Delta\rho/(\rho_a u^2_*) \tag{5-19}$$

where lift-off will occur if $L_p > 30$ (Meroney, 1984). Here, g is the acceleration due to gravity (m/s^2), h is the height of the cloud (m), $\Delta\rho$ is the difference in density between the air and the plume (kg/m^3), ρ_a is the density of air (kg/m^3), and u_* is the friction velocity (m/s).

For UF_6, HF, and ammonia, the SACRUNCH computer model calculates L_p at distances downwind of the transition point at which the plume ceases to be denser than air. If L_p exceeds 30, in any weather condition, this information will be printed out, and the user must judge whether there will be more than trivial plume rise. Table 5-9 contains an illustration of the potential for lift-off for a 1,000 lb/min release of flashing liquid ammonia. As can be seen, there appears to be no potential for lift-off until the plume has diluted below the toxic endpoint

Table 5-9. Illustration of the Potential for Lift-Off

Distance Downwind (m)	L_p	Average Concentration (kg/m^3)	Peak Concentration (kg/m^3)
1,950	6.4	2×10^{-4}	5.9×10^{-4}
2,400	20.5	8.1×10^{-5}	2.4×10^{-4}
3,000	31.9	4.4×10^{-5}	1.3×10^{-4}
4,500	48.0	1.9×10^{-5}	3.8×10^{-5}

Assumptions:
- Anhydrous Ammonia, flashing liquid release
- Release Rate 1,000 lb/min
- Worst-Case Weather Conditions, Rural Site
- RH = 75%

Results:
- Cloud evolves out of denser-than-air phase ~ 1800 m downwind with mean concentration ~ 4×10^{-4} kg/m^3
- Toxic endpoint: 1.4×10^{-4} kg/m^3 (200 ppm) at ~ 2,900 m based on peak concentration

Conclusion:
- No lift-off until after toxic endpoint
- No counter-examples found in sensitivity studies

CHAPTER 6: EFFECT OF AMMONIA RELEASES ON STRUCTURES

The purpose of this chapter is to discuss the consequences of releases inside rooms, such as the compressor room in an ammonia refrigeration plant or a room containing chlorine or sulfur dioxide vessels at WWTPs. The work presented here has been used as the basis for building mitigation models in the AR and WWTP guidance, but not in OCAG.

This chapter provides methods for prediction of pressures inside buildings and the subsequent rate of release to the atmosphere. Important parameters include the quantity of ammonia, chlorine, or sulfur dioxide available for release, the time over which the release takes place, the volume of the room, the presence of airborne liquid droplets, leakpaths in the structure, and the characteristics of the ventilation system.

As discussed in Chapter 3, experimental evidence indicates that in the case of unobstructed releases, ammonia, chlorine, or sulfur dioxide droplets formed in the release remain suspended in the vapor phase and evaporate. Obstructions can be effective in facilitating the rain-out of droplets with removal efficiencies on the order of 75 percent of the liquid reported. The remaining 25 percent of the liquid release is assumed to be entrained in the vapor release. Chapter 3 presents an approximate rule-of-thumb: if released inside a building as a flashing liquid release, 60 percent collects on the floor as a relatively slowly evaporating pool, and 40 percent remains airborne as a 50:50 mixture of vapor and liquid droplets.

Evaluation of building structural integrity and effectiveness of mitigation for intact structures was based on consideration of single-phase releases of vapor into buildings containing leakpaths and engineered vents capable of relieving pressure. The vapor release for the analysis included the contribution of vapor formed during depressurization of liquefied gas stored under pressure (flashing). Building release attenuation factors estimated in this chapter are applicable to both the entrained liquid and gaseous portions of the release.

This document considers releases over 10 minutes. EPA also analyzed sudden releases. Its analysis indicated that for pressure-tight buildings, a sudden release could damage the building sufficiently to eliminate its ability to mitigate the release unless the size of the building is large in relation to the mass of the chemical. In the more likely case of a building with leakpaths and ventilation, a sudden release will generally not damage the building.

6.1 PROLONGED RELEASES

Gradual releases of stored material as vapor may not be capable of producing the pressure differentials predicted for instantaneous releases. Over periods of 10 minutes, ammonia, chlorine, or sulfur dioxide may escape through leakpath and ventilation system flowpaths at rates large enough to relieve the initial pressure disturbance. The potential magnitude of this behavior was investigated for a leakpath flow that would produce a room change-over rate of one-half volume per hour at undisturbed flow conditions. This assumption does not preclude the possibility that there may be significantly different change-over rates to be investigated on a case-by-case basis. The approach applied was to estimate leakpath resistance factors for

representative conditions and use these resistance factor estimates to evaluate the building pressure response to a specified rate of either ammonia, chlorine, or sulfur dioxide release from a vessel inside the building.

Leakpath flow areas were estimated based on the assumption that one-half of a volume of the room is lost per hour (ASTM, 1986) and that the driving force for this loss is developed by air flow around the building. For a given windspeed, the pressure differential may be estimated using correlations based on experimental data (Blevins, 1984). The pressure differential may then be used in conjunction with the assumed normal condition leakage rate to estimate resistances for the in- and out-leakage paths. This leakage resistance calibration procedure also assumed that the cross-sectional area of each leakpath was proportional to the length of the building and that the building length was twice the building width. Engineered vent areas were estimated based on the assumption that linear air velocities through the vent were 8 m/s (1,600 ft/min), a value consistent with standard practice (ACGIH, 1986). Release rate of stored material into the room (i.e., R_i) was represented as a piecewise continuous function, allowing simulation of transient release with variable dependence on time. Room density and pressure conditions and vent flow rates were estimated using FIRAC (Gregory and Nichols, 1986), a computer code capable of simulating ventilation system response to accident conditions. FIRAC is a node/branch network model in which nodes represent rooms and branches represent ducts, blowers, and filters. In this case, leakpaths were modeled as ducts of small size, and the ammonia release was represented as mass injection with associated evaporative energy loss.

6.1.1 Building Structural Response

Potential conditions that could be established were investigated for a 10-minute release of liquid ammonia stored at 310 K (98 °F) and 1.4 MPa (206 psia). The simulation estimated the ammonia injection rate required to produce an overpressure large enough to threaten structural integrity. An overpressure value of 6,895 Pa (1 psia) was adopted for this criterion. Release modeling predicted immediate evaporation of approximately 20 percent of the ammonia flow with subsequent evaporation of the remaining mass. High-accident condition leakpath flows were predicted for room volumes from 500 m^3 to 10,000 m^3 with 6,710 kg/10 min (14,790 lb/10 min) required to produce the 6,895 Pa (1 psia) overpressure for the 500 m^3 room. Very large release rates were required to approach the overpressure criterion for rooms in the 1,000 m^3 to 10,000 m^3 range. This general conclusion was verified using the single-room mass balance model. Because ammonia has lower density than either chlorine or sulfur dioxide, the results of this ammonia analysis also indicate that prolonged releases of chlorine or sulfur dioxide will not threaten building integrity.

6.1.2 Building Attenuation of Release

Continuous release of either ammonia, chlorine, or sulfur dioxide into a ventilated room will produce an increase in concentration of gas which approaches a constant level determined by the gas injection rate, ventilation rate, and room volume. Once steady state conditions are established the removal rate equals the injection rate and the fractional release factor equals unity. For transient conditions occurring before establishment of a steady state, such as may occur for ten-minute release periods, the fractional release factor (FR_{10}) may be less than unity. A single-room mass balance model was used to estimate FR_{10} for set of values of θ (ratio of

room volume to the amount of ammonia, chlorine, or sulfur dioxide vapor release) and N_v (ventilation rate as number of room changes per hour) at constant rate of gas addition. The results of these calculations are presented in Table 6-1 for ammonia and Table 6-2 for chlorine and sulfur dioxide. Results for chlorine and sulfur dioxide are similar due to similarity in molecular weight of the gases. As expected, for high ventilation rates and small rooms, steady state is quickly established and fractional release factors approach unity. For larger rooms and lower ventilation rates, building attenuation of a release can be appreciable. For cases in which overpressurization effects are small, an analytical solution to Equation 6-1 may be used to corroborate the results presented in Tables 6-1 and 6-2.

$$P_{1,i} = F_{sat}(T_{1,i}) \tag{6-1}$$

where:

$P_{1,i}$ = equilibrium partial pressure of the i'th component, either ammonia, chlorine, or sulfur dioxide at temperature $T_{1,i}$, Pa

F_{sat} = equilibrium relation between pressure and temperature for the i'th component, either ammonia, chlorine, or sulfur dioxide

$T_{1,i}$ = temperature of ammonia, chlorine, or sulfur dioxide at the end of the first step K

The vapor/liquid equilibrium relationship is available in tabular form for ammonia (ASHRAE, 1981), chlorine and sulfur dioxide (Perry and Chilton, 1973).

For negligible overpressurization, constant gas addition and constant ventilation rate, fractional release rate is given by:

$$FR = 1 - (1/N_v t)\{1 - \exp(-N_v t)\} \tag{6-2}$$

where all variables are as defined above. Evaluation of Equation 6-2 for time of 0.1667 hours (10 minutes) and values of N_v of 1, 5, 10, 20, 30, and 40 hr^{-1} yields values of FR_{10} of 0.08, 0.32, 0.51, 0.71, 0.80, and 0.85, respectively. These values are in agreement with the values of Tables 6-1 and 6-2 for the high room volume to vapor mass release case (i.e., $\theta = 10$) which would produce the smallest overpressures.

6.2 SUMMARY OF CONCLUSIONS

For prolonged releases, including those occurring over ten-minute periods, failure of buildings of industrial size would not be expected. The presence of the building serves to attenuate transient releases and attenuation is effective for relatively small buildings ventilated at low rates. Attenuation is small for buildings ventilated at high rates as would occur if emergency ventilation systems were used.

Table 6-1. Ten-Minute Building Release Attenuation Factors for Continuous Releases of Ammonia

θ* (m^3/kg)	N_v (hr^{-1})	FR_{10} (dim)
10.0	0	0.07
	1	0.08
	5	0.32
	10	0.51
	20	0.71
	30	0.80
	40	0.85
5.0	0	0.13
	1	0.13
	5	0.32
	10	0.51
	20	0.71
	30	0.80
	40	0.85
2.0	0	0.29
	1	0.29
	5	0.32
	10	0.51
	20	0.71
	30	0.80
	40	0.85
1.0	0	0.47
	1	0.47
	5	0.47
	10	0.51
	20	0.71
	30	0.80
	40	0.85

θ* (m^3/kg)	N_v (hr^{-1})	FR_{10} (dim)
0.5	0	0.67
	1	0.67
	5	0.67
	10	0.67
	20	0.71
	30	0.80
	40	0.85
0.25	0	0.83
	1	0.83
	5	0.83
	10	0.83
	20	0.83
	30	0.83
	40	0.85
0.05	0	0.97
	1	0.97
	5	0.97
	10	0.97
	20	0.97
	30	0.97
	40	0.97
0.02	0	0.99
	1	0.99
	5	0.99
	10	0.99
	20	0.99
	30	0.99
	40	0.99

* Values of θ in m^3/kg can be converted to values of θ in ft^3/lb by multiplying by 16.

Table 6-2. Ten-Minute Building Release Attenuation Factors for Prolonged Releases of Chlorine and Sulfur Dioxide

θ* (m^3/kg)	N_v (hr^{-1})	FR_{10} (dim)
10.0	0	0.02
	1	0.08
	5	0.32
	10	0.51
	20	0.71
	30	0.80
	40	0.85
5.0	0	0.03
	1	0.08
	5	0.32
	10	0.51
	20	0.71
	30	0.80
	40	0.85
2.0	0	0.08
	1	0.08
	5	0.32
	10	0.51
	20	0.71
	30	0.80
	40	0.85
1.0	0	0.15
	1	0.15
	5	0.32
	10	0.51
	20	0.71
	30	0.80
	40	0.85

θ* (m^3/kg)	N_v (hr^{-1})	FR_{10} (dim)
0.5	0	0.28
	1	0.28
	5	0.32
	10	0.51
	20	0.71
	30	0.80
	40	0.85
0.25	0	0.46
	1	0.46
	5	0.46
	10	0.51
	20	0.71
	30	0.80
	40	0.85
0.05	0	0.85
	1	0.86
	5	0.86
	10	0.86
	20	0.86
	30	0.86
	40	0.86
0.02	0	0.94
	1	0.94
	5	0.94
	10	0.94
	20	0.94
	30	0.94
	40	0.94

* Values of θ in m^3/kg can be converted to values of θ in ft^3/lb by multiplying by 16.

REFERENCES

American Conference of Governmental Industrial Hygienists (ACGIH), Industrial Ventilation, ACGIH, Lansing, MI, 1986.

American Institute Hygiene Association (AIHA), "Emergency Response Planning Guidelines," Akron, OH, 1988-1992.

American Society of Heating, Refrigerating, and Air-Conditioning Engineers, Inc., (ASHRAE), "*ASHRAE Handbook 1981 Fundamentals*," ASHRAE, Atlanta, GA, 1981.

American Society of Testing and Materials (ASTM), "Measured Air Leakage of Buildings," ASTM, Philadelphia, PA, 1986.

American Waterworks Research Association Research Foundation (AWWARF), "*Model RM Plan for the Water Industry*," February 1998 (Draft).

Barr, S. and Gifford, F.A., "The Random Force Theory Applied to Regional Scale Tropospheric Diffusion," *Atmospheric Environment* 26A pp. 1053-1062, 1987.

Blevins, R.D., "*Applied Fluid Dynamics Handbook*," Van Nostrand Rheinhold, New York, NY, 1984.

Blewitt, D.N., J.F. Yohn and D.L. Ermak, "An Evaluation of SLAB and DEGADIS Heavy Gas Dispersion Models Using the HF Spill Test Data," in CCPS, 1987.

Briggs, G.A., "Diffusion Estimates for Small Emissions," ATDL Contribution File No. 79, National Oceanic and Atmospheric Administration, Atmospheric Turbulence and Diffusion Laboratory, Oak Ridge, TN, 1973a.

Briggs, G.A., "Lift Off of Buoyant Gas Initially on the Ground," Environmental Research Laboratories, Air Resources, Atmospheric Turbulence and Diffusion Laboratory, ATDL Contribution File No. 87 (draft), National Oceanic and Atmospheric Administration, Oak Ridge, TN, 1973b.

Briggs, G.A., "Plume Dispersion in the Convective Boundary Layer. Part III: Analysis of CONDORS Field Experiment Data," *Journal of Applied Meteorology*, 32 pp. 1388-1425, 1993.

Brighton, P.W.M., "Continuous Chlorine Releases Inside Buildings: Concentrations on Emission to Atmosphere," SRD R 468, United Kingdom Atomic Energy Authority Health and Safety Directorate, Culcheth, UK, 1989.

Britter, R.E., "Atmospheric Dispersion of Dense Gases," *Annual Review of Fluid Mechanics*, 21 pp. 317-344, 1989.

Britter, R.E. and S.T. Cole, "The Evaluation of Technical Models Used for Major Accident Hazard Installations," Report # EUR 14774 EN, Directorate-General, Science, Research and Development, Commission of the European Communities, Brussels, 1994.

Carpenter, R.J., R.P. Cleaver, P.J. Waite and M.A. English, "The Calibration of a Simple Model for Dense Gas Dispersion Using the Thorney Island Phase I Trials Data," United Kingdom Health and Safety Executive, Second Symposium on Heavy Gas Dispersion Trials at Thorney Island, Sheffield, UK, 1986.

Center for Chemical Process Safety (CCPS), "*Guidelines for Use of Vapor Cloud and Source Dispersion Models, with Worked Examples*", American Institute of Chemical Engineers, New York, NY, 1986.

Center for Chemical Process Safety (CCPS), *International Conference on Vapor Cloud Modeling*, Boston, MA, November 2-4, 1987, American Institute of Chemical Engineers, New York, NY, 1987.

Center for Chemical Process Safety (CCPS), "*Guidelines for Chemical Process Quantitative Risk Analysis*," American Institute of Chemical Engineers, 1989.

Center for Chemical Process Safety (CCPS), *International Conference and Workshop on Modeling and Mitigating the Consequences of Accidental Releases of Hazardous Materials*, New Orleans, LA, May 20-24, 1991, American Institute of Chemical Engineers, New York, NY, 1991.

Center for Chemical Process Safety (CCPS), *International Conference and Workshop on Modeling and Mitigating the Consequences of Accidental Releases of Hazardous Materials*, New Orleans, LA, September 26-29, 1995, American Institute of Chemical Engineers, New York, NY 1995.

Chamberlain, A.C. and R.C. Chadwick, "Deposition of Airborne Radio-iodine Vapour," Nucleonics 8, 22-25: Chamberlain, A.C. (1966), "Transport of Gases To and From Grass and Grass-Like Surfaces," *Proceedings of the Royal Society* A290, 236-265, 1953.

Chan, S.T., H.C. Rodean and D.N. Blewitt, "FEM3 Modeling of Ammonia and Hydrofluoric Acid Dispersion," in CCPS (1987) pp. 116-154, 1987.

Clough, P.N., D.R. Grist and C.J. Wheatley, "The Mixing of Anhydrous Hydrogen Fluoride with Moist Air," International Conference on Vapor Cloud Modeling, American Institute of Chemical Engineers, New York, pp. 39-55, 1987.

Cox, R.A. and R.J. Carpenter, "Cloud Dispersion Model for Hazard Analysis," *Proc. 1st Heavy Gas and Risk Assessment Symposium*, Battelle Institute, Frankfurt, West Germany, 1979.

Erisman, J.W. and G.P.J. Draaijers, "Atmospheric Deposition in Relation to Acidification and Eutrophication," ISBN 0-444-82247-X, Elsevier, Amsterdam, The Netherlands, 1996.

Ermak, D.L., "User's Manual for the SLAB Model, An Atmospheric Dispersion Model for Denser-than-Air Releases," Lawrence Livermore Laboratory, Livermore, CA, 1989.

Fryer, L.S. and G.D. Kaiser, "DENZ - A Computer Program for the Calculation of the Dispersion of Dense Toxic or Explosive Gases in the Atmosphere," United Kingdom Atomic Energy Authority and Reliability Directorate Report SRD R152, Culcheth, Cheshire, UK, 1979.

Gephart, L. and S. Moses, "An Approach to Evaluate the Acute Imports from Simulated Accidental Releases of Chlorine and Ammonia," *Plant/Operation Progress*, Vol. 8, no. 1, pp. 8-11, 1989.

Gregory, W.S. and B.D. Nichols, "FIRAC User's Manual: A Computer Code to Simulate Fire Accidents in Nuclear Facilities," NUREG/CR-4561, Los Alamos National Laboratory, Los Alamos, NM, 1986.

Goldwire, Jr., H.C., T.G. McRae, G.W. Johnson, D.L.Hipple, R.P. Koopman, J.W. McLure, L.K. Morris, and R.T. Cedarwall, "Desert Tortoise Series Data Report – 1983 Pressurized Ammonia Spills," Lawrence Livermore National Laboratories Report UCID-20562, Livermore, CA, 1985.

Hanna, S.R. and R.P. Hosker, "Atmospheric Removal Processes for Toxic Chemicals," ATDL Contribution File No. 80/25, Air Resources, Atmospheric Turbulence and Diffusion Laboratory, National Oceanographic and Atmospheric Administration, Oak Ridge, TN, 1980.

Hanna, S.R., T.C. Chang and D.G. Strimaitis, "Hazardous Gas Model Evaluation with Field Observations," *Atmospheric Environment*, 27A pp. 2265-2285, 1993.

Havens, J.A. and T.O. Spicer, "*A Dispersion Model for Elevated Dense Gas Chemical Releases," Volume I & II*, EPA 450/4-88-006a/b, U.S. Environmental Protection Agency, Research Triangle Park, NC, 1988.

Heinrich, M.E., E. Gerold and P. Wietfeld, "Large Scale Propane Release Experiments Over Land at Different Atmospheric Stability Classes," *Journal of Hazardous Materials* 20, pp 287-301, 1988: Corrigendum, *Journal of Hazardous Materials* 22, pp 407-413, 1989. For more details, see the report by the same authors, APraxisgerechte Bestimmung der Zundentfernungen bei der Freisetzung Schwere Gases," BMFT 326-7591-01-RG-8402, TUV (Technischer Uberwachungs-Verein Norddeutscheland e.V.), Hamburg, 1988.

Hoot, T.G., R.N. Meroney and J.A. Peterka, "Wind Tunnel Tests of Negatively Buoyant Plumes," Report CER73-74TGH-RNM-JAP-13, Fluid Dynamics and Diffusion Laboratory, Colorado State University, 1973.

Hosker, Jr., R.P., "Estimates of Dry Deposition and Plume Depletion over Forests and Grassland," in *Physical Behavior of Radioactive Contaminants in the Atmosphere*, IAEA STI/PUB/354, pp. 291-, 1974.

Ianello, V., P.H. Rothe, G.B. Wallis, R. Diener and S. Schreiber, "Aerosol Research Program: Improved Source Term Definition for Modeling the Ambient Impact of Accidental Releases of Hazardous Liquids,"6th International Symposium on Loss Prevention and Safety Promotion in the Process Industries, June, 1989, Oslo, Norway, 1989.

Iman, R.L. and M.J. Shortencarier, "A Fortran 77 Program and User's Guide for the Generation of Latin Hypercube and Random Samples for Use with Computer Models," NUREG/CR-3624 (SAND83-2365), prepared for the U.S. Nuclear Regulatory Commission, Washington, D.C., 1984.

International Institute of Ammonia Refrigeration (IIAR), "Guidelines for: Ammonia Machinery Room Ventilation," Bulletin No. 111, IIAR, Washington, DC, 1991.

Jagger, S.F., "Development of CRUNCH: A Dispersion Model for Continuous Releases of Denser-than-Air Vapor into the Atmosphere," United Kingdom Atomic Energy Authority Safety and Reliability Directorate Report SRD R229, 1983.

Johnson, D.J., "Prediction of Aerosol Formation from the Release of Pressurized, Superheated Liquids to the Atmosphere" in CCPS, 1991.

Kaiser, G.D., "Examples of the Successful Application of a Simple Model for the Atmospheric Dispersion of Dense, Cold Vapors to the Accidental Release of Anhydrous Ammonia from Pressurized Containers," United Kingdom Atomic Energy Authority Safety and Reliability Directorate Report SRD R150, Culcheth, UK, 1979.

Kaiser, G.D., "A Review of Models for Predicting the Dispersion of Ammonia in the Atmosphere," *Plant/Operations Progress*, Vol. 8 No. 1, pp 58-64, 1989.

Keenan, J.H. and F.G. Keyes, *Steam Tables*, John Wiley and Sons, Inc., New York, NY, 1969.

Lonsdale, H., "Ammonia Tank Failure - South Africa," *Ammonia Plant Safety* 17 (1975), 126-131, 1975.

Lees, F.P., "*Loss Prevention in the Process Industries*," Butterworths, London, UK, 1980.

Markham, R.S., "A Review of Damages from Ammonia Spills," presented at the 1986 Ammonia Symposium on Safety in Ammonia Plants and Related Facilities, American Institute of Chemical Engineers, Boston, MA, 1986.

McMullen, G., "A Review of the 11th May Ammonia Truck Accident," City of Houston Health Department Report (unnumbered), Houston, TX, 1976.

McQuaid, J. (Ed.), "Heavy Gas Dispersion at Thorney Island," *Journal of Hazardous Materials* 11 (Special Issue), 1986

Meroney, R.N., "Lift-Off of Buoyant Gas Initially on the Ground," *J. Industrial Mathematics*, Vol. 5, 1979.

Mueller, S.F. and L.M. Reisinger, "Measured Plume Width versus Sampling Time: A Look Beyond 10 Kilometers," *Atmospheric Environment* 20 pp. 895-900, 1986.

Muralidhar, R., G.R. Jersey, F.J. Krambeck and S. Sundaresan, "A Two-Phase Model for Subcooled and Superheated Liquid Jets," in CCPS, 1995.

Nair, S.K., D.B. Chambers, S.H. Park, Z.R. Radonjic, P.T. Coutts, C.J. Lewis, J.S. Hammonds, and F.O. Hoffman, "Review of Models for Determining Consequences of UF_6 Release," NUREG CR/6481, U.S. Nuclear Regulatory Commission, Washington, D.C., 1997.

National Oceanic and Atmospheric Administration (NOAA) and U.S. Environmental Protection Agency (USEPA), "User's Manual for the ALOHA Model, ALOHA 5.0, Areal Locations of Hazardous Atmospheres," Washington, D.C., 1995.

National Transportation Safety Board (NTSB), "Railroad Accident Report; Chicago, Burlington and Quincy Railroad Company Train 64 and Train 824 Derailment and Collision with Tank Car Explosion, Crete, Nebraska, February 18, 1969," Report Number NTSB-RAR-71-2, Washington, D.C., 1971.

National Transportation Safety Board (NTSB), "Railroad Accident Report; Louisville and Nashville Railroad Company Freight Train Derailment and Puncture of Anhydrous Ammonia Truck Cars at Pensacola, Florida, November 9, 1977," Report Number NTSB-RAR-78-4, Washington, D.C., 1978.

Ooms, G., "A New Method for the Calculation of the Plume Path of Gases Emitted by a Stack," *Atmospheric Environment* 6, pp. 899-909, 1972.

Perry, R.H. and C.H. Chilton (ed.), *Chemical Engineer's Handbook*, McGraw-Hill Book Co., New York, NY, 1973.

Picknett, R.G., "Field Experiments on the Behavior of Dense Clouds," Chemical Defense Establishment Report PTN, IL 1154-78-1, Porton Down, UK, 1978.

Resplandy, A., *Chimie et Industrie Genie Chimique*, 102, pp. 691-702 (1969).

Scarborough, J.B., *Numerical Mathematical Analysis*, Johns Hopkins Press, Baltimore, MD, 1966.

Schotte, W., "Fog Formation of Hydrogen Fluoride in Air," *Ind. Chem. Eng. Chem. Res.* 26, pp 300-306, 1987.

Science Applications International Corporation (SAIC), "SAIC's Computer Programs for Modeling the Atmospheric Dispersion of Hazardous Vapors–Model Description and User's Guide," prepared by Science Applications International Corporation, McLean, VA, 1994.

Smith, J.M. and H.C. Van Ness, *Introduction to Chemical Engineering Thermodynamics*, McGraw-Hill Book Co., New York, NY, 1975.

South Coast Air Quality Management District (SCAQMD), "Supporting Document for: Proposed Rule 1410: Hydrogen Fluoride Storage and Use," El Monte, CA, 1991a.

South Coast Air Quality Management District (SCAQMD), "Guideline to Comply with Proposed Rule 1410: Hydrogen Fluoride Storage and Use," El Monte, CA, 1991b.

Spicer, T.O., J.A. Havens and L.E. Kay, "Extension of DEGADIS for Modeling Aerosol Releases," in CCPS (1987) pp. 416-438, 1987.

The Fertilizer Institute (TFI), "Guidance Document for Fertilizer Retailers/Wholesalers/ Distributors, SIC 5191, EPA's Risk Management Program, Clean Air Act Section 112(r), Anhydrous Ammonia, Aqua Ammonia," Washington, D.C., 1998.

United States Environmental Protection Agency (USEPA), "Technical Guidance for Hazards Analysis," in collaboration with the Federal Emergency Management Agency and the U.S. Department of Transportation, Washington D.C., 1987.

United States Environmental Protection Agency (USEPA), "User's Guide for the DEGADIS 2.1 Dense Gas Dispersion Model," EPA-450/4-89-019 (NTIS PB 90-213893), Research Triangle Park, NC, 1989.

United States Environmental Protection Agency (USEPA), "Evaluation of Dense Gas Simulation Models," EPA-450/4-90-018, prepared by TRC Environmental Corporation under EPA Contract 68-02-4399, 1991.

Wheatley, C.J., P.W.M. Brighton and A.J. Prince, "Comparison Between Data from the Heavy Gas Dispersion at Thorney Island and Predictions of Simple Models," United Kingdom Atomic Energy Authority Safety and Reliability Directorate Report, Warrington, UK, 1986.

Wheatley, C.J., "Discharge of Liquid Ammonia to Moist Atmospheres - Survey of Experimental Data and Model for Estimating Initial Conditions for Dispersion Calculations", SRD/HSE/R 410, United Kingdom Atomic Energy Authority, Culcheth, UK, April, 1987.

Wilson, D.J., *Concentration Fluctuations and Averaging Time in Vapor Clouds*, Center for Chemical Process Safety of the American Institute of Mechanical Engineers, New York, NY, 1995.

Woodward, J.L. and A. Papadourakis, "Modeling of Droplet Entrainment and Evaporation in a Dispersing Jet" in CCPS (1991), pp. 147-167, 1991.

Woodward, J.L., J. Cook and A. Papadourakis, "Modeling and Validation of a Dispersing Aerosol Jet," *Journal of Hazardous Materials* 44, pp 195-207, 1995.

Woodward, J.L., "Improving the Effect of Atmospheric Stability Class for Dispersion Modeling," *Process Safety Progress* 17, pp 1-8, 1998.

Yersel, M., R. Goble and J. Morrill, "Short Range Dispersion Experiments in an Urban Area," *Atmospheric Environment*, 17 pp. 275-282, 1993.

APPENDIX A

SAIC'S COMPUTER PROGRAMS FOR MODELING THE ATMOSPHERIC DISPERSION OF LARGE SCALE ACCIDENTAL RELEASES OF HAZARDOUS VAPORS IN INDUSTRIAL ENVIRONMENTS

TABLE OF CONTENTS

Page

A.1 INTRODUCTION **A-1**

A.2 SACRUNCH **A-1**

A.3 SADENZ **A-1**

A.4 SAPLUME **A-2**

A.5 COMMON FEATURES OF THE COMPUTER PROGRAMS **A-3**

A.5.1 VAPORS WITH COMPLEX THERMODYNAMIC PROPERTIES A-3
A.5.2 BEHAVIOR IN THE PASSIVE REGIME A-3
A.5.3 PROBABILISTIC SHELL A-4
A.5.4 DRY DEPOSITION A-4
A.5.5 CHEMICAL AGENTS A-4
A.5.6 MODELING OF MIXTURES A-4
A.5.7 MODELING VAPOR CLOUD EXPLOSIONS A-4

A.6 DEFINITION OF "SOURCE TERMS" FOR THE CODES **A-4**

A.7 COMPARISONS WITH EXPERIMENTS AND OTHER MODELS **A-5**

LIST OF FIGURES

Page

Figure A-1. Predictions for Concentration as a Function of Non-Dimensionalized Time from the SRD and SADENZ Models Compared with Area-Averaged Concentrations Determined from the Data for Trials 13 and 17 ..... A-10

Figure A-2. A Comparison of the BG/C&W and SADENZ Models with Data Derived from the Photographic Records of Trial 13 by the UKAEA SRD. A-11

Figure A-3a. Temperature Data at 100m, Height of 1.0m. A-12

Figure A3-b. Temperature Data at 100m, Height of 2.5m A-13

Figure A-3c. DTI Temperature Data at 800m, Height of 1.0 m A-14

Figure A-4. Maximum Observed Concentration and Maximum Predicted Concentrations Using DEGADIS and Pasquill-Hanna Gaussian Plume Model for DT4. ..... A-15

Figure A-5. Comparison Among DEGADIS, SACRUNCH, and Data "Goldfish" HF Experiments. A-16

Figure A-6. FEM3, SACRUNCH, and AMOCO Series Test 1: (a) 300 m, (b) 1000 m - Height: 1 m A-17

Figure A-7. Maximum HF Concentration vs. Time at an Elevation of 1m for Two Downwind Locations for AMOCO HF Spill Test 3: (a) x = 300 m, (b) x = 1000 m A-18

LIST OF TABLES

Page

Table A-1. Comparison Between SAPLUME and Experiment A-7

Table A-2. Comparison Between Schotte's Results and Theory Mixing HF Vapor and Air with 80% RH A-8

Table A-3. Comparison Between Experimental Results and Theory A-9

A.1 INTRODUCTION

SAIC makes use of three atmospheric dispersion computer programs to simulate the range of possible large-scale accidental releases of hazardous vapors from units in the chemical, petrochemical or refining industries. They are known as SADENZ, SACRUNCH, and SAPLUME. The purpose of this appendix is to describe the models that are included in the computer codes, to give the reader a representative selection of comparisons with data, and to assess how the computer programs compare with other state-of-the art models.

A.2 SACRUNCH

SACRUNCH is a computer program that models the atmospheric dispersion of continuous releases of heavy vapors at ground level. SACRUNCH has its origins in an earlier code, CRUNCH (Jagger, 1983)[1], that was developed in the UK with funding provided by the UK Health and Safety Executive. SACRUNCH has also undergone extensive modifications during the 1980s. It has been validated against:

- Continuous releases of heavy vapors that were done at Thorney Island;
- The "Desert Tortoise" series of large scale releases of anhydrous ammonia at the Nevada Test Site; and
- The "Goldfish" series of large-scale releases of anhydrous HF.

The important features of SACRUNCH are as follows:

- Accepts input describing the dimensions of the source (which is approximated as a rectangle through which the vapor is flowing), the initial mass flux of heavy vapor, the initial mass flux of air (if any), the initial momentum flux, and the initial temperature.
- Takes account of:
  - Gravitational slumping
  - Entrainment of air at the edge of the cloud during the slumping
  - Entrainment of air at the top of the cloud that is strongly influenced by the presence of a density gradient
  - Conservation of momentum
  - Heating of the cloud by the ground
  - Eventual transition to behavior as a passive plume when the difference in density between the cloud and the surrounding air becomes small

A.3 SADENZ

SADENZ models the atmospheric dispersion of puff releases of heavy vapors. SADENZ is based on a code called DENZ (Fryer and Kaiser, 1979) which was developed during the late '70s

[1] See References in the main report for a list of references.

and early '80s at the Safety and Reliability Directorate in the United Kingdom. Funding for the development of DENZ was provided by the United Kingdom Health and Safety Executive, which is the body that regulates the chemical industry in the UK. DENZ has been used in the UK's CIMAH (Control of Industrial Major Accident Hazards) program. CIMAH is a risk management program, which has elements in common with California's Risk Management and Prevention Program and other state-mandated risk management programs in the United States.

SADENZ has been updated from time to time during the 1980s to take account of experimental and theoretical developments. In particular, considerable modifications were made on the basis of the Thorney Island Experiments, which are the best available large-scale experimental results on the atmospheric dispersion of puffs of heavy vapor. SADENZ compares well with the Thorney Island results.

The important features of SADENZ are as follows:

- Accepts input on the initial configuration, density, temperature, and composition of a heavy vapor puff
- Takes into account:
  - Gravitational slumping
  - Entrainment of air at the edge of the cloud during the slumping
  - Entrainment of air at the top of the cloud that is strongly influenced by the presence of a density gradient
  - Conservation of momentum
  - Heating of the cloud by the ground
  - Eventual transition to behavior as a passive plume when the difference in density between the cloud and the surrounding air becomes small

A.4 SAPLUME

The SAPLUME computer program simulates the atmospheric dispersion of heavy or buoyant vapors emitted from stacks, relief valves, or ruptured pipework. It is based on the well-known Ooms (1972) model that was originally developed by workers at Shell's research laboratories in the Netherlands.

The important features of SAPLUME are as follows:

- Accepts data describing the initial dimensions of the plume or jet, its orientation, its momentum flux, the initial mass flux of heavy gas, the initial mass flux of air (if any), and the temperature and density.
- Takes into account entrainment of air by the following mechanisms:
  - Entrainment into a high speed jet
  - Entrainment into a rising or falling buoyant or dense plume due to the action of its internally generated turbulence

- Action of the ambient turbulence in the surrounding atmosphere

- Also takes into account:
  - Temperature gradient in the atmosphere
  - Velocity gradient in the atmosphere
  - Conservation of momentum in both the horizontal and vertical directions
  - The influence of gravitational forces
  - The rate of change of temperature of the plume due to the entrainment of air
  - Transition to behavior as a passive plume when either the density difference becomes small or plume's velocity falls to close to that of the surrounding air
  - For buoyant plumes, termination of plume rise by a number of alternative mechanisms that take into account both mechanical and convective turbulence in the atmosphere and the presence of inversion lids.

SAPLUME has been successfully compared to wind tunnel experiences on the release of heavy plumes from stacks. There are no large-scale data against which a comparison can be made.

A.5 COMMON FEATURES OF THE COMPUTER PROGRAMS

A.5.1 Vapors with Complex Thermodynamic Properties

For vapors with complex thermodynamic properties, such as HF and ammonia, the user can input an array of vapor cloud properties: air/gas mass mixing ratio, cloud temperature and cloud density. The computer programs then interpolate among the values in this array each time a temperature or a density is needed. The array must be independently calculated.

A.5.2 Behavior in the Passive Regime

In all three computer programs, once the difference in density between the plume and the surroundings becomes small, the model reverts to the traditional Gaussian formulation. There are two user-selected alternatives for the vertical and horizontal standard deviations. The first is due to Briggs (1973), who allows a further choice between a rural and an urban case. Briggs' model is virtually identical to that in ALOHA, the Gaussian model that was developed by the National Oceanic and Atmospheric Administration (NOAA, 1988) and has been widely disseminated among agencies and industry. Test runs have shown that the SAIC codes and ALOHA give the same results for the dispersion of passive plumes. The Briggs model has also been included in Technical Guidance issued by the EPA (USEPA, 1987).

The second option that a user has is to call on standard deviations in a formulation given by Hosker (1974) wherein the vertical standard deviations are functions of meteorological roughness length, thus allowing the user to account for sites where the terrain differs widely. However, Hosker's model does not take into account the additional dilution caused by thermal effects in urban areas, so that the Hosker approach tends to be conservative for city sites.

A.5.3 Probabilistic Shell

All three of SAIC's computer programs are embedded within a probabilistic "shell" that allows the user to calculate various measures of risk. These measures include "f-n" lines, which are plots of the frequency f with which a given consequence equal exceeds a magnitude n. The quantity n is the number of people exposed above various levels chosen by the user, such as the LC_{50} (the concentration that would prove fatal to 50 percent of those exposed to it), the IDLH (Immediately Dangerous to Life or Health) or the ERPG (Emergency Response Planning Guideline). "n" can also be the areas affected by concentrations exceeding the levels given above, or the distances downwind to which those areas extend. The codes can also be used to calculate quantities such as mean societal risk and individual risk.

The computer programs generate the information on risk by carrying out the calculations for a variety of different weather conditions (the codes accept the meteorological data in the STAR format) and wind directions, as well as different release scenarios. The codes keep track of the frequencies associated with each combination of scenario, atmospheric stability category, windspeed, and wind direction and contain subroutines that store the results and manipulate them into the various measures of risk.

A.5.4 Dry Deposition

All of the computer programs contain the option of activating a dry deposition mechanism that depletes the plume by deposition of reactive gases or particulates onto the ground, using the well-established concept of dry deposition velocity.

A.5.5 Chemical Agents

All of the computer programs contain the option of modeling chemical agent releases. The models contain chemical agent-specific vapor pressure relationships and probit equations for consequence assessment.

A.5.6 Modeling of Mixtures

All of the computer programs can handle the releases of mixtures of ideal vapors.

A.5.7 Modeling Vapor Cloud Explosions

All of the computer programs can predict the potential for vapor cloud explosions. They can predict if a cloud will make contact with a given ignition source. If such contact is predicted, then the models also calculate the inventory of materials in the cloud, the cloud geometry and the time elapsed since the release.

A.6 DEFINITION OF "SOURCE TERMS" FOR THE CODES

SAIC believes that, among them, the three computer programs described above are capable of simulating the atmospheric dispersion of most of the accidental releases of toxic or flammable

vapors that might occur at industrial facilities. However, the use of codes is not trivial, because the codes are deliberately not set up as "black boxes" that purport to simulate every conceivable case without much thoughtful effort by the user. The range of possible releases from industrial facilities is so large, and the variety of subtle physical and chemical phenomena to be considered is so wide, that no dispersion model can be used without careful consideration of whether it is appropriate for the type of release being considered and what approximations are needed to formulate the input in a way that the code can handle without sacrificing physical reality.

SAIC uses the full array of models that are available for calculating release rates, such as the standard formulas for evaporating pools. The techniques are reviewed in the "Guidelines for Use of Vapor Cloud Dispersion Models," published by the Center for Chemical Process Safety (Hanna and Drivas, 1987) or the CCPS' Quantitative Risk Assessment Guidance Document (CCPS, 1989). The user makes use of these techniques to generate input for the atmospheric dispersion computer programs.

A.7 COMPARISONS WITH EXPERIMENTS AND OTHER MODELS

SAIC's computer programs, including their theoretical basis and how they compare with experiment, are documented in SAIC's internal report, "SAIC's Computer Programs for the Atmospheric Dispersion of Hazardous Vapors." For the purposes of this summary, a selection of comparisons is shown in Figures A-1 to A-7. Much of the modeling basis for SADENZ and SACRUNCH depends on the series of large-scale releases of Freon-12 (refrigerant-12) that were carried out at Thorney Island (McQuaid, 1985). Figure A-1 shows how SADENZ compares with the concentration results of two of the trials from Thorney Island and with the DENZ model that has been independently updated in the UK by the Safety and Reliability Directorate (Wheatley et al., 1986). Agreement between experiment and both models is good. Figure A-2 shows experimental results for the position of the puff centerline, the puff height, and the area of the base of the puff as a function of time. In addition, Figure A-2 shows the predictions of a model developed in the UK by British Gas Corporation and Cremer and Warner (Carpenter et al., 1986). Again, agreement between both models and the data is good.

Figure A-3 shows some results from the "Desert Tortoise" series of large-scale anhydrous ammonia releases (Goldwire et al., 1985). The figure contains experimentally measured temperatures as a function of time, compared with the predictions of SACRUNCH. The predicted temperature of a cloud is a very sensitive function of, for example, the predicted rate of entrainment of air. Small differences in the entrainment can easily lead to temperature differences of tens of degrees. Therefore, it is gratifying that SACRUNCH does so well with modeling that was fixed by comparison with the Thorney Island Experiments, in which temperature effects were unimportant. Figure A-4 shows how SACRUNCH and DEGADIS (Spicer et al., (1987) predict the peak centerline concentrations in the fourth of the Desert Tortoise experiments, DT4. SACRUNCH reproduces the data with a goodness of fit at least comparable to that of DEGADIS. Incidentally, the differences between the predictions of the two models and between each of the models and the data lie within the combined error band that is to be expected from the models and the data.

Figure A-5 shows how SACRUNCH and DEGADIS reproduce the predicted peak centerline concentrations that were observed in the "Goldfish" series of HF experiments (Blewitt et al.,

1987). Again, the way the two codes fit the data is comparable. Figures A-6 and A-7 show how SACRUNCH and FEM3 (Chen et al., 1987) fit some of the "Goldfish" data. These figures are instructive because, while SACRUNCH (and DEGADIS) are examples of relatively simple "box" models that, in the main, deal with averaged quantities, FEM3 is a sophisticated three dimensional code that solves the underlying conservation equations and turbulence closure assumptions numerically. The goodness of fit achieved by SACRUNCH, both to the concentration data and the time of arrival and time of departure of the plume, is at least comparable to that achieved by FEM3. This confirms an opinion that is widely accepted in the community of those who develop and use heavy vapor dispersion models, namely that, for the purposes of risk assessment, the simple box models do at least as good a job as the more sophisticated three dimensional codes at a fraction of the cost.

As discussed above, the code SAPLUME is based on the well-known Ooms model for stack releases. The comparable module in DEGADIS is based on exactly the same model. Unfortunately, there are relatively few data against which to compare the releases of heavy vapors from stacks or as jets from relief valves. One good data set of heavy vapor releases from stacks has been prepared by Hoot et al. using a wind tunnel at Colorado State University (Hoot et al., 1973). Table A-1 shows a selection of data from those experiments and how they compare with the predictions of SAPLUME. As can be seen, agreement is quite good. The authors of DEGADIS used the same data set to validate the Ooms module. SAIC has reviewed the DEGADIS manual (Havens and Spicer, 1988), where the comparisons are presented, and has concluded that SAPLUME reproduces the data with a goodness of fit that is at least as good as that achieved by DEGADIS. Finally, Tables A-2 and A-3 show a comparison between the predictions of the HF model in SACRUNCH and data on the mixing of HF and air or nitrogen collected by workers at DuPont (Schotte, 1987). Agreement is good.

In conclusion, SAIC's toxic vapor dispersion models compare well with data from a variety of sources and with other state-of-the-art models.

Table A-1. Comparison Between SAPLUME and Experiment

Exit Velocity	Velocity Ratio	Specific Gravity	Height of Rise (IN)		Touchdown Dist. (IN)		Touchdown Conc. (kg/m^3)	
			EXPT.	SAPLUME	EXPT.	SAPLUME	EXPT.	SAPLUME
3.712	5.1	1.077	3.7	3.6	beyond experimental range			
15.022	20.72	1.572	10.8	13	56	50	0.006	0.004
11.137	15.3	2.158	7.78	9.45	28	24	0.015	0.015
7.424	10.2	3.278	5.24	5.88	13	10.5	0.038	0.055
7.511	10.32	4.16	5.12	6.05	9.7	7.8	0.054	0.088
7.597	10.1	1.608	3.22	3.77	31.5	31.2	0.0052	0.0037
3.799	5.05	2.217	1.38	1.64	21.23	14	0.013	0.01
6.216	8.80	3.044	2.88	3.2	14.05	13	0.017	0.017

Spot comparisons of SAPLUME predictions with experiments of Hoot, Meroney and Peterka. "Wind Tunnel Tests of Negatively Buoyant Plumes" PB-231 590 (1973)

Table A-2. Comparison Between Schotte's Results and Theory
Mixing HF Vapor and Air with 80% RH

Total Mol% HF	Mixing Ratio[1]	Temperature				X_{HF}[2]		% HF Condensed	
		Air	HF-N_2	Fog Exp	Fog (SAIC)	expt	(SAIC)	expt	(SAIC)
0.373	387	298.9	299.6	300.1	300.8	0.261	0.263	26.7	26.29
0.696	207	299.1	299.7	303.8	302.8	0.306	0.302	29.5	28.33
1.13	127	299	299.7	305.5	304.2	0.346	0.340	29.8	29.11
1.52	94.7	298.9	299.8	306.8	305.1	0.370	0.351	29.8	28.04
1.90	75.8	298.8	299.7	307.2	305.7	0.389	0.374	29.7	28.35
2.86	50.3	299	298.9	308.9	306.9	0.423	0.421	29.3	29.21
5.55	25.9	298.7	299.2	308.6	307	0.490	0.476	28.7	27.92
8.85	16.3	298.7	298.8	305.0	303.8	0.553	0.524	28.8	26.83
12.07	11.9	298.5	298.1	296.2	299.2	0.620	0.597	29.5	28.69
15.68	9.18	25.6	25.0	12.0	15.1	0.687	0.677	29.9	28.4
19.63	7.34	25.7	25.2	7.0	8.8	0.737	0.726	29.2	27.4

1 Air/HF mass mixing ratio
2 Mole percent of HF in HF/water droplets
Source: Schotte (1987)

Table A-3. Comparison Between Experimental Results and Theory Mixing a 50/50 Mixture of Nitrogen and HF with Air at 80% RH

Total Mol% HF	Mixing Ratio[1]	Temperature				X_{HF}[2]		% HF Condensed	
		Air	HF-N_2	Fog Exp	Fog (SAIC)	expt	(SAIC)	expt	(SAIC)
0.197	732	26.4	26.7	28.5	27.4	0.215	0.213	16.0	10.3
0.482	298.	26.4	26.6	29.7	30.1	0.282	0.280	21.5	17.3
0.951	151	26.3	26.6	33.5	33.7	0.33	0.331	21.8	18.7
1.41	101	26.3	26.4	35.0	34.7	0.36	0.361	21.0	18.1
1.87	75.8	26.2	26.4	35.9	35.8	0.38	0.382	20.1	18.1
2.85	49.2	25.8	25.7	39.7	38.7	0.41	0.415	18.6	17.5
5.26	26.0	25.9	25.6	41.3	40.4	0.46	0.465	15.8	15.9
7.29	18.4	25.4	26.7	42.7	42.7	0.49	0.493	13.1	14.6
10.18	12.8	25.4	26.2	43.4	41.9	0.52	0.526	12.2	14.0
12.76	9.9	25.5	25.8	42.1	41.1	0.55	0.554	11.7	13.7
14.95	8.2	25.7	25.8	40.8	39.9	0.57	0.577	11.1	13.3

1 Air/HF mass mixing ratio
2 Mole percent of HF in HF/water droplets
Source: Schotte (1987)

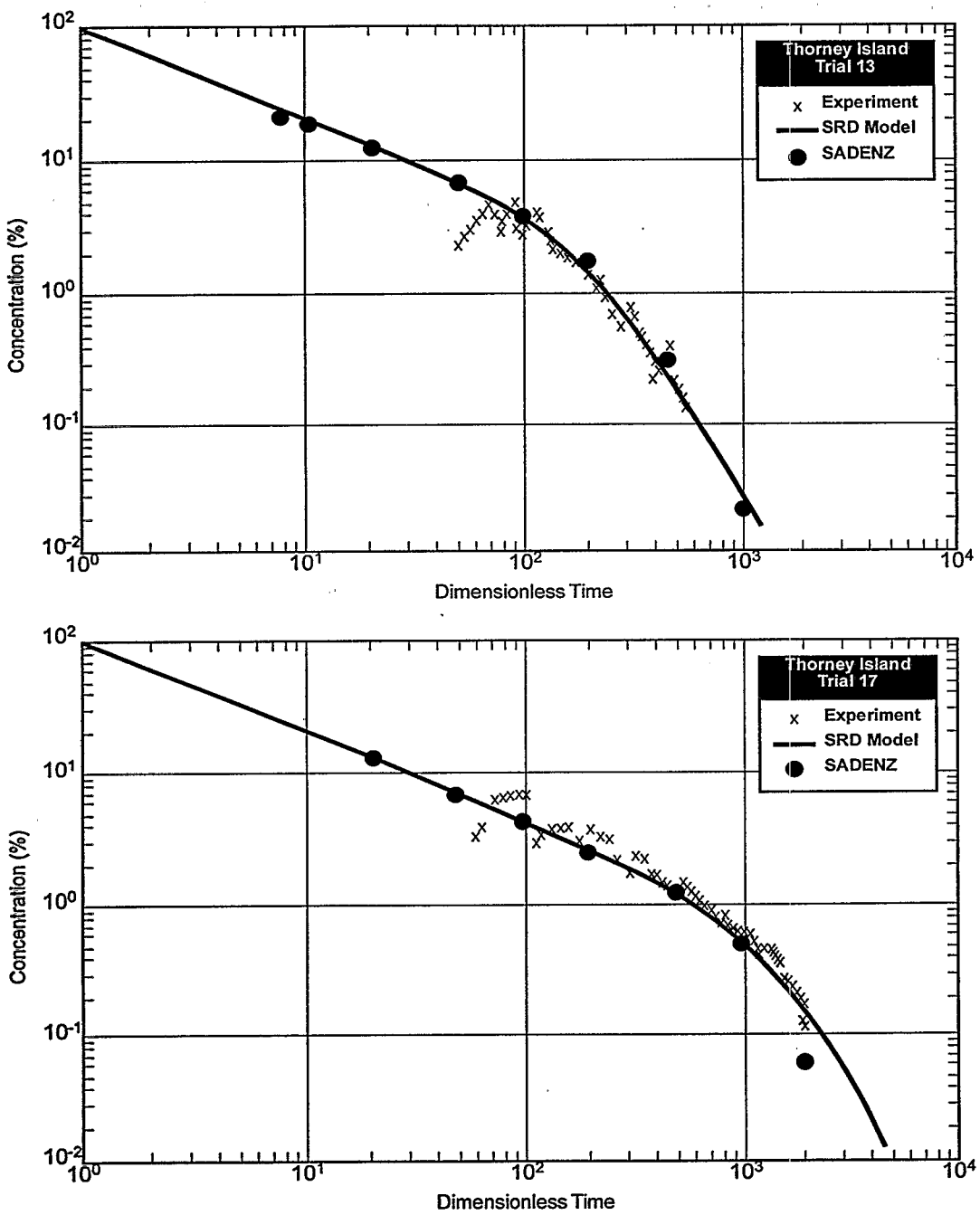

Source: Wheatley et al. (1985)

Figure A-1. Predictions for Concentration as a Function of Non-Dimensionalized Time from the SRD and SADENZ Models Compared with Area-Averaged Concentrations Determined from the Data for Trials 13 and 17.

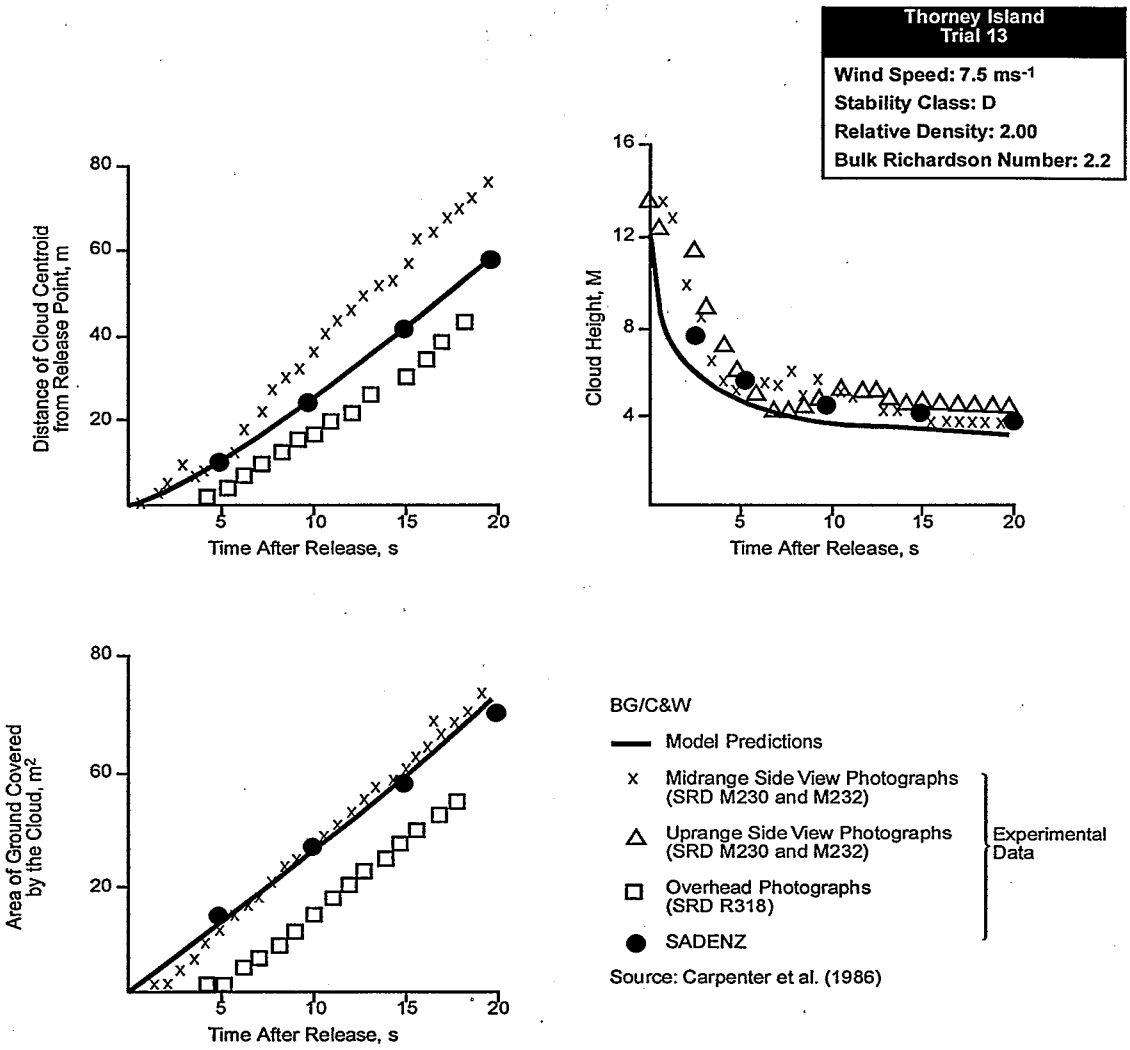

Figure A-2. A Comparison of the BG/C&W and SADENZ Models with Data Derived from the Photographic Records of Trial 13 by the UKAEA SRD.

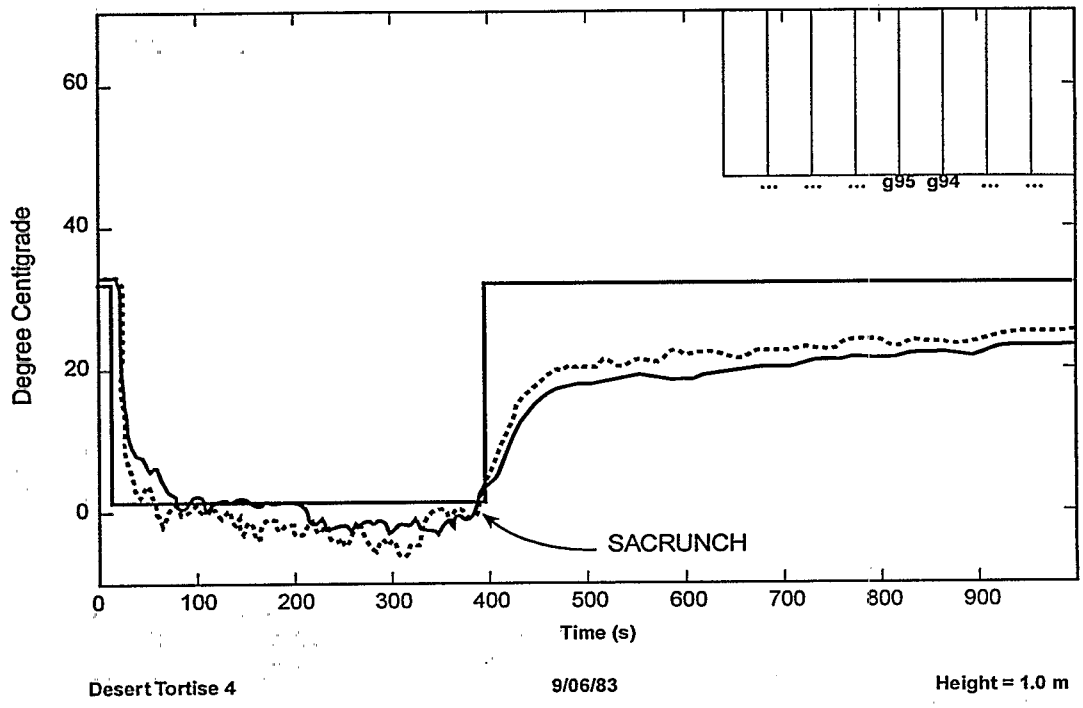

Figure A-3a. Temperature Data at 100m, Height of 1.0m.

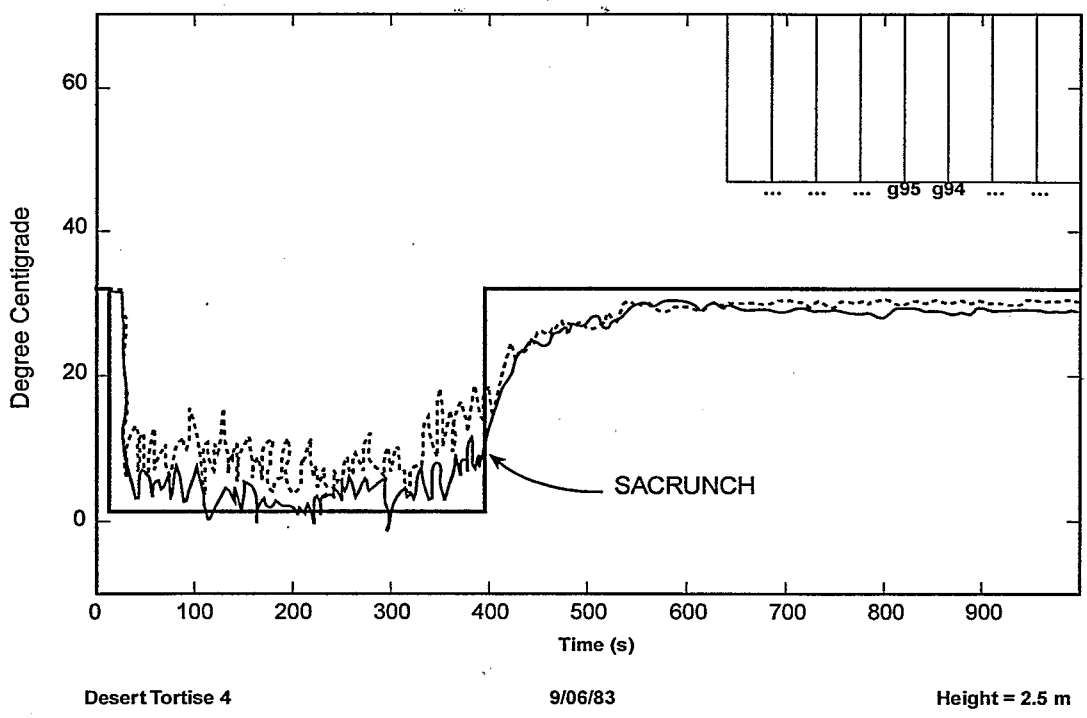

Figure A3-b. Temperature Data at 100m, Height of 2.5m

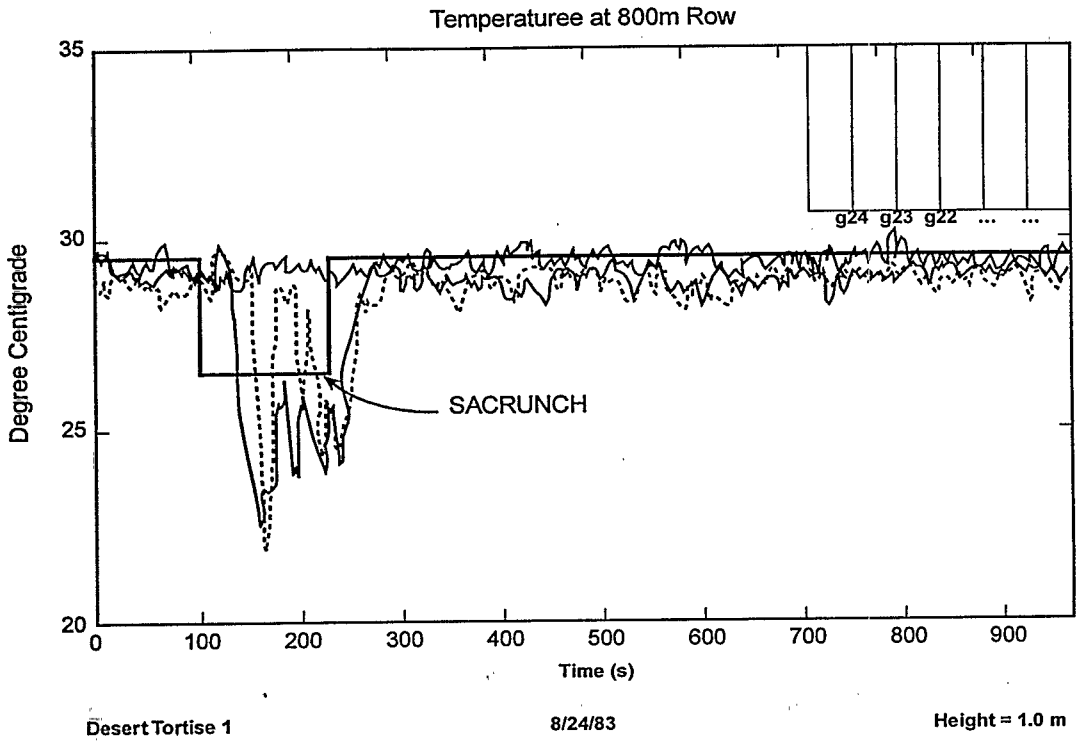

Figure A-3c. DTI Temperature Data at 800m, Height of 1.0 m

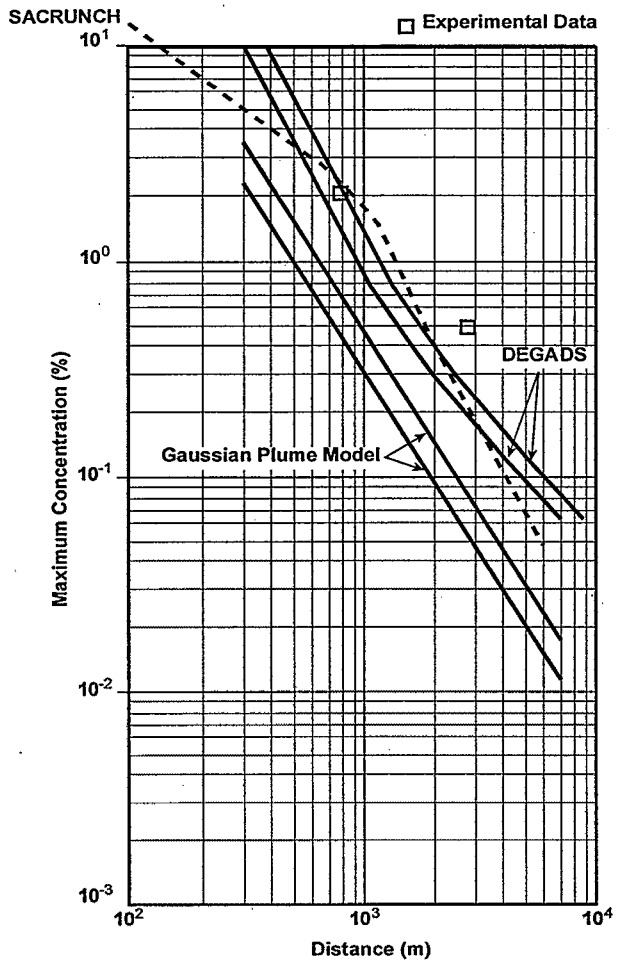

Figure A-4. Maximum Observed Concentration and Maximum Predicted Concentrations Using DEGADIS and Pasquill-Hanna Gaussian Plume Model for DT4.

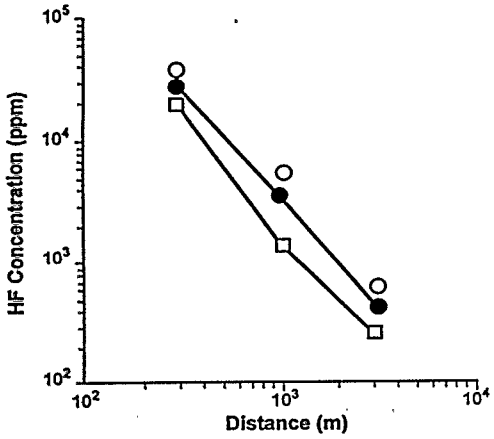

Comparison of Observed and DEGADIS Predicted Plume Centerline Concentrations for Test 1 (1 Meter Height)

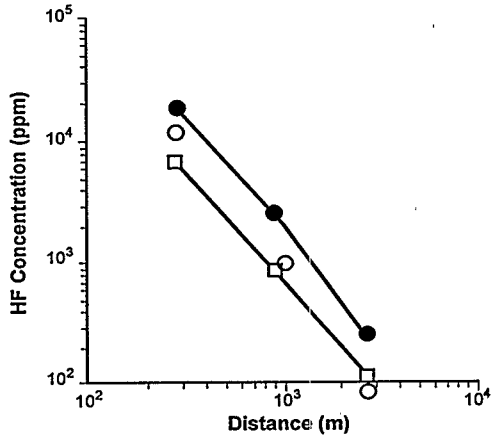

Comparison of Observed and DEGADIS Predicted Plume Centerline Concentrations for Test 2 (1 Meter Height)

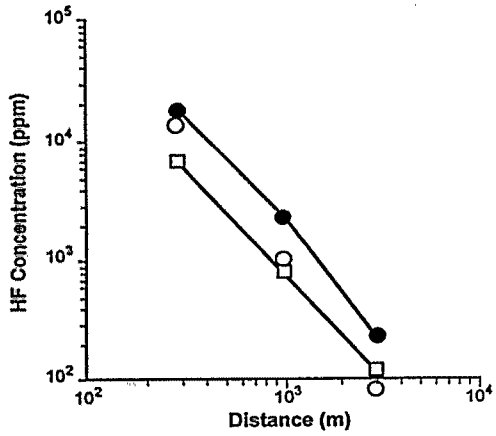

Comparison of Observed and DEGADIS Predicted Plume Centerline Concentrations for Test 3 (1 Meter Height)

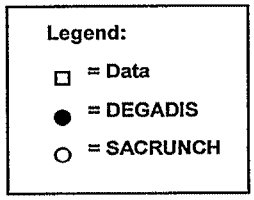

Figure A-5. Comparison Among DEGADIS, SACRUNCH, and Data "Goldfish" HF Experiments.

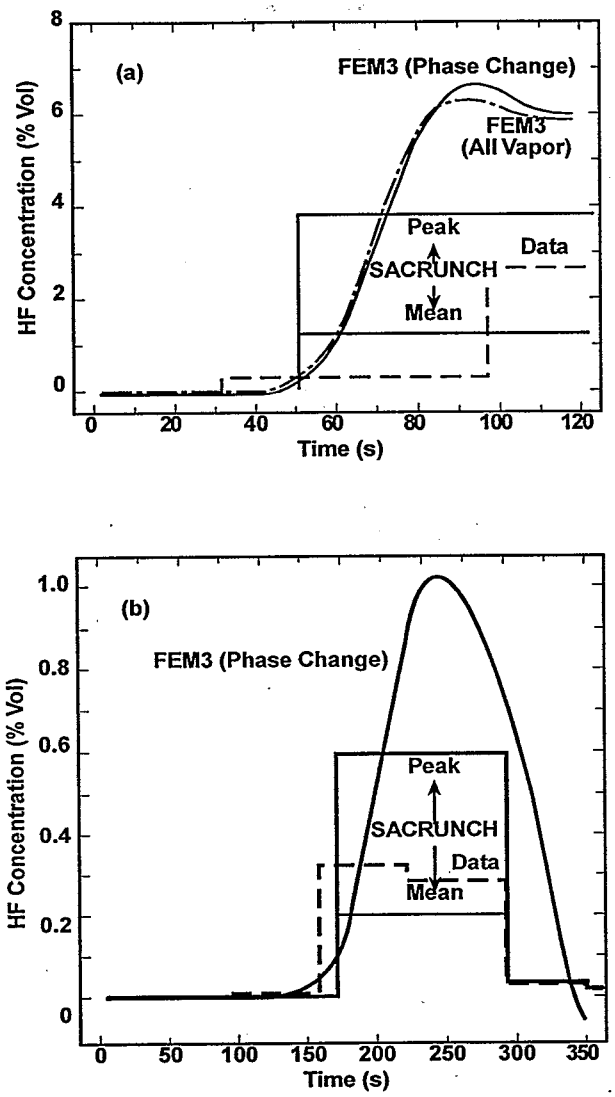

Figure A-6. FEM3, SACRUNCH, and AMOCO Series Test 1: (a) 300 m, (b) 1000 m - Height: 1 m

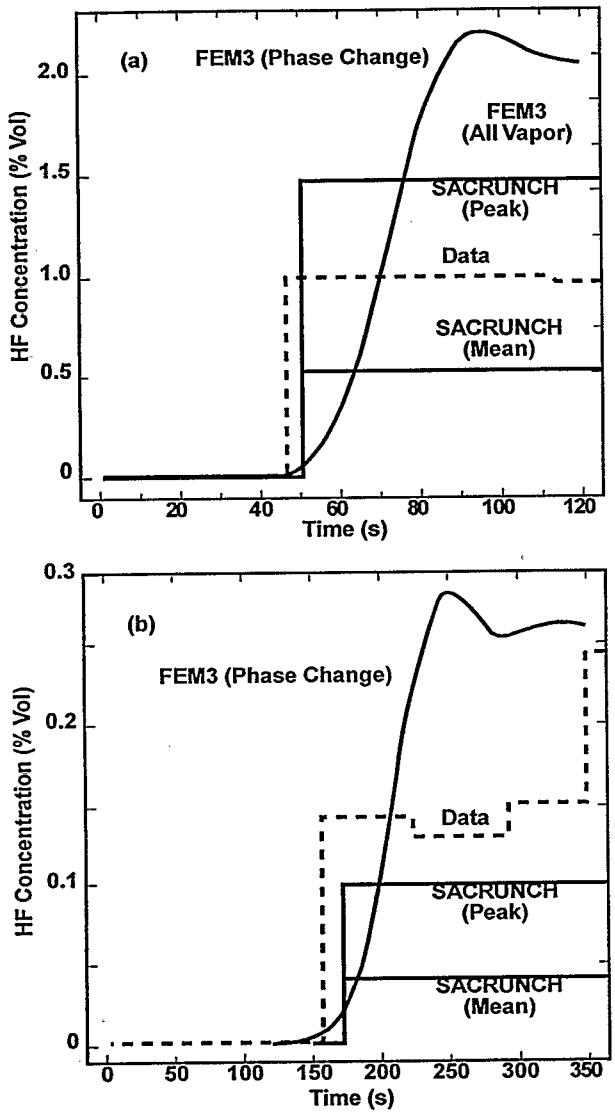

Figure A-7. Maximum HF Concentration vs. Time at an Elevation of 1m for Two Downwind Locations for AMOCO HF Spill Test 3: (a) x = 300 m, (b) x = 1000 m